Investigating Synthetic Lethal Interactions with the Wall Teichoic Acid Pathway of Staphylococcus aureus

Investigating Synthetic Lethal Interactions with the Wall Teichoic Acid Pathway of *Staphylococcus aureus*

Abstract

The peptidoglycan of many Gram-positive bacteria is densely functionalized with anionic glycopolymers called wall teichoic acids (WTAs). Recent studies have shown that these polymers play crucial roles in cell shape determination, regulation of cell division, and other fundamental aspects of Gram-positive bacterial physiology. Furthermore, in pathogens they are important in host infection and play key roles in antibiotic resistance. In many cases, precise mechanisms for WTA involvement in these processes have not been established. In order to better understand the roles of WTAs in the biology of the human pathogen *Staphylococcus aureus*, we sought to identify their interactions with other cellular pathways. By employing a transposon screen, we found that lipoteichoic acid (LTA) synthesis, D-alanylation of teichoic acids, cell wall stress sensors, CAAX-like proteases, and peptidoglycan biosynthesis were all synthetically lethal with depletion of WTAs in *Staphylococcus aureus*. Further investigations revealed that several genes required when WTAs were depleted were not essential when LTAs were removed. Unexpectedly, TA D-alanylation, became essential in the absence of WTAs, but not LTAs. Examination of terminal phenotypes following WTA depletion revealed that strains lacking LTA D-alanine esters died from envelope rupture during ongoing cell division whereas strains lacking LTAs were unable to form Z rings, stopped dividing, and had altered PG biosynthesis. Finally, we designed and implemented parallel, pathway-specific chemical screens to identify inhibitors that specifically kill mutants deficient in WTAs or D-alanylation of TAs. In addition to elucidating new interactions between cell envelope pathways, and establishing distinct roles

LTAs and WTAs in the cell envelope of *S. aureus*, these experiments provide a list of potential targets and a strategy for identifying inhibitors for these targets, in compound combinations as therapeutics against antibiotic-resistant *S. aureus* infections.

Acknowledgements

The journey of my PhD started long before graduate school and continued only with the encouragement of countless friends, students, and mentors along the way. In this way, I consider this body not my own work, but the manifestation of others' efforts through my hands, as inefficient and clumsy as they sometimes were!

First and foremost, I thank my parents, who provided unwavering support for me in my academic pursuits, despite how far they took me away from home (even while I was physically home). Thank you for always being there when I called, for pushing me to never give up, for excusing my absence, and for always making an effort to learn and hear my science. And much gratitude to my sister Olivia, whom I'm proud to say, will be adroitly applying her science as a physical therapist.

Thank you to my friends, particularly Kristina Quirolgico, Daphne Rich, Jaemin Bae, Stefan Ringel, Amaad Rivera, and especially Nadia Chernyak, who understood my pain best as a fellow graduate student (I look forward to potential professorships together). You visited me, fed me, watered me, listened to me, and always made me feel loved. And thank you to my experimental partners Stephanie Brown, Yuriy Rebets, Jennifer Campbell, Mithila Rajagopal, Samir Moussa, and Lincoln Pasquina, as well as other members of the Walker Lab who kept me coming in everyday despite failed experiments and with whom I've embarked on many exciting excursions into the environs of greater Boston (climbing, curling, dancing, drinking, eating, hiking, we did it all!).

I owe a debt of thanks to teachers such as Drs. David Niedosik and the late Charlie Russell, who instilled within me scientific curiosity and a desire to pursue science in greater depth than we could pursue in the classroom. I am very grateful for mentors such as Drs. Amy Hark and Keri Colabroy, who provided formative preparatory research experiences and continued to provide great advice even after I graduated from Muhlenberg College. I am indebted to Drs. Thomas Bernhardt, Christopher T. Walsh, and Eric Rubin as my dissertation advisory committee for their advice on experiments and for keeping me on track, as well as Jason Milberg, KeyAnna Schmiedl, and Samantha Reed as caring and attentive administrators for the Chemical Biology Program.

Even since before he was a graduate student, Mark Kalinich has provided perspicacious scientific insight and more importantly has been a loving partner. I do not think that I could have completed my PhD in one piece, were it not for his strong arms holding me together (I look forward to potential professorships together). I look forward to providing reciprocal support (really, spoiling) him over the duration of his graduate career.

And Dr. Suzanne Walker – ineffable is the depth of my gratitude for your patience and mentorship and my admiration of your intellect. I really don't know how you stuck by me all this time. I will miss our time together, analyzing data and conjecturing in your office.

Chapter 1: Wall Teichoic Acid Biosynthesis and Function

This chapter is an amalgamation of two reviews, published in the 2013 issues of Annual Reviews in Microbiology and Current Opinion in Microbiology

Brown, S, Santa Maria, JP, and Walker, S. (2013) Wall teichoic acids of Gram-positive bacteria. *Ann Rev Microbiol*. **67**: 313-336.
Pasquina, L, Santa Maria, JP, and Walker, S. (2013) Teichoic acid biosynthesis as an antibiotic target. *Curr Op Microbio* **16**: 531-537.

1.1 Introduction

Bacteria are surrounded by a complex cell envelope that performs a variety of functions (202). Cell envelopes are varied in structure, but all contain layers of peptidoglycan (PG), a cross-linked matrix of linear carbohydrate (glycan) chains connected to one another via covalent bonds between attached peptides (228). This PG matrix is essential for survival, and in gram-positive organisms it is densely functionalized with other polymers. Wall teichoic acids (WTAs) are the most abundant PG-linked polymers in many gram-positive organisms (166). They are intimately involved in many aspects of cell division and are essential for maintaining cell shape in rod-shaped organisms (211). WTAs are required for β-lactam resistance in methicillin-resistant *Staphylococcus aureus* (MRSA), and they modulate susceptibility to cationic antibiotics in several organisms (42; 44; 247). Due to their importance in pathogenesis, WTAs are possible targets for new therapeutics to overcome resistant bacterial infections. Here we review recent work on WTAs and discuss studies implicating the pathway as a therapeutic target.

1.2 Teichoic Acid Definition

Armstrong *et al*. discovered teichoic acids in 1958 while trying to determine the function of CDP-glycerol and CDP-ribitol in *Lactobacillus arabinosus, Bacillus subtilis,* and several other bacteria (9). The term teichoic acid encompasses a diverse family of cell surface glycopolymers containing phosphodiester-linked polyol repeat units (235). Teichoic acids include both lipoteichoic acids (LTAs), which are anchored in the bacterial membrane via a glycolipid, and WTAs, which are covalently attached to PG (166; 235) (Figure 1.1).

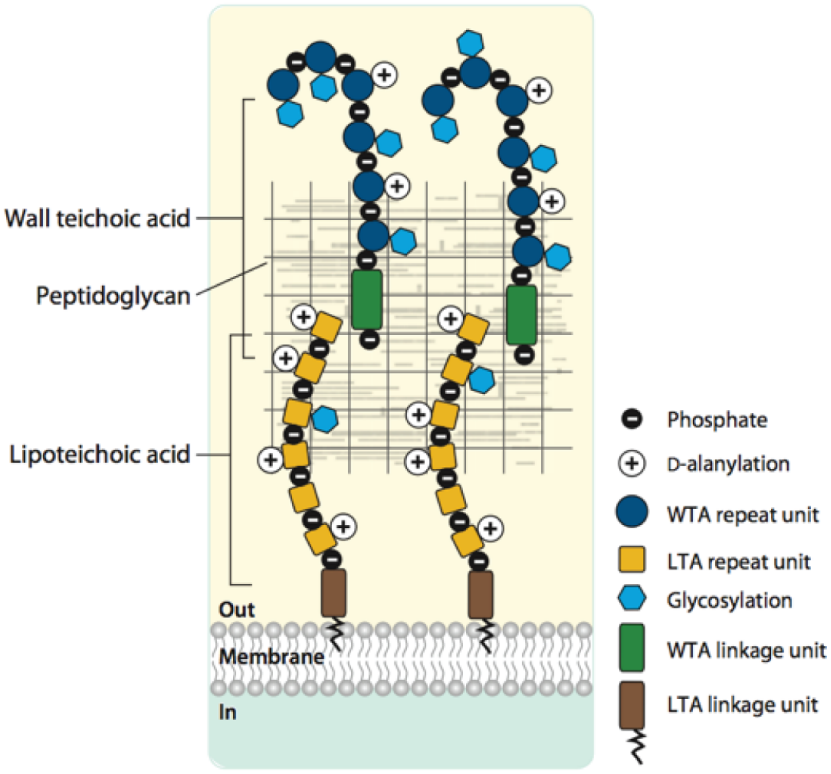

Figure 1.1: Teichoic acid polymers are located within the gram-positive cell wall. This schematic of the gram-positive cell wall shows that WTAs are covalently anchored to PG and LTAs are tethered to the membrane. The WTAs extend beyond the PG layer, whereas fully extended LTAs may not be able to reach past the PG layer. Abbreviations: LTA, lipoteichoic acid; PG, peptidoglycan; WTA, wall teichoic acid.

1.3 Wall Teichoic Acid Backbone Structure

WTAs are highly abundant modifications of gram-positive cell walls (165). In *B. subtilis* and *S. aureus,* it has been estimated that every ninth PG *N*-acetylmuramic acid (MurNAc) residue contains an attached WTA polymer containing 40 to 60 polyol repeats (20; 127). The total mass of WTAs in these and other organisms constitutes up to 60% of the cell wall (74; 217). Cryo-electron microscopy images suggest that, consistent with their

estimated length, *S. aureus* WTAs extend well beyond the PG layer (150; 151; 189).

The WTA polymer can be divided into two components: a disaccharide linkage unit and a main chain polymer composed of phosphodiester-linked polyol repeat units (166) (Figure 1.2). The disaccharide linkage unit, which is highly conserved across bacterial species, is composed of *N*-acetylmannosamine (β1→4) *N*-acetylglucosamine 1-phosphate [ManNAc(β1→4)GlcNAc- 1P] with one to two glycerol 3-phosphate units attached to the C4 oxygen of ManNAc (8; 127; 166). The anomeric phosphate of the linkage unit is covalently attached to PG via a phosphodiester bond to the C6 hydroxyl of MurNAc. The phosphodiester-linked polyol repeats extend from the GroP end of the linkage unit (166; 235).

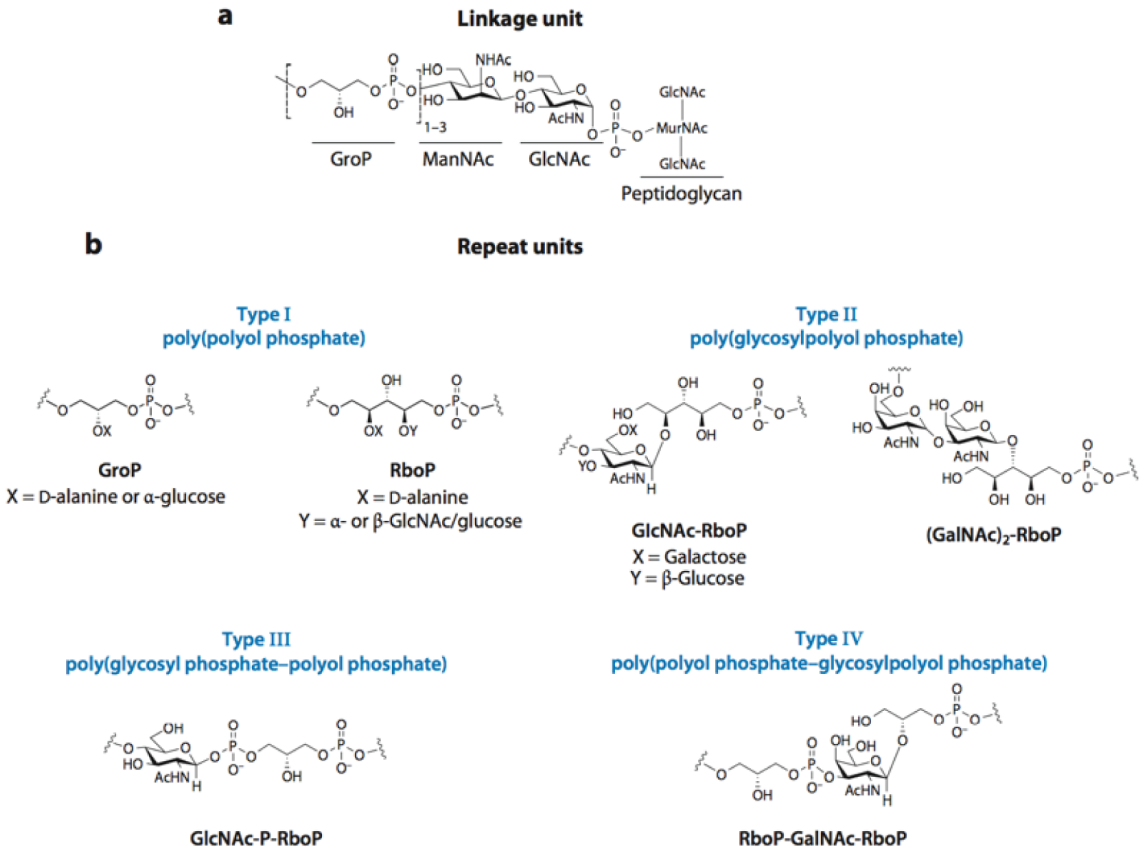

Figure 1.2: WTA polymers share a common linkage unit but exhibit structural diversity in their repeat units. (a) The commonly characterized WTA linkage unit consists of a GroP-ManNAc-GlcNAc-P that is covalently attached to peptidoglycan. Although the stereochemistry of the glycosidic linkage has not been clearly established, it is assumed to be retained as α on the basis of predicted enymatic catalysis. (b) Four different classes of WTA repeat units found in gram-positive bacteria as adapted from Naumova, *et al.* (165). Abbreviations: GalNAc, N-acetylgalactosamine; GlcNAc, N-acetylglucosamine; GroP, glycerol 3-phosphate; ManNAc, N-acetylmannosamine; MurNAc, N-acetylmuramic acid; P, phosphate; RboP, ribitol 5-phosphate.

The best-characterized WTA structures contain repeat units of ribitol 5-phosphate (RboP) or glycerol 3-phosphate (GroP), but WTA monomer structures can be highly diverse, and many published structures are more unusual (75; 76; 165). Other WTA repeat units include variations of glycosylpolyol phosphate or glycosyl phosphate–polyol phosphate (165; 166) (Figure 1.2). WTA structural diversity can exist within the same species, as in *B. subtilis,* in which strains 168 and W23 contain GroP and RboP repeat units, respectively. *Lactobacillus plantarum* has the ability to switch backbone composition (39). Furthermore, single strains of *S. aureus* and *Bacillus coagulans* can contain polymers with distinct repeats expressed simultaneously but at different levels (182; 226). WTA structural variations may represent adaptations to different environments. Relatedly, bacteria are known to modulate transcription of WTA biosynthetic genes in response to stress conditions (159). Despite their diversity, all WTAs contain a negatively charged anionic backbone and share common functions.

1.4 Tailoring Modifications of the Wall Teichoic Acid Polymer

Additional WTA structural diversity arises from the presence or absence of substituents attached to the repeating monomers (Figure 1.3). The repeat unit hydroxyls can be tailored with cationic D-alanine esters or a variety of mono- or oligosaccharides, commonly glucose or GlcNAc (166). In RboP polymers, D-alanyl residues are installed at position 2 of ribitol and sugars are commonly found at position 4 (166; 226). D-Alanine ester content is variable and depends on several factors, including pH, salt concentration, and temperature (117; 166). In contrast, the WTA sugar substituents do not appear to fluctuate with changes in the cellular environment (53). These tailoring modifications are typically highly abundant. For example, nearly all of the RboP repeats in *S. aureus* contain *O*-GlcNAc substituents (117). Depending on the bacterial strain, the anomeric glycosidic linkage to the repeat unit can be exclusively α, exclusively β, or a mixture of the two (49; 75; 76; 163). Some *S. aureus* strains have been found to contain, in the same cell wall, two different poly(RboP) WTAs, one fully α-glycosylated and the other fully β-glycosylated (218). In *B. subtilis* W23 it was observed that some WTA strands were fully glycosylated, whereas other strands contained no sugar substituents (49).

1.5 Wall Teichoic Acid Biosynthesis

1.5.1 Overview

Much of the early work to understand WTA biosynthesis used particulate enzyme preparations. Though this work enabled characterization of the enzymatic steps in WTA polymer formation, the identities of the enzymes responsible for these steps remained elusive

(235). Later, genetic analyses of temperature-sensitive and phage-resistant mutants led to the identification of the poly(GroP) WTA gene cluster in *B. subtilis* 168 and the poly(RboP) WTA gene cluster in *B. subtilis* W23 (119; 253). Sequence analysis led to proposals for the enzymatic activity encoded by each gene (136; 166; 235). However, it proved challenging to fully characterize the pathway using genetics because many of the biosynthetic genes are essential (25; 26; 58; 59; 125). Efforts to characterize WTA enzymes biochemically were hampered because the substrates contain 55-carbon lipid chains that make them difficult to handle. Moreover, these lipid-linked substrates are present in very low abundance and cannot be isolated in useful quantities from bacterial cells. The development of chemoenzymatic methods to make WTA substrates has not only allowed elucidation of biosynthetic pathways but also permitted mechanistic studies on purified teichoic acid enzymes in the absence of membranes (40; 43; 93; 196; 201; 255).

1.5.2 Linkage Unit Synthesis

In 1978 Archibald and colleagues used electron microscopy to show that WTA synthesis begins in the cytoplasm at the wall-membrane interface and that the WTA polymer subsequently appears on the outer surface of the cell (6; 235). TagO catalyzes the first synthetic step: the transfer of GlcNAc-1-P from UDP-GlcNAc to a membrane-anchored undecaprenyl phosphate carrier lipid, an intermediate shared with PG biosynthesis (191; 204). The TagO product is used in the synthesis of several *B. subtilis* 168 cell wall polymers, including the major WTA [poly(GroP)], the minor teichoic acid (TA) [poly(glucosyl *N*-*acetylgalactosamine* 1-phosphate)], and teichuronic acid [poly(glucuronyl *N*-acetylgalactosamine)] (204). Consequently, the first committed step in WTA biosynthesis is

the transfer of ManNAc from UDP-ManNAc to the C4 hydroxyl of GlcNAc to form the ManNAc(β1→4)GlcNAc disaccharide, catalyzed by TarA (57; 93; 255). The UDP-ManNAc donor sugar is derived from UDP-GlcNAc via MnaA (*yvyH),* an epimerase that catalyzes stereochemical inversion at the C2 position (205). TagB, a glycerophosphotransferase, catalyzes the transfer of a GroP unit from CDP-glycerol to the C4 position of ManNAc (27; 93). These first three steps to complete the synthesis of the WTA linkage unit are highly conserved across all strains characterized thus far (Figure 1.3). After these steps, WTA pathways diverge.

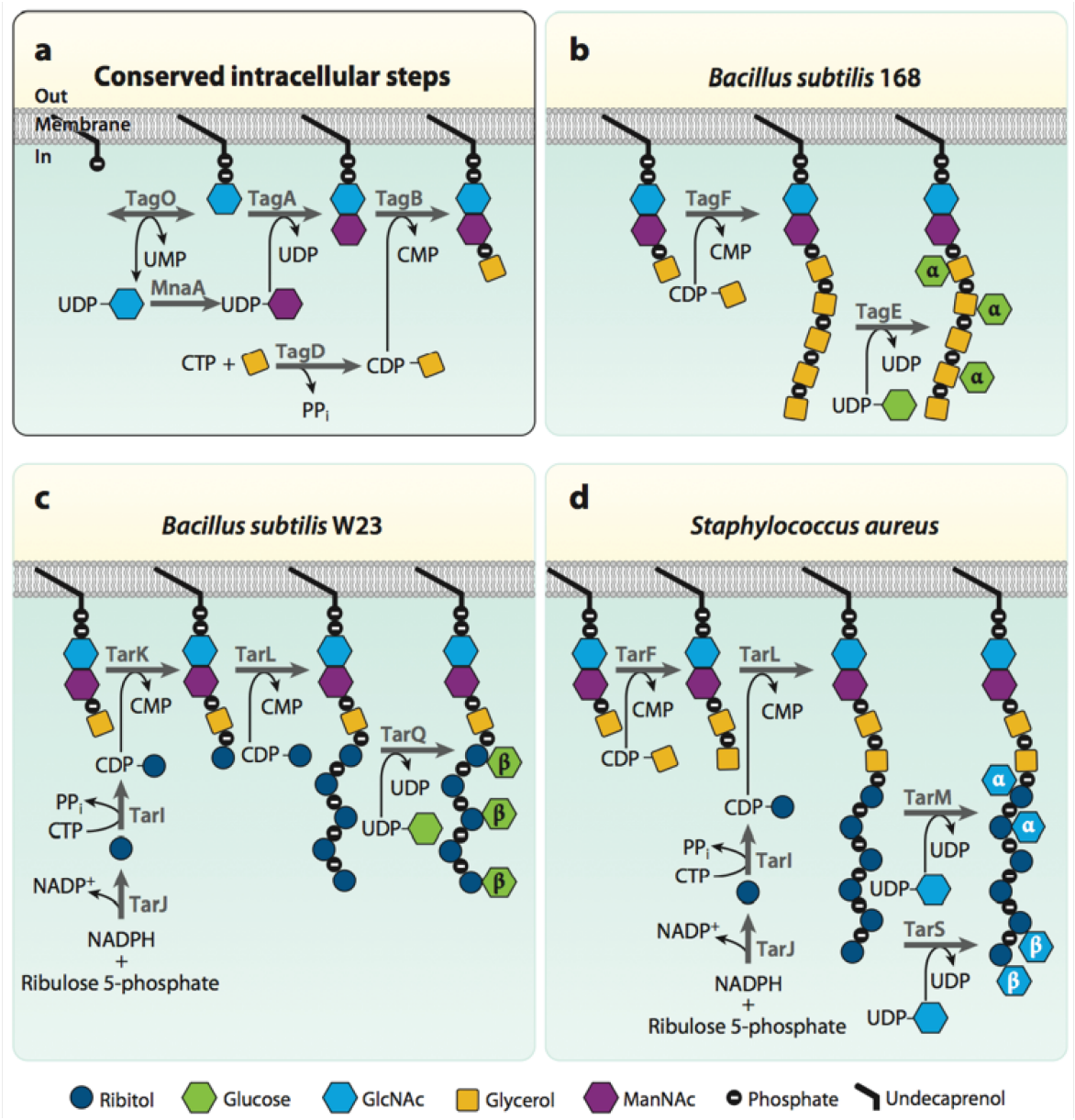

Figure 1.3: In different organisms, WTA biosynthesis begins with the same initial steps but then the pathways diverge. (a) The initial steps to WTA polymer formation that have been found in all pathways characterized thus far. (b-d) The end-stage intracellular steps to form the WTA poylmer in (b) *Bacillus subtilis*, (c) *B. subtilis* W23, and (d) *Staphylococcus aureus*. TarIJ reactions to form CDP-ribitol exist in both *B. subtilis* W23 and *S. aureus*. The α or β within the sugar denotes the stereochemistry of attachment. We have shown α- and β -

GlcNAc attachment to *S. aureus* occurring on the same strand, but it is possible that the TarS and TarM enzymes do not attach GlcNAc to the same polymer.

1.5.3 Poly(Glycerol 3-Phosphate) Wall Teichoic Acid Synthesis

The genes encoding proteins involved in poly(GroP) WTA synthesis are annotated as *tag* genes (teichoic acid glycerol) (36). *B. subtilis* 168 is the most studied of the poly(GroP) WTA–producing organisms (Figure 1.3). After the action of TagO, TagA, and TagB to complete synthesis of the linkage unit, TagF adds 45–60 GroP units to the TagB product to assemble the polymer (145; 178; 195; 196; 201). The GroP moiety originates from the activated precursor CDP-glycerol, which is synthesized by TagD, a cytidylyltransferase that catalyzes the transfer of L-α-glycerol 3-phosphate to CTP, releasing pyrophosphate (172). Although the Tag enzymes from *B. subtilis* 168 remain the most characterized of the poly(GroP) WTA biosynthetic enzymes, homologs have been identified and loosely characterized in other bacteria known to contain poly(GroP) WTAs, including *Enterococcus faecalis, L. plantarum, Staphylococcus epidermidis,* and several species of *Streptomyces* (60; 65; 85; 158; 164).

In 2010, Strynadka and colleagues published the first and so far only crystal structure of a teichoic acid enzyme involved in polymer synthesis (145). The structure showed that *S. epidermidis* TagF possesses a GT-B glycosyltransferase fold and an extended open active site that appears capable of accommodating the rebinding of CDP-glycerol without product release. Whereas this observation suggests a processive mechanism, kinetic studies found that polymer length depended on the ratio of CDP-glycerol to lipid acceptor, supporting a distributive mechanism (178; 196; 201). The crystal structure of TagF should allow for further mechanistic studies on this class of phosphotransferases. TagB and TagF share 50%

similarity in their catalytic domains, but features governing primase versus polymerase activity await identification.

1.5.4 Poly(Ribitol 5-Phosphate) Wall Teichoic Acid Synthesis

Enzymes making poly(RboP) WTAs are designated Tar for teichoic acid ribitol (36), but it should be noted that TarO, TarA, TarB, and TarD have the same biochemical functions as TagO, TagA, TagB, and TagD, respectively. In *S. aureus,* following formation of the lipid-PP-ManNAc- GlcNAc-GroP product by TarO, TarA, and TarB, poly(RboP) synthesis continues with the TarF- mediated transfer of a (predominantly) single unit of GroP from CDP-glycerol, synthesized by TarD (14; 40; 43; 157; 237). As described above, the synthesis of poly(GroP) WTAs requires a GroP primase (TagB) as well as a GroP polymerase (TagF), and it was proposed that poly(RboP) WTA synthesis in *S. aureus* requires both a RboP primase and a RboP polymerase to make the main chain polymer (136; 185). Recent work has shown, however, that *S. aureus* contains a single enzyme, TarL, that primes the linkage unit and then attaches more than 40 RboP units to complete the polymer (43; 157; 177) (Figure 3). The CDP-ribitol substrate utilized by TarL is made by the combined action of TarI, a cytidylyltransferase, and TarJ, an alcohol dehydrogenase (176; 257). All *S. aureus* strains contain two sets of *tarIJL* genes (the second set is designated *tarI'J'K)* (185). The significance of these duplications is still unclear (157; 177; 185; 211; 247).

Whereas poly(GroP) WTA biosynthesis has been fully characterized in only one organism, *B. subtilis* 168, poly(RboP) WTA biosynthesis has been characterized in both *B. subtilis* W23 and *S. aureus* (40; 43) (Figure 1.3). These two organisms produce very similar poly(RboP) WTAs, which differ only in the number of GroP repeats in the linkage unit (one versus two) and in the sugar tailoring modifications (the addition of Glc versus GlcNAc)

(166; 251). Both organisms appear to contain the same *tar* genes (136; 185), but their WTA biosynthetic pathways differ. Although *S. aureus* uses a single enzyme to prime the linkage unit and build the RboP polymer chain, *B. subtilis* W23 requires an RboP primase, TarK (40; 157). Furthermore, TarK acts directly on the TagB product. Thus, *B. subtilis* W23 does not require the enzymatic activity of TarF even though it contains a *tarF* gene. In *S. aureus tarF* is essential, but genetic analysis has established that *B. subtilis tarF* is neither essential nor transcribed under laboratory culture conditions (40). The WTA polymer in *B. subtilis* W23 is completed by the RboP polymerase TarL, which can attach upward of 40 RboP units (251). Thus, *B. subtilis* W23 TarL is not a bifunctional primase-polymerase like its *S. aureus* homolog but can utilize only WTA lipid-linked substrates that are primed with RboP by TarK (40; 157).

The biochemical and genetic studies of WTA biosynthesis described above have substantially expanded our understanding of how WTA polymers are made, but they also highlight challenges in predicting enzymatic pathways from genome sequences. Other pathways will most likely begin with the same initial steps but may then diverge (Figure 1.3). In principle, the presence of *tagD* and *tarIJ* genes, required to make CDP-glycerol (tagD) and CDP-ribitol (tarIJ) substrates, should facilitate prediction of WTA polymer composition (18; 65; 217). It should be noted, however, that strains containing both types of genes may produce only one type of polymer. For example, some strains of *L. plantarum* that make only poly(GroP) polymers contain both *tarIJKL* and *tagDF* homologs, but the *tarIJ* gene homologs are not transcribed (39; 217). More perplexing is a recent report of an *E. faecalis* strain that makes a WTA poly(RboP) polymer but does not have a *tarJ* homolog (214).

1.5.5 Attachment of Sugars to the Polyol Chain

Data suggests WTA glycosylation occurs inside the cell after polymer synthesis is complete prior to WTA export to the cell surface (4; 42). In the past few years several WTA glycosyltransferases have been identified. In *B. subtilis* 168, TagE modifies WTAs with α-glucose using UDP-glucose as a donor substrate (4; 17). In *B. subtilis* W23, TarQ attaches β-glucose units to poly(RboP) WTAs (42). In *S. aureus,* RboP WTA α-O-GlcNAc modifications are installed by TarM (248), and β-O-GlcNAc modifications are installed by TarS (42). As mentioned above, WTAs extracted from cells appear to be heavily modified with sugars of the same stereochemistry or not modified at all (49; 75; 76; 218), suggesting that the glycosyltransferases are processive enzymes that fully glycosylate WTAs. Processivity may ensure that individual polymers are densely modified and, in organisms that contain more than one glycosyltransferase, may also prevent the attachment of sugars of different stereochemistries to the same polymer. The presence or absence of sugars and the glycosidic linkage conformation affect polymer structure and likely influence interactions with other components in the cell envelope or at the cell interface (24). Strains lacking modifications have altered phenotypes with regard to antibiotic susceptibility and virulence (42; 247). Although progress has been made with regard to the roles of the WTA sugar substituents, numerous questions remain.

1.5.6 Polymer Export

The final steps in the WTA biosynthetic pathway, those following polymer formation and sugar tailoring, are not as clearly defined as are earlier steps. For both poly(GroP) and poly(RboP) WTA polymers, the polymer is translocated through the membrane by a two-

component ABC (ATP-binding cassette) transporter (TagGH and TarGH, respectively) (137). TagH, containing an ATPase domain, provides energy to drive a conformational change in the transmembrane component, TagG, which somehow facilitates translocation across the membrane (137; 189). The WTA transporter exports polymers containing main chains that can be more than ten times longer than the width of the lipid bilayer. In principle, there are two models for how export may occur: one involves a threading mechanism in which the polymer is fed through the transporter from the nonreducing end, eventually pulling the linkage unit across; the other involves a flipping mechanism in which the lipid-PP-GlcNAc-ManNAc linkage unit is somehow flipped across the membrane, with the polymer chain following (Figure 1.4). The former model is conceptually simpler, but experimental studies support the latter model in that they show that the linkage unit, and not the main chain, is recognized by TagGH (39; 199). It is not known whether translocation occurs concomitantly with or following polymerization. Reconstitution of the translocation process in proteoliposomes would provide valuable mechanistic insight and may be possible now that all previous steps have been characterized and enzymes to make the precursors are available.

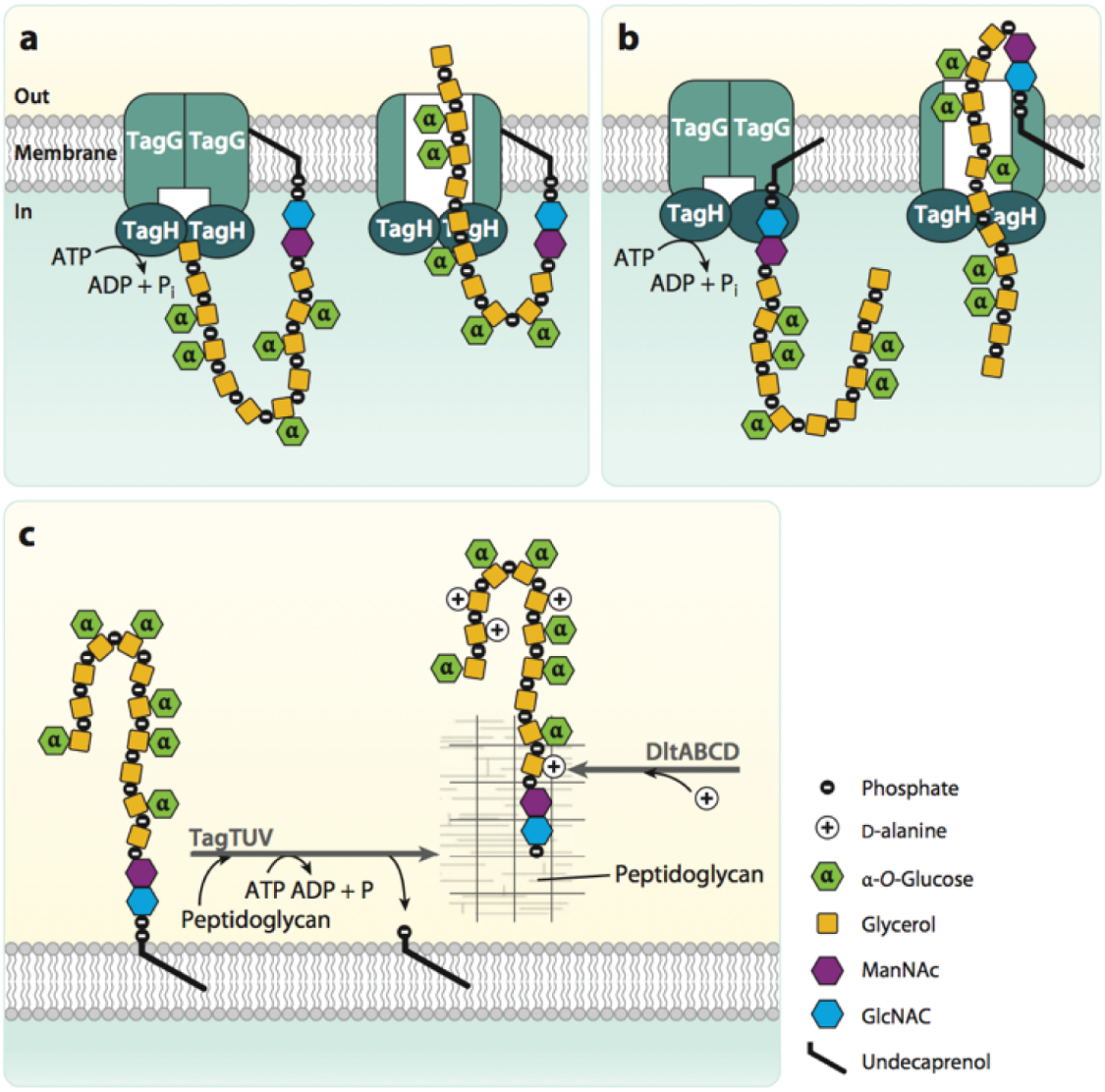

Figure 1.4: WTA polymer flipping and attachment to PG in Bacillus subtilis 168 proceeds through a series of enzymes. In this schematic, the poly(GroP) WTA polymer is transported through the cell membrane by TagGH. Homology suggests that the energy generated by TagH ATP hydrolysis drives a conformational change that allows for polymer transport. TagGH can presumably either (a) thread the polymer through the membrane by the nonreducing end or (b) recognize the disaccharide linkage unit and flip the polymer across. (c) Following transport, the poylmer is covalently attached to PG by TagTUV. It is unknown

whether the TagTUV enzymes work independently or together to ligate WTA to PG. The energy source for this ligation reaction, which we designated here as ATP hydrolysis, is undetermined. It remains unknown whether extracellular D-alanylation by DltABCD occurs before or after WTAs are covalently attached to PG.

1.5.7 Wall Teichoic Acid Attachment to Peptidoglycan

Once the polymer is outside the cell, the final stage of WTA biosynthesis is the formation of a phosphodiester linkage between the WTA polymer and the C6 hydroxyl of the PG MurNAc unit. On the basis of genetic evidence, a set of redundant enzymes, TagTUV, was recently proposed to be responsible for catalyzing this coupling reaction in *B. subtilis* 168 (121), and similar evidence supports a related function for three homologous enzymes in *S. aureus* (66; 112; 169) (Figure 4). TagT has geranyl pyrophosphatase activity (70; 121), which is presumed to be a surrogate for attack of the WTA phosphodiester bond by the C6 MurNAc hydroxyl of PG, but an authentic coupling reaction must be reconstituted to confirm the proposed WTA ligase activity.

The question of when and where WTAs are synthesized and attached to PG is still debated. Decades ago, some studies suggested the WTA polymer is attached to nascent (new) PG, whereas others indicated that it may be attached to mature (old) PG. Still others suggested it can be attached to concurrently synthesized as well as preexisting PG (38; 152; 216; 235; 244). Recently, the timing and location of WTA synthesis has been revisited. In cryo-electron microscopy images, Matias & Beveridge (149-151) identified densely staining material at the septa of *B. subtilis* and *S. aureus* as WTA and proposed that WTAs are attached to new PG during cell division. Consistent with this hypothesis, this densely staining material disappears in a time-dependent fashion when the first step in WTA synthesis is

inhibited (44). Furthermore, studies using fluorescent protein fusions show that WTA biosynthetic proteins localize predominantly to the septum in *B. subtilis* and *S. aureus* (11; 27; 86), suggesting that WTAs are attached to nascent PG during cell division (septum formation). However, other studies suggest that WTAs are attached to older PG (7; 200). Fluorescently labeled concanavalin A, a lectin reported to bind to α-GlcNAcylated WTAs, was used to probe the location of WTAs in *S. aureus*. Fluorescent concanavalin A bound to the half of the cell containing old PG but not to the half containing PG produced during cross wall formation (cell division) (7; 200). Additional studies using alternative detection methods are required to resolve the location of WTA attachment.

1.5.8 D-Alanylation of the Wall Teichoic Acid Repeat Unit

Attachment of D-alanine esters to WTAs is an important mechanism by which bacteria modulate surface charge (53). Unlike glycosylation, which occurs inside the cell, D-alanylation occurs following export of WTAs to the cell surface. Four enzymes, encoded by the *dltABCD* operon, attach D-alanines to both LTAs and WTAs (128; 153; 175) (Figure 1.5). DltA resembles the adenylation domains of nonribosomal peptide synthetases. It is responsible for activating D-alanine as an AMP ester (104) and then transferring the aminoacyl adenylate to DltC. DltC possesses a pantothenate cofactor that forms a thioester with D-alanine through nucleophilic attack of the sulfhydryl on the mixed anhydride (105; 227). What happens after DltC is charged with D-alanine is unclear, but it involves both DltB and DltD (Figure 1.5). DltB, which contains several predicted membrane-spanning helices, is an uncharacterized membrane protein of the membrane-bound *O*-acetyltransferase (MBOAT) family. DltD is a membrane-anchored protein shown to possess a short, cytoplasmic N-

terminus and a large extracellular C-terminal domain (188). DltD was shown to hydrolyze D-alanine from acyl carrier protein, which is normally involved in fatty acid biosynthesis; on this basis DltD was suggested to have an editing function and to remove D-alanine from mischarged acyl carrier protein (61). It was also shown to modestly accelerate the rate of transfer of D-alanine to DltC, suggesting an accessory role in the transfer reaction (61). These proposals for DltD require it to function in the cytoplasm, which is inconsistent with its topology (188). At this point, the specific function of DltD is unclear, though recent evidence shows its direct interaction with YpfP, LtaA, and LtaS of the LTA biosynthetic pathway (187).

Early experiments proposed on the basis of pulse-chase radiolabeling that D-alanines are transferred to LTAs by DltC and then to WTAs in an isoenthalpic transesterification reaction (101). Two lines of evidence support such a mechanism: D-alanyl esters can be transferred between LTAs of differing lengths in nonnative micelles without an enzyme catalyst, though the reaction is slow (48), and an LTA-deficient *S. aureus* mutant was found to have highly reduced D-alanylation of its WTAs (188). Alternatively, D-alanyl esters could be transferred back from LTAs to DltC and then to WTAs (123). Because this transfer reaction requires bacterial membranes, other factors may also play a role in the process. DltB is also required for D-alanylation, and it has been suggested to facilitate membrane translocation of D-alanine-charged DltC so that it can serve as the direct donor to LTA (166). DltC has not been identified in any proteomic analyses of secreted proteins, and the evidence that it serves as the direct D-alanylation donor is limited (68; 123; 166). Recent experiments confirmed that DltC is exclusively cytoplasmic (188). An alternate hypothesis was proposed by Heaton & Neuhaus, where undecaprenyl phosphate could serve as a substrate for D-

alanylation and subsequent flipping by DltB (83; 105). They cited homology between this protein and undecaprenol phosphate transferases, as well as sensitivity of the reaction to tunicamycin and amphomycin. Other D-alanylated phospholipids have been identified that could theoretically serve as donors, including D-alanylcardiolipin and D-alanylphosphatidylglycerol, however, these lipids have not been detected innately in *S. aureus* (203). This proposal is more consistent with predicted enzymatic functionality for DltB as an MBOAT family protein. Furthermore, it was recently shown that Gram-negative organisms attach positively-charged amino acids to LPS through proteins analogous/homologous to the Dlt pathway, including one with an annotated lysophospholipid acyltransferase (LPLAT) domain (103). Although it is clear that D-alanylation of LTAs and WTAs requires the same biosynthetic machinery, many questions remain regarding the enzymology of the process.

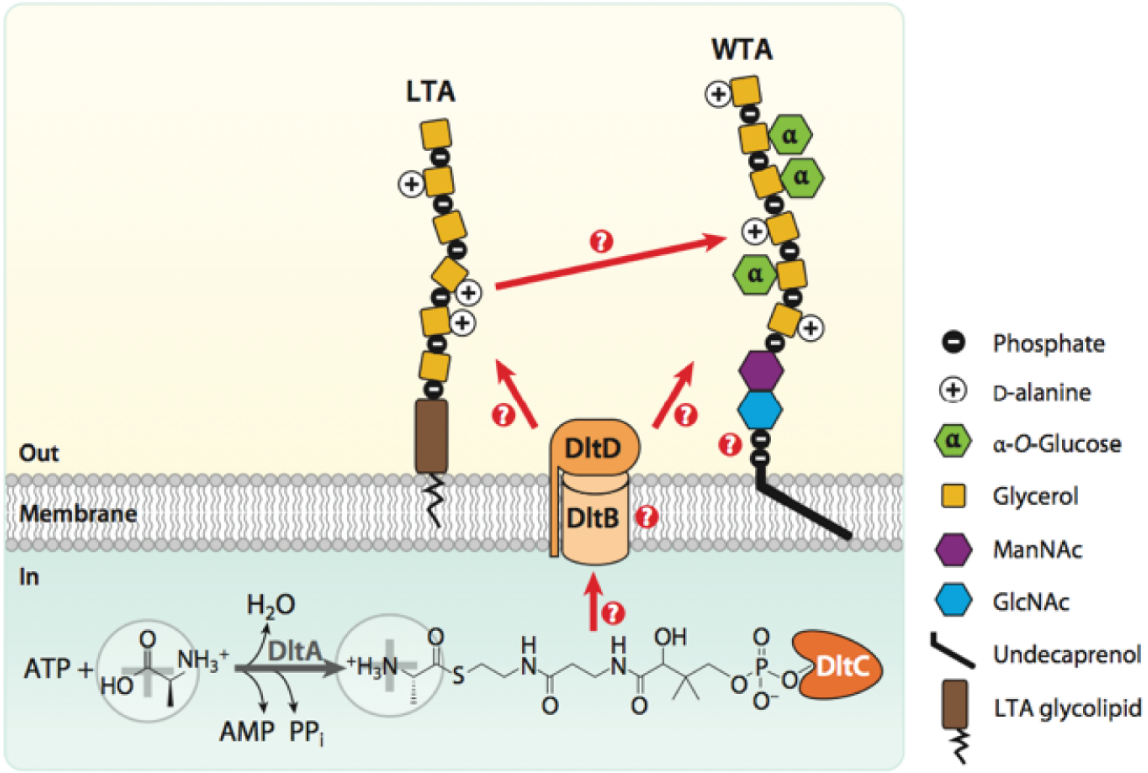

Figure 1.5: D-alanylation of teichoic acids. The DltABCD machinery is responsible for the activation and attachment of D-alanines to extracellular teichoic acids. Many questions remain regarding the roles of DltB and DltD, the nature of their substrates, and whether D-alanine transesterification is enzymatically catalyzed.

1.6 Nonessential and Conditionally Essential Wall Teichoic Acid Genes

Deletion of *tagO* or *tagA,* the first two genes in the WTA biosynthetic pathway, produces bacteria lacking WTA polymers. These bacteria display a range of defects, but are viable in traditional laboratory conditions. With the exception of the tailoring enzymes, however, most of the downstream WTA genes are essential, and their deletion results in a lethal phenotype unless flux into the WTA pathway is blocked at an early stage (58; 59). The lethality of a late-stage block may be due to accumulation of toxic intermediates in the cell or to depletion of cellular pools of undecaprenyl phosphate, which is also required for the synthesis of PG (57-59; 211; 247). Conditionally essential genes are found in pathways for other cell wall polysaccharides that are synthesized on the undecaprenyl phosphate carrier lipid. For example, deletion of late-stage genes involved in synthesis of the capsular polysaccharide of *Streptococcus pneumonia* generates bacteria with suppressor mutations in the initiating enzyme that turns off capsule production (116; 245).

1.7 Roles of Wall Teichoic Acids

WTA polymers play numerous, varied roles in the cell wall owing to their location, abundance, and polyanionic nature (Figure 1.6). The molecular mechanisms underlying their many critical functions are not well understood. Genetic and small-molecule tools are enabling more detailed studies to elucidate these mechanisms.

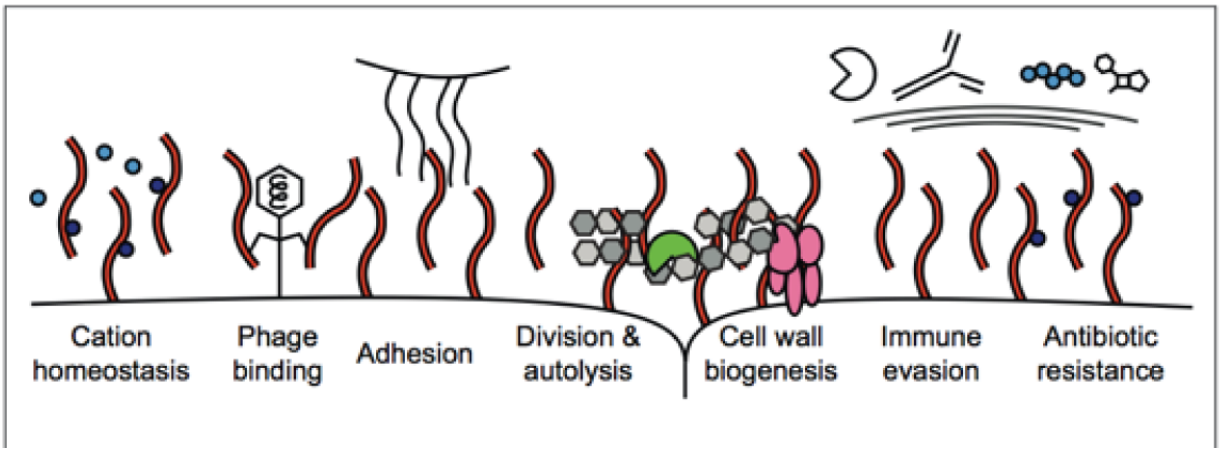

Figure 1.6: Teichoic acids are responsible for a wide variety of functions involved in cell division, charge homeostasis, and infection.

1.7.1 Regulation of Cell Morphology and Division

Bacteria lacking WTAs grow slower than wild-type bacteria, and they clump in solution. These strains exhibit numerous morphological abnormalities, including a nonuniform thickening of the PG cell wall, increased cell size, and defects in septal positioning and number (7; 44; 52; 58; 171; 200). Furthermore, rod-shaped bacteria such as *B. subtilis* and *Listeria monocytogenes* lose their shape, becoming spherical (25; 36; 72; 77; 204; 205). These phenotypes imply that WTAs are necessary for proper localization, assembly, and/or activation of cell wall elongation and division machinery. Consistent with this idea, many WTA and PG biosynthetic enzymes have been shown to colocalize and physically interact in *B. subtilis* (86; 121).

Evidence for functional interactions between WTAs and PG machinery comes from *S. aureus,* in which the putative PG cross-linking enzymes PBP4 and FmtA lose septal localization in the absence of WTAs (11; 184). This mislocalization correlates with decreased PG cross-linking found in Δ*tarO* mutants (200). In addition, Campbell *et al*.

showed that TarO inhibitors potentiate β-lactams in MRSA strains, indicating a functional connection between the PG and WTA biosynthetic pathways (44). Farha *et al*. used a panel of β-lactams to argue that this synthetic lethality was specifically due to combined disruption of the PG cross-linking enzymes PBP2 (via β-lactams) and PBP4 (via WTA biosynthesis inhibition) (80). Although many details remain to be clarified, there is considerable evidence that WTAs regulate the function of PG biosynthetic machinery, and the recruitment of cell wall assembly proteins is one mechanism through which they do so.

1.7.2 Regulation of Autolytic Activity

The failure of mutants to effectively septate and separate during cell division implicates WTAs in coordinating the localization, stability, and/or activity of PG lytic proteins. Strains lacking WTAs have altered endogenous autolysin expression profiles and increased autolysis rates (31; 146; 200; 236). *In vitro* studies performed with purified LTAs, enzymes, and cell wall substrates explain these observations using a recruitment model, in which polyanionic phosphate backbones bind and sequester positively charged autolysins (29; 84; 166). Positively charged D-alanyl esters help mask this charge and free autolysins to degrade PG. This model requires WTAs to be either absent from the septum or present in a highly D-alanylated state, as autolytic activity must be regulated to ensure separation specifically at the cross wall during cell division (249). Recent studies support an exclusion model (89; 200). Finally, others have proposed that WTAs could indirectly modulate enzyme activity through ion chelation (13; 31; 107). Whether directly or indirectly, or by recruitment or exclusion, WTAs clearly play a role in the localization of autolytic enzymes (89; 184; 200).

1.7.3 Regulation of Ion Homeostasis

It is thought that WTAs can bind extracellular metal cations by extending beyond the PG layer (122; 242). WTAs have a high affinity for metals, and their biosynthesis is upregulated under metal limitation (13; 75). WTAs also bind protons, and cells lacking WTAs have a 23% decrease in their proton binding capacity (31). Although WTAs do not influence the pH gradient across the cell wall, it has been suggested that they can create localized changes in pH, indirectly modulating the function of some enzymes (*e.g.*, autolysins) (31). WTA ion binding is also thought to minimize repulsion between nearby phosphate groups, which can affect polymer structure and therefore cell wall integrity (122; 242). D-Alanylation masks negatively charged sites on the polymer, reducing WTAs' binding capacity for cations (107). Some have also speculated that ion binding to WTAs could help prevent fluctuations in osmotic pressure between the inside and the outside of the cell (7; 107; 211).

1.7.4 Protection from Host Defenses and Antibiotics

WTAs and their attached substituents contribute to bacterial cell surface charge and hydrophobicity, which in turn affect binding of extracellular molecules. By affecting cell surface characteristics, WTAs therefore play a role in protecting bacteria from various threats and adverse conditions. In the absence of WTAs, bacteria are sensitive to high temperatures and unable to grow in high-salt media, indicating that WTAs are involved in temperature tolerance and osmotic stress (11; 109; 205; 225). WTA-deficient cells are more susceptible to human antibacterial fatty acids, presumably because hydrophobic antibacterial fatty acids penetrate the less hydrophilic mutant cell wall more easily and bind more efficiently to the

cell membrane, where they can cause damage (126).

Preventing D-alanylation through gene deletion removes D-alanine esters from both LTAs and WTAs; consequently, researchers have not yet been able to identify roles specific to each polymer. Nevertheless, it has been established that teichoic acid D-alanylation protects against host-defense mechanisms (130; 131). *S. aureus* lacking D-alanine has an increased susceptibility to phagocytes, to neutrophil killing (53), and to lysostaphin and lysozyme (180). A reduction in the D-alanyl content of the cell wall results in increased susceptibility to glycopeptide antibiotics and to certain cationic antimicrobial peptides (CAMPs) (53; 179; 180; 220; 231). It was reasoned that the absence of D-alanyl esters increases the overall negative cell surface charge (220), attracting cationic molecules and thus increasing susceptibility to CAMPs. Accordingly, *B. subtilis* and *S. aureus* lacking teichoic acid D-alanine modifications bind more positively charged cytochrome *c* than their wild-type counterparts do (179; 236). In group B *streptococci*, however, D-alanylation shows little influence on the surface association of fluorescently labeled CAMPs (192). These data suggest that charge effects are not solely responsible for the observed changes in CAMP susceptibility. Saar-Dover *et al*. suggested that the increased cell wall density observed in strains with D-alanylation prevents penetration of CAMPs, thereby conferring protection (192). The effect of TA D-alanylation on susceptibility toward other drugs appears variable. In both *B. subtilis* and *S. aureus*, deletion of *dltA* rendered the bacteria more sensitive to methicillin and a subset of other β-lactams, but more resistant to others (42; 236). However, a *S. aureus* transposon mutant in *dltB* possessed increased resistance to methicillin (162). Studies in *B. subtilis* have revealed that TA D-alanylation plays a role in the stability and folding of cell envelope proteins as well as signaling by cell envelope stress two-component

sensors, which may be one mechanism by which D-alanines have varying effects on antibiotic susceptibility (113; 114).

Blocking WTA synthesis renders *B. subtilis* and MRSA sensitive to β-lactam antibiotics (42; 44; 81; 146; 179; 210; 236). Recent studies have replicated this sensitivity through the specific removal of WTA β-GlcNAc modifications (42). It has been speculated that the WTA β-GlcNAc moieties scaffold proteins involved in resistance. Accordingly, recent work has shown that *S. aureus* WTAs specifically interact with PBP2A (184), the resistant transpeptidase found in MRSA. Because WTA glycosyl substituents are also receptors for phage (17; 246), there is a precedent for WTA sugar residues mediating protein binding. It is possible that glycosylated WTAs function as ligands for cell surface proteins with carbohydrate recognition sites.

1.7.5 Effects on Adhesion and Colonization

The presence of WTAs and their D-alanyl esters influences bacterial interactions with various surfaces (166). WTA-deficient cells have a reduced capability to form biofilms (98; 109; 225; 231). Removal of D-alanine esters also decreases biofilm formation and bacterial adhesion to plastic and glass surfaces. Decreased adherence is potentially linked to the resultant increase in negative cell surface charge creating increased repulsive forces between bacteria and a stratum (98; 109).

In 1980, Aly *et al*. showed a 71% reduction of *S. aureus* binding to nasal epithelial cells that were preincubated with teichoic acid (5). Since that time, several animal studies have established that bacteria lacking teichoic acid D-alanine esters or WTAs are attenuated in host colonization and infection (53; 81; 131; 209; 210; 231; 233; 237; 238; 241).

Lactobacilli lacking teichoic acid D-alanylation colonize mice gastrointestinal tracts at 1% of wild-type levels (231). Similarly, WTA-free *S. aureus* cells colonize rat nares at levels 90% lower than those of wild-type *S. aureus,* and in rabbits these mutant cells were unable to proliferate to adjacent organs (237; 241). Teichoic acid D-alanine esters are considered virulence factors, because their deletion attenuates pathogenicity but does not cause major cellular defects under laboratory growth conditions (7; 25; 44; 46; 52). WTAs have also been categorized as virulence factors, although they exhibit such profound defects *in vitro* that they may be better described as "*in vivo* essential" (50; 240). The decreased ability of WTA null mutants to survive in challenging host environments is due to the combined effects of an inability to adhere to host tissue, an increased susceptibility to host defenses, and cell division defects (131; 166; 231; 239).

1.8 The Wall Teichoic Acid Pathway as an Antibiotic Target

The vital roles of WTAs in physiology and pathogenesis promote this pathway as a target for antibacterial drugs and vaccines (211; 239). The WTA pathway contains three distinct target categories: antivirulence targets, β-lactam potentiator targets, and essential targets (Figure 1.7).

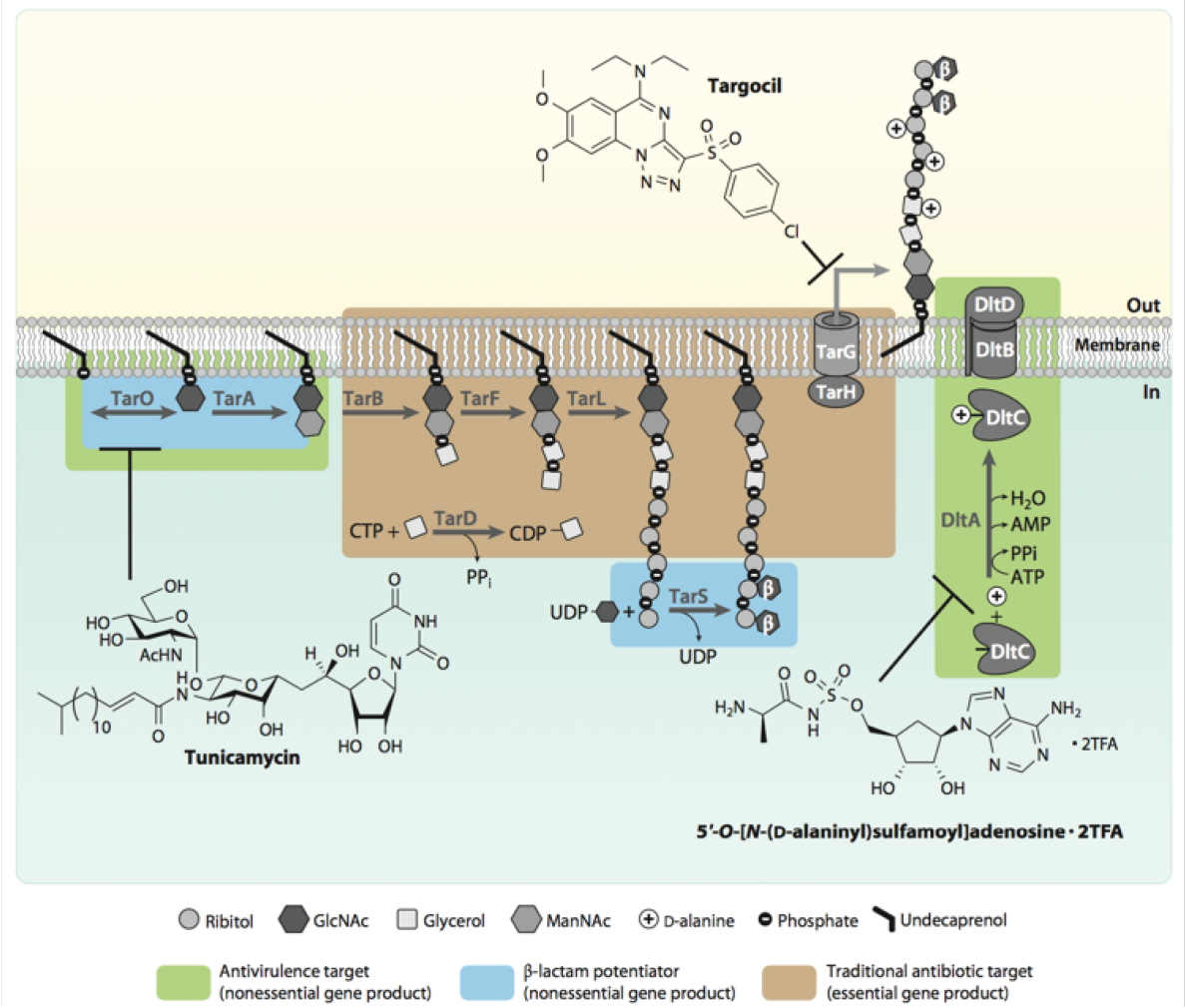

Figure 1.7: WTA biosynthetic enzymes are potential antibiotic targets. The schematic shows the three types of antibacterial targets present in the Staphylococcus aureus WTA pathway. Enzymes that are traditional antibiotic targets (tan), β-lactam potentiators (blue), or antivirulence antimicrobial targets (green) are boxed. The three chemical structures illustrated are small molecules known to inhibit WTA enzymes TarO, TarG, and DltA.

1.8.1 Antivirulence Targets

Proponents of virulence factors as antibacterial targets argue that resistance to virulence factor inhibitors is less likely to emerge, because there is no selection pressure for

survival (50). Although some argue that these inhibitors are unable to cure established infections and may create unforeseen *in vivo* host selection pressures, it is nonetheless worth investigating virulence factor targets, particularly for resistant pathogens. Enzymes of the *dlt* operon are targets for antivirulence agents because strains lacking teichoic acid D-alanine esters are strongly attenuated in animal infection models but show minimal growth defects under laboratory growth conditions (239). A DltA inhibitor was reported in 2005 but was not further optimized and is likely not specific (153). The enzymes involved in initiating WTA polymer synthesis, TarO and TarA, have also been described as virulence factor targets, but as noted above, these deletion strains are more than attenuated in animal hosts: they are nonviable (237). Hence, inhibitors of these initiating enzymes may behave more like traditional antibiotics *in vivo*, although this remains to be established.

The natural product tunicamycin inhibits TarO at very low concentrations (44; 102; 181), but at higher concentrations it also blocks MraY, an essential UDP-MurNAc-pentapeptide transferase involved in PG biosynthesis (183). Tunicamycin has been used to probe the effects of inhibiting WTA biosynthesis in bacteria; unfortunately, however, it cannot be used in animals because it inhibits GPT, an essential phosphotransferase involved in eukaryotic N-linked glycan biosynthesis (183). Hence, there is still a need for specific nontoxic inhibitors that target TarO, TarA, and Dlt enzymes for use in infection models.

1.8.2 β-Lactam Potentiator Targets

β-Lactams are one of the safest and most widely used classes of antibiotics (91), and there is considerable interest in compounds that restore β-lactam sensitivity to resistant microorganisms. B-Lactamase inhibitors, for example, have been highly successful as

components of compound combinations to treat many β-lactam resistant infections (91). B-Lactam resistance in MRSA is not mediated by β-lactamases but by the resistant transpeptidase PBP2A (254). Because the activity of this transpeptidase depends on the function of various host factors, compound combinations are possible as therapeutic modalities (254). TarO, TarA, and TarS are β-lactam potentiator targets. Unlike Δ*tarO* and Δ*tarA* strains, Δ*tarS* mutants divide normally and do not show appreciable growth defects (42). Furthermore, they are not strongly attenuated in virulence. Hence, TarS inhibitors should act exclusively as potentiators, whereas inhibitors of TarO and TarA would serve as both β-lactam potentiators and antivirulence agents. A cell-based high-throughput β-lactam potentiation screen recently identified the clinically used antiplatelet drug ticlopidine as a TarO inhibitor, although target selectivity was not demonstrated (81). It should also be possible to identify TarS inhibitors from β-lactam potentiation screens, as they can be readily discriminated from TarO or TarA inhibitors on the basis of their cellular effects (42).

1.8.3 Traditional Antibiotic Targets

Inhibitors of the essential late-stage WTA biosynthetic enzymes TarB through TarH should have lethal effects on bacterial cells and thus would be akin to traditional antibiotics. Late-stage WTA pathway inhibitors (e.g., targocil) were discovered by screening a Δ*tarO* mutant and a wild-type strain against the same library to identify compounds that selectively killed the wild-type strain. All identified compounds inhibited TarG (138; 212; 233). The identification of several different inhibitors of TarG indicates that this may be a druggable target. This may indicate that WTA precursor export is the rate-limiting step in the pathway, and TarG may also be more accessible to inhibitors than are most other WTA targets because

it spans the membrane. All identified TarG inhibitors suffer from a relatively high frequency of resistance (45; 233). Consequently, in an MRSA infection model, the TarG inhibitors were effective only in combination with β-lactams (233). It would be desirable to identify compounds with a lower frequency of resistance to validate late-stage enzymes as targets independent of β-lactams.

1.9 Conclusion

WTAs compose a huge percentage of the gram-positive cell wall and are thus extremely important for cell wall integrity. They are important for pathogenesis and play fundamental roles in bacterial physiology. Furthermore, their tailoring modifications modulate their structures and interactions with other molecules and cells in complex ways. The variety of enzyme classes involved in WTA biosynthesis (glycosyltransferases, polymerases, ABC transporters) and the diverse functions of WTAs make the ongoing study of this pathway challenging. Small-molecule inhibitors of WTA enzymes can be used to probe enzyme mechanism and WTA function in cells and to explore the potential of the different antibacterial target types.

Chapter 2: Construction and Analysis of a *S. aureus mariner* Transposon Library

Portions of this chapter are featured in "Genes contributing to *Staphylococcus aureus* success in infection-related ecologies" by Valentino, M.D., *et. al.* (2014) *Submitted.*

2.1 Abstract

Transposon libraries can facilitate large-scale reverse genetic experiments in many organisms. When combined with high-throughput sequencing, these libraries can provide genome-wide phenotypic assessment at high resolution. In order to facilitate these studies in *S. aureus*, we needed to construct a high coverage transposon library. Here I describe the creation and initial characterization of this library, performed in collaboration with Dr. Ama Sadaka of the Gilmore lab. I also describe several statistical methods for the assessment of conditional gene essentiality.

2.2 Introduction

Transposable elements (TEs) are DNA fragments that can move their chromosomal positions, either within or between genomes. They have been identified in all domains of life, in some cases comprising large fractions of an organism's genetic material. Tes fall into two broad classes – retrotransposons (class I) function via an RNA intermediate, which is reverse-transcribed and inserted using enzymes encoded within the element. Class II transposons are DNA-based and are mobilized via a transposase. The required transposase is often encoded within the transposon, and surrounded by two terminal inverted repeats (TIRs), though some transposons are mobilized via enzymes supplied in *trans* or coopted from other transposons in the genome. TE insertion requires the activity of host DNA repair enzymes to fill in sequence gaps, generating unique target site duplications. Transposons can be further classified into superfamilies based on their sequence, TIRs, and target site duplications.

2.2.1 Superfamily Tc1/*mariner*

Tc1 and *mariner* superfamily members are the most widespread transposons and include some that have retained functionality. They are generally 1-5kb in length and are possess a transposase of 282-345 amino acids, with TIRs that are <100bp long (160). While the transposases of this superfamily diverge significantly in sequence similarity, they are all similarly organized into an N-terminal DNA/TIR binding domain, an intervening nuclear localization signal that promotes transposase entry into cell nuclei, and a C-terminal catalytic domain responsible for DNA cleaving and joining reactions. This catalytic domain possesses a characteristic DDD (or in the case of *mariner*, DDE) motif that was found to be functionally non-interchangeable with opposite superfamily members (143).

Members of the Tc1/*mariner* superfamily replicate through a cut-and-paste mechanism. First, monomers of the transposase bind each of the two TIRs flanking the transposon in single-end complexes. The transposase monomers then catalyze hydrolysis of the phosphodiester backbone at the 5' termini flanking the transposon TIRs. Through a transposase dimerization, the two single-end complexes are brought together to form a paired-end complex, after which excision takes place via cleavage of the phosphodiester backbone at the 3' ends. This leaves a double-stranded DNA break (DSB). The excised transposon, complexed with the transposase dimer, then mobilizes to a target location in the host genome – Tc1 and *mariner* transposons preferentially target TA dinucleotides. After insertion, transposon 5' gaps are filled in, generating transposon-specific target site duplications, while the DSB at the transposons origin is filled in using host DNA repair enzymes, often generating a transposon footprint.

2.2.2 Effects of Transposon Mobilization

Because of their dynamic nature, TEs can contribute to genetic organization, regulation, stability, and evolution (154; 186). The effects of their mobilization are most often mediated near their insertion location. Transposons can directly alter the expression of a gene by inserting within its exon/open reading frame, or they can indirectly alter expression by inserting in regulatory elements, such as promoters or terminators. TEs can also cause polar effects by inserting within polycistronic operons (124). These effects can be exacerbated in transposons containing transcriptional terminators or outward facing promoters (232). Nevertheless, transposons may also carry adjacent chromosomal regions during the processes of excision and insertion, promoting recombination events with distal regions of chromosomes. Through all of these mechanisms, transposons can alter the fitness of their host, in turn impacting their own probability of carriage.

A variety of host and TE regulatory mechanisms have evolved in order to mitigate the potentially deleterious effects of transposition. In order to maintain function, the ratio of TEs to their transposases must be carefully balanced and each must encode active versions – deviations in this ratio or mutations can lead to inhibition, potentially through the formation of inactive complexes or by diluting active subunits (133; 144). Some transposons, such as those encoding drug resistance factors, include regulatory elements that respond specifically to environmental cues to induce transposition (124). In eukaryotic hosts, epigenetic mechanisms, such as DNA methylation, or RNAi can suppress transposon activity (110; 224). Furthermore, systems that detect and degrade foreign DNA, such as CRISPR and restriction-modification, can prevent TE horizontal transfer (28; 56; 148; 229).

2.2.3 Use of Transposon Mutagenesis to Determine Gene Essentiality in *S. aureus*

Given enough insertional coverage, the fitness cost of transposition into a locus can be used to assess gene essentiality across the genome. Saturating transposon mutagenesis has been used to assess the essentiality of genes in a variety of organisms, as a way to better understand physiology and identify strong candidates for interventional therapeutics. Transposon libraries can supersede the predictive power of comparative genomics in assessing the core genome, particularly for organisms with distant homology and encoded functional redundancies. Furthermore, transposon libraries can be grown in a variety of conditions, enabling rapid assessment of conditionally essential genes.

Bae *et a*l. previously used the *bursa aurealis mariner*-based transposon system to generate a library in strain Newman consisting of approximately 8,400 mutants with defined unique insertion sites, which was screened for loss-of function mutants in a *C. elegans* infection model (15). Seventy-one genes responsible for virulence were identified, representing the first genome-wide query of genes critical for fitness *in vivo* (*i.e.* the *C. elegans* gut). While providing proof of principle, the library was reported to have disruptions in only 67% of all ORFs. More recently, Chaudhuri and colleagues utilized a modified *E. coli* Tn5-based transposon, coupled with microarray mapping and PCR-based verification, to identify genes that were intolerant of transposon insertion (47). A total of 351 genes were identified as incapable of being disrupted by transposon insertion and still yielding cells capable of growth in laboratory medium. Unfortunately, few Tn5 insertions were directly sequenced, so the actual level of genome saturation used in these experiments is unclear.

2.2.4 Statistical Methods for Determining Gene Essentiality in Transposon Libraries

In principle, the absence of mapped transposons in a genomic locus corresponds to the inviability of insertional mutants. In reality, this could be attributed to several factors, including insertion bias, PCR jackpotting, and insufficient sensitivity of detection. Several studies have also noted that known essential genes can harbor insertions, but that these have a higher probability of appearing in the immediate 5' and 3' regions of an ORF, where they may preserve functional translation (2; 96). Early experimenters often excluded these extreme insertions from subsequent analyses, however more modern analytical methods can accommodate them by grouping them with insertions from adjacent regions.

Several statistical methods have been developed to determine gene essentiality from transposon insertion data in organisms with annotated genomes. Blades and Bowman used a Bayesian method called Gibbs sampling (a Markov Chain Monte Carlo algorithm) and Jacobs, *et al*. used parametric bootstrapping to estimate the total number of essential genes, assuming that transposon insertions followed a multinomial distribution (32; 115). A rigorous analysis of these approaches demonstrated that these methods required libraries with a large number of clones or accurate probabilistic models *a priori* for transposon insertions (243). Another approach utilizes likelihood ratio tests (*e.g*. D-values and ESSENTIALS (221; 258)). Others have modeled TA insertions as a Bernoulli process, where stretches of consecutive TA sites lacking insertions corroborate essentiality (96). This method had the advantage of finely tuning essentiality scores to provide insight on essential regions within an ORF, such as independently expressed protein domains. However, this model depended on *a priori* estimation of insertion frequency for non-essential genes, and was subsequently improved via more rigorous statistical methods, including Bayesian analysis with mixing and Hidden Markov modeling (62; 63).

2.2.5 Selection of a Transposon Delivery System for *S. aureus*

Screening or selection of mutagenized cell pools can facilitate the identification of genotypes pertaining to a phenotype or physiological process. Classical mutagenesis, often performed using chemical mutagens or radiation, must be carefully dosed to ensure single mutations in each cell. Alterations of the chromosome can then be identified through whole-genome sequencing or complex mapping. In contrast, transposons traditionally enable finer dosage control and disruption stability, and through their known sequence, afford rapid identification of insertion loci via PCR. Furthermore, when combined with advances in DNA sequencing technologies, transposons enable massively parallel assays for mutant pools (223). These mutant pools can be prepared *de novo*, or characterized and arrayed into archived libraries for distribution.

Several aspects of transposon and host were taken into consideration in selecting an appropriate transposon system for our genetic studies. We chose *S. aureus* HG003 as a methicillin-sensitive strain for the library, as this strain shares lineage with many other common laboratory strains (NCTC8325), is repaired in the *tcaR* and *rsbU* loci, and does not require the BL2+ safety precautions of methicillin-resistant brethren (108). Unlike RN4220, HG003 has been preserved from phage curing via successive rounds of UV-irradiation and chemical mutagenesis and has no defects in its restriction-modification system (161). While these characteristics help reduce artifacts introduced by laboratory handling, the presence of resident phage can lead to host heterogeneity due to spontaneous activation, and restriction requires passage of DNA first through a strain that installs modifications. This precluded the use of transposons assembled *in vitro*, such as EZ-Tn5 and Mu (170).

Historically, transposons such as *Tn917* and *Tn551*, have proved useful in elucidating important aspects of *Staphylococcal* biology, but suffer from strong biases in insertion locations (15; 22). At the onset of our genetic studies, the *Himar1*-based system, *bursa aurealis*, appeared as the best candidate, due to its high efficiency of transposition and *in vivo* transposition approach (Figure 2.1) (15; 16; 47). The modified horn fly transposon contains an *ermC* erythromycin resistance gene, an R6K origin of replication, and a green fluorescence protein. This transposon is supplied on plasmid pBursa, which possesses the chloramphenicol selection marker *cat* and a *S. aureus* temperature-sensitive origin of replication. The transposase is supplied *in trans* under the xylose-inducible promoter *xylA* on plasmid pFA545, which contains the tetracycline resistance genes *tetBD*, the xylose repressor, *xylR*, and a temperature-sensitive origin of replication compatible with pBursa. Through mechanisms that remain elusive, temperature shift promotes transposon mobilization and plasmid curing, enabling selection of stable insertion mutants. This system was used to develop the Nebraska Transposon Mutant Library, a repository of 1,952 transposon mutants in the community-acquired methicillin-resistant strain USA300 (82), and recent work by Bose, *et al*. has generated tools to exchange transposon mutants with alternative selection markers or fluorescent probes through allelic replacement (35). A phage-based system has subsequently been developed that delivers pre-assembled *Tn551* transposon cassettes at high efficiency without high temperature treatment or resident transposase-expressing plasmids (232). This system is being improved further through continuing efforts in the Walker and Bernhardt laboratories.

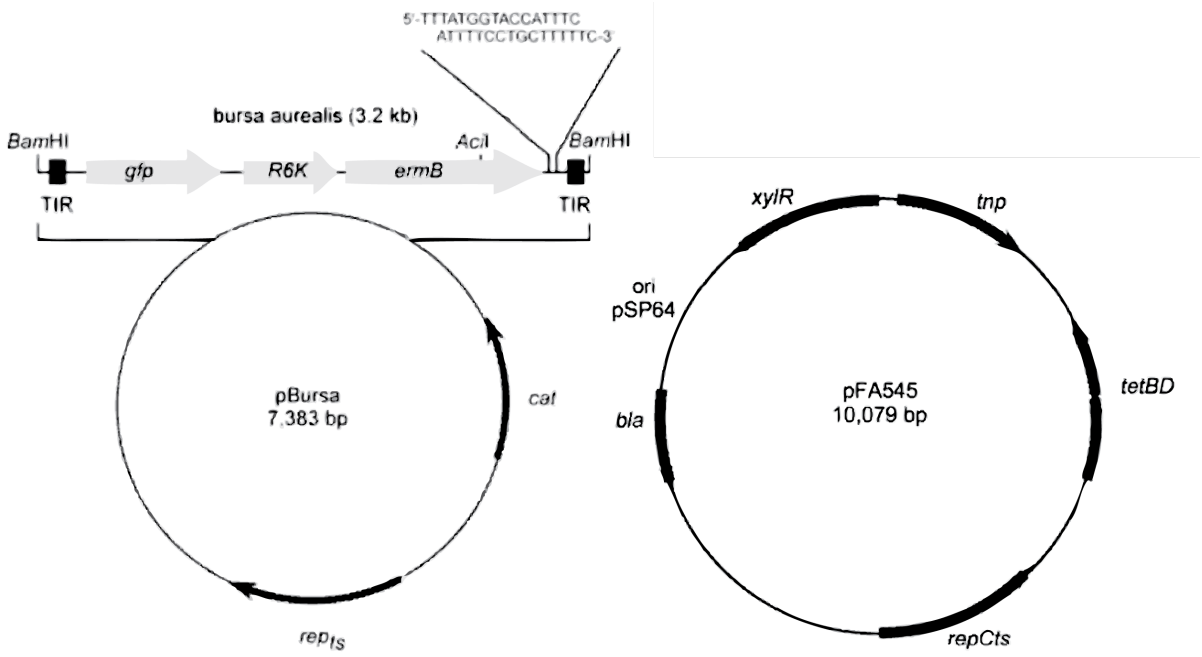

Figure 2.1 Plasmids used for construction of a *bursa aurealis* transposon library. pBursa contains a modified *Himar1* transposon, while pFA545 encodes the transposase in *trans*. Figure adapted directly from Bae & colleagues (16).

2.3 Methods

2.3.1 Bacterial Strains, Reagents, and General Methods

Plasmids were introduced into restriction-negative *S. aureus* strain RN4220 by electroporation (142). To prepare electrocompetent cells, overnight cultures of *S. aureus* were diluted approximately 1:200 into media with tunicamycin and harvested in mid-exponential phase. Cells were washed four times in 20mL of sterile 20% glycerol (v/v), before resuspension in approximately 600uL of sterile 20% glycerol and storage at -80°C. Plasmids were purified from *S. aureus* RN4220 by first washing cells with a 1:1 mixture of cold acetone:ethanol, then pretreating cells with lysostaphin (50 µg/ml, 10 min, 37°C) prior to isolation using a standard plasmid miniprep protocol (Qiagen). Plasmids were then introduced into restriction-positive wild-type strains by electroporation. *S. aureus* was grown

primarily in tryptic soy broth (TSB) medium at 30°C. Antibiotic markers were selected with erythromycin (Em) (10 μg/ml), tetracycline (Tet) (2.5 μg/mL), carbenicillin (Carb) (100μg/mL), and chloramphenicol (Cm) (5 μg/mL). Tunicamycin (Tm) purchased from Sigma Aldritch was dissolved in DMSO to a final concentration of 0.4μg/mL. Novagen KOD Hot Start Polymerase was used for inverse PCRs, restriction enzymes and T4 DNA ligase from New England Biolabs, terminal deoxynucleotidyl transferase (TdT) was purchased from Promega, and PCRs for Illumina sequencing were prepared using Easy A high-fidelity cloning enzyme from Agilent. Strains and oligonucleotides used for this work are listed in Table 2.1.

Table 2.1: Bacterial strains, plasmids, and oligonucleotides used in this work.

Strains	Relevant Genotype	Reference
RN4220	RN450 partial *agr* defect ST8; CC8; codon in both *hsdR* and *sauUSI*	(161)
HG003	*rsbU* and *tcaR* repaired NCTC 8325	2010 Herbert
JSM060	HG003 pBursa pFA545 Tet^R Cm^R Erm^R	
Plasmids	**Description**	**Reference**
pBursa	Mariner transposon plasmid, *bursa aurealis*, Em^R, Cm^R, rep^{TS}	(15)
pFA545	Transposase plasmid, Tet^R, rep^{TS}	(15)
Oligonucleotide	**Sequence**	
Martn-F	5′-TTTATGGTACCATTCATTTTCCTGCTTTTTC-3’	
Martn-ermR	5′-AAACTGATTTTTAGTAAACAGTTGACGATATTC-3’	
olj510	5’-CCAAAATCCGTTCCTTTTTCATAGTTCCTATATAGTTATACGC-3’	
olj376	5’-GTGACTGGAGTTCAGACGTGTGCTCTTCCGATCTGGGGGGGGGGGGGGGG-3’	
olj511	5’-	

	AATGATACGGCGACCACCGAGATCTACACTCTTTGACCGGGGACTTATCAGCCAACCTGTTA-3’
olj512	5’-ACACTCTTTGACCGGGGACTTATCAGCCAACCTGTTA-3’
BC1	5’-CAGCAGAAGACGGCATACGAGATAAAAAAGTGACTGGAGTTCAGACGTGTGCTCTTCCGATCT-3’
BC2	5’-CAGCAGAAGACGGCATACGAGATACACACGTGACTGGAGTTCAGACGTGTGCTCTTCCGATCT-3’
BC3	5’-CAGCAGAAGACGGCATACGAGATAGAGAGGTGACTGGAGTTCAGACGTGTGCTCTTCCGATCT-3’
BC4	5’-CAGCAGAAGACGGCATACGAGATATATATGTGACTGGAGTTCAGACGTGTGCTCTTCCGATCT-3’
BC5	5’-CAGCAGAAGACGGCATACGAGATCACACAGTGACTGGAGTTCAGACGTGTGCTCTTCCGATCT-3’
BC6	5’-CAGCAGAAGACGGCATACGAGATCCCCCCGTGACTGGAGTTCAGACGTGTGCTCTTCCGATCT-3’
BC7	5’-CAGCAGAAGACGGCATACGAGATCGCGCGGTGACTGGAGTTCAGACGTGTGCTCTTCCGATCT-3’
BC8	5’-CAGCAGAAGACGGCATACGAGATCTCTCTGTGACTGGAGTTCAGACGTGTGCTCTTCCGATCT-3’

2.3.2 Construction of the *bursa aurealis* Transposon Library

S. aureus HG003 was electroporated sequentially with pFA545 and pBursa, then mutagenized using the *bursa aurealis* system as previously reported (15; 16; 108). Approximately 5,000 colonies from 20 plates were harvested directly using 5 mL BHI with Em to wash each plate, which was mixed with 5 mL 50% glycerol to generate 20 separate 10 mL aliquots each representing a subset of the library. Before freezing at -80°C, each tube was thoroughly homogenized by vortexing and 1 mL was pooled into a single aliquot representing the entire library encompassing approximately 100,000 individual transposon insertions.

2.3.3 Library Analysis

Genomic DNA was extracted using a Wizard Genomic DNA Preparation Kit. Initial analysis of insertions was performed using inverse PCR and sequencing per protocol (16). For complete characterization of the library, extracted DNA was sonicated, then a poly-C tail was addended using TdT. The reaction was purified using an EdgeBio PERFORMA column, then subjected to PCR with oligonucleotide primers olj510 and olj376. A small aliquot was then subjected to a second round of PCR using primer olj511 and one of the barcoding (BC) primers, and olj512 was provided for sequencing. Single-end Illumina sequencing was performed at the Tufts Genome Sequencing Facility. Reads were processed using the Galaxy Web Server (33; 92; 94). After sequences were clipped to remove the poly-C tail, filtered by quality (q = 7, p-95), and mapped with Bowtie to the NCTC 8325 genome. Mapped reads were assigned Dvals using the Tufts Med Galaxy Web Server AggCount algorithm.

2.4 Results

2.4.1 Characterization of the *S. aureus* HG003 *mariner* Library

We performed initial mobilization of the transposon library in small batches, in efforts to determine parameters for minimal clonal expansion, maximal diversity, and transposase plasmid curing. Inverse PCR and targeted sequencing for initial platings revealed diverse insertion sites (Figure 2.2, Table 2.2). A small fraction of mutants appeared to possess multiple insertions, as revealed by distinct transductants in unlinked loci originating from a single progenitor.

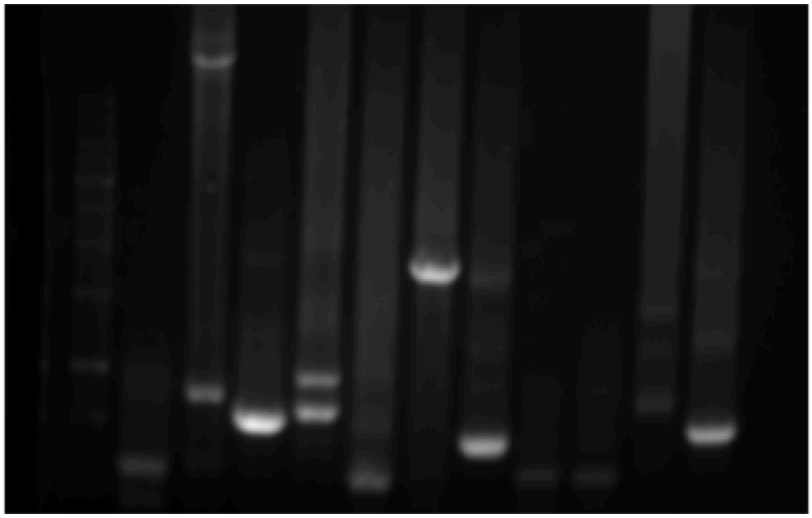

Figure 2.2: Inverse PCR for transposon insertions in 12 individual mutagenized *S. aureus* colonies.

Table 2.2: Sample identified transposon insertion sites through targeted sequencing		
Genomic Site of Transposon Insertion	NCTC 8325 ORF #	Annotated Function
1322640	SAOUHSC_01377	Oligopeptide transporter
2323757	SAOUSHC_2519/2520	GNAT acetyltransferase or sugar transporter
99539	SAOUHSC_00093	Superoxide dismutase
152720	SAOUHSC_00144	Aureolysin NRPS
1531492	SAOUHSC_01606	Peptidase T
213259	SAOUHSC_00192	Coagulase
649578	SAOUHSC_00661	Lipase/hydrolase
2657937	SAOUHSC_02885	PG acetyltransferase OatA

While inverse PCR afforded accurate identification of transposon insertion sites, this technique was recalcitrant toward scale-up and analysis of pooled mutants. Previous studies employed signature tagging (e.g. Signature Tagged Mutagenesis, STM (106)) and microarray-based approaches (e.g. Transposon Site Hybridization, TraSH (193), and Genomic Array Footprinting, GAF (30)), but these may lead to ambiguous assignment of transposon location through cross-hybridization and poor resolution. Modern techniques,

such as Tn-Seq/InSeq and TraDIS (95; 135; 222) can exploit the higher sensitivity and throughput afforded by next-generation sequencing.

In order to obtain detailed information about library composition, we sent library samples to the Tufts University Genomics Core Facility, where they were analyzed using 50bp single-end reads on an Illumina HiSeq 2500. Raw reads were trimmed and mapped onto the NCTC 8325 genome. A large number of sequencing reads were successfully mapped to diverse loci (Figure 2.3, Table 2.3). A total of 72,699 unique insertion sites were detected in 6,246,137 PCR reads with 80% in genic regions – this approaches the 85% of the total chromosome occupied by genes. For the *S. aureus* genome, this represents coverage of 24X, higher than all other reported libraries, providing an average of 1 insertion per 38.8 base pairs (15; 19; 47; 139; 156). A second assessment of the library, grown for 24 hours in BHI media after dilution from an overnight starter culture, showed a moderate decrease (16%) in the number of genic insertion sites, despite a higher proportion of mapped reads. This suggested that a number of initially identified transposon mutants were either inviable, susceptible to freeze-thawing of the library, or highly compromised for growth and outcompeted by other library members. For both data sets, approximately equal numbers of insertions were identified on each strand of the chromosome. Out of 2969 total ORFs, 339 lacked transposon insertions (345 for the sample post-24 hours growth). The ORF with the largest number of unique insertions (550 in the initial, 391 post-outgrowth) was *ebhB*, though at 28.6kb this is the largest gene on the chromosome. Normalizing for gene size, the ORF with the largest number of unique insertions was SAOUHSC_00636, annotated as an ABC transporter for chelated iron. As observed in other organisms, a greater number of sequenced

insertions were identified near the chromosomal origin in comparison to the terminus (Figure 2.4).

Table 2.3 Transposon Library Sample Reads

	Initial Library	+24 hrs
Total Insertion Sites	72,699	61,061
Total Genic Insertion Sites	57,825	48,317
Total Intergenic Insertion Sites	14,874	12,744
Total Reads	6,246,137	10,497,679
Total +Strand	3,139,416	4,880,073
Total -Strand	3,106,721	5,617,606
Total Genic Reads	5,051,212	8,239,326
Total Intergenic Reads	1,194,925	2,258,353
Genome Size	2,821,361	
Genic Regions	2,397,907	
Intergenic Regions	423,454	
Total TA Sites	269,582	
Total ORFs	2969	
Calculated Coverage	24.49	20.57

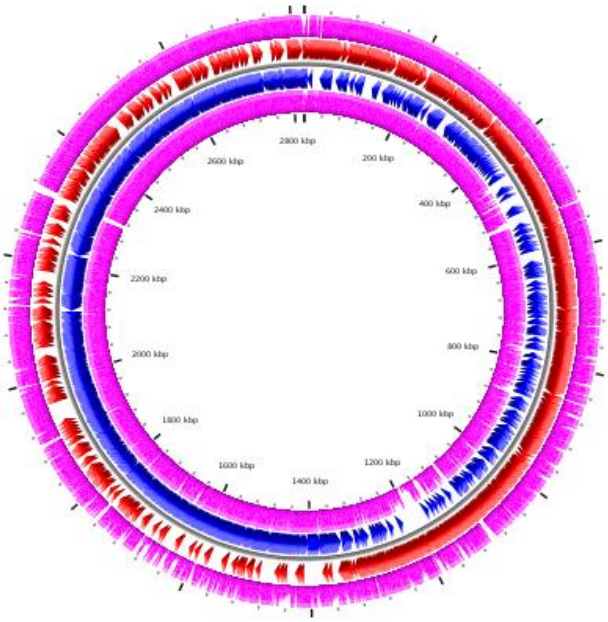

Figure 2.3: Mapped transposon insertions across the NCTC 8325 genome. Genes on the forward strand are denoted in red, and those on the reverse strand are denoted in blue, while

insertions are denoted in pink above (outermost circle) and below (innermost circle) for each strand.

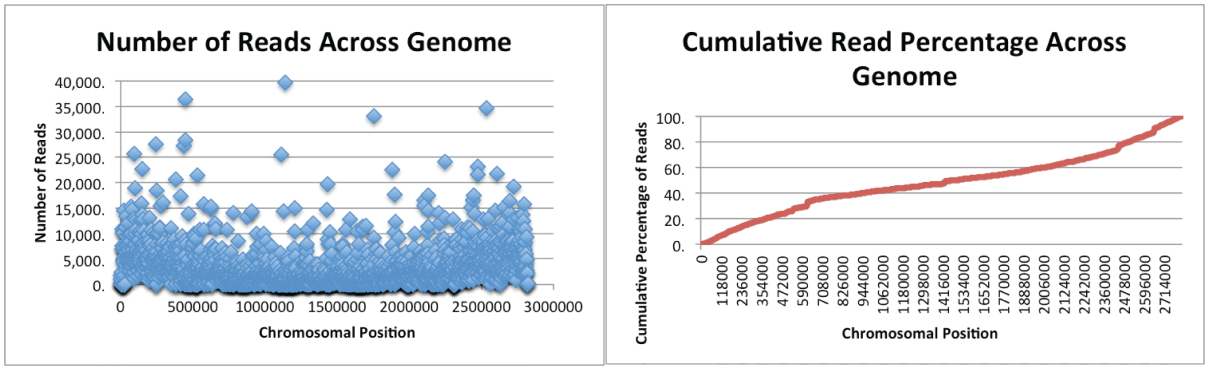

Figure 2.4 Plots of identified insertions based on chromosome position reveal an uneven distribution with bias toward the chromosomal origin of replication.

2.4.2. Statistical Analysis of Essential Genes in the Transposon Library

The first approach that we used in order to quantitatively analyze our insertional data was to calculate a Dval. Each gene's Dval represents the observed number of mappable reads of insertions in a gene, divided by the number of mappable reads of insertions predicted for a gene based on its size relative to the genome and the total number of mappable reads obtained for that experiment. Thus, Dval is normalized the total number of insertion amplicon reads occurring in a specific gene to the number expected for that gene bases solely on its size and assuming complete randomness of insertion. For example, in our library, the gene *dnaA* encoding DNA replication initiation protein has a length of 1361 bp, in a genome of size 2,821,361bp. If one assumed that the reads obtained were equally distributed across the genome, then the expected number of insertions within *dnaA* is 0.048% of the total number of reads (6246137) or 2994 reads. We observed only 48 reads in *dnaA*, a Dval of .016, suggesting transposon mutants in this gene are underrepresented in the library. Dvals >1 suggest that transposon mutants are overrepresented within a given gene. For example,

SAOUSHC_00636 had Dval >100, with ~6% of the total reads. In addition to the 339 ORFs lacking transposons entirely, 13 possessed Dvals ≤ 0.01 strongly suggesting their essentiality. Approximately 70 more genes possessed Dvals ≤0.10 but > 0.01 and several of these were manually curated for essentiality based on their possession of transposons insertions at densities below 0.00285 (1 insertion every 350bp, approximately 1/10 the expected insertion frequency). This overall number of essential genes (approximately 420) is in accord with several literature studies, though somewhat higher than observed for bacteria such as *E. coli* and *M. tuberculosis*. We categorized multiple genes as nonessential that have been previously reported as essential and vice-versa (Table 2.4) (47). In some cases, such as for fructose bisphosphate aldolase, the identified insertions were all outside of a protein domain or active site, suggesting that these mutants retained gene function and are false negatives for essentiality. Estimation of the number of essential genes using a Hidden Markov Model gave 982 essential genes, which reduced to 681 in subsequent samples with higher coverage (Table 2.5). We hypothesize that the tendency of the HMM method to predict a higher number of essential genes is due to sampling only about one quarter of the total genomic TA sites, which is lower saturation than the transposon libraries for which this algorithm was initially developed.

Table 2.4: Genes With Different Essentiality Than Reported *In Vitro*

Gene	Our Finding	ProteinID	Length
SAOUHSC_00003	Essential	Hypothetical protein	245
SAOUSHC_00345	Essential	Hypothetical protein	203
secE	Essential	preprotein translocase subunit	182
SAOUSHC_00884	Essential	Putative monovalent cation/H+ antiporter subunit F	293
SAOUHSC_00887	Essential	Putative monovalent cation/H+ antiporter subunit C	329
SAOUHSC_00892	Essential	Hypothetical protein	344
SAOUHSC_01721	Essential	Hypothetical protein	260
SAOUHSC_A01041	Nonessential	Hypothetical protein	224

SAOUHSC_02805	Nonessential	Hypothetical protein	302
SAOUHSC_02575	Nonessential	Hypothetical protein	422
SAOUHSC_02366	Nonessential	Fructose-bisphosphate aldolase	860
SAOUHSC_01979	Nonessential	Hypothetical protein	464
SAOUHSC_01782	Nonessential	Hypothetical protein	608
SAOUHSC_00998	Nonessential	FmtA	1193
SAOUHSC_00760	Nonessential	Hypothetical protein	1070

Table 2.5 Hidden Markov Model for Transposon Library

Category	Total	Avg. Insertions	Avg. Reads
Essential	681	0.06	172.6
Growth Depleted	431	0.103	210.8
Nonessential	1759	0.178	324.3
Growth Advantage	0	0	0

2.5 Conclusion

Using the *bursa aurealis* system, we constructed a highly saturated transposon library in *S. aureus* HG003. By employing TnSeq, we were able to accurately map the locations of transposon insertions to positions in the genome. Using several different statistical methods, we were then able to predict the likelihood of gene essentiality based on the presence or absence of PCR reads from a genomic locus. Together, these tools enabled us to determine the conditional essentiality of genes upon treatment of the library with tunicamycin to deplete wall teichoic acids from the population.

Chapter 3: A Chemical Genetic Strategy to Map Interactions with Wall Teichoic Acids in *Staphylococcus aureus*

The majority of this chapter is included in the article "Compound-gene interaction mapping reveals distinct roles for *Staphylococcus aureus* teichoic acids" by Santa Maria Jr., J.P., *et al.* (2014) *Submitted*.

3.1 Abstract

The bacterial cell envelope was historically viewed as a protective barrier that enables survival in challenging environments, but recent evidence shows that envelope constituents also play roles in physiological processes such as cell division. In Staphylococcus aureus, deletion of either lipoteichoic (LTA) or wall teichoic acid (WTA) polymers results in doubled and misoriented septa as well as impaired cell separation. To gain insight into TA function, we employed a small molecule inhibitor to screen a highly saturated transposon library for cellular factors that become essential when WTAs are depleted. Based on the results and follow up validation we constructed a network connecting WTAs with genes involved in LTA synthesis, peptidoglycan synthesis, surface protein display, and D-alanine cell envelope modifications. Unexpectedly, D-alanylation, a shared modification of LTAs and WTAs, became essential in the absence of WTAs, but not LTAs.

3.2 Introduction

Bacteria are surrounded by a complex cell envelope that performs many different functions important for survival. In Gram-positive organisms such as *Staphylococcus aureus*, the major components of the cell envelope are peptidoglycan (PG) and teichoic acids (Figure 3.1). PG, a polymer of highly crosslinked carbohydrate chains that encapsulates the cell, is a well-established target for clinically useful antibiotics, due to its essential role in providing structural support and protection from osmotic lysis. *S. aureus* teichoic acids are anionic polymers of two main types: lipoteichoic acids (LTAs), which are embedded in the cell membrane and comprise a poly(glycerolphosphate) backbone tailored with D-alanine esters, and wall teichoic acids (WTAs), which are covalently attached to PG and possess a poly(ribitolphosphate) backbone functionalized with D-alanine and N-acetylglucosamine

(GlcNAc) moieties (41; 189). Unlike PG, LTAs and WTAs are individually dispensable for survival *in vitro*, but they play critical roles in pathogenesis (168; 237). Moreover, strains lacking either TA polymer have severe septal defects and compromised fitness even *in vitro*, implying that these pathways are also possible targets for antibiotics (44; 46; 168; 173; 199; 200). Efforts to make strains lacking both LTA and WTA polymers have not been successful, suggesting that simultaneous inactivation of the two pathways is lethal (168; 198). While their importance is readily apparent, TAs are still not well understood. LTAs and WTAs are thought to play partially redundant roles in *S. aureus* cell division and envelope integrity, and this view is bolstered by the fact that the same D-alanylation machinery is used to install D-alanine esters on both polymers (166). It has been difficult to identify unique roles for the two polymers through phenotypic analysis because deletion has pleiotropic effects and the observed phenotypes are similar. We reasoned that more insight into distinct functions of LTAs and WTAs could be gleaned by identifying the genes that become essential when either polymer is removed. Therefore, we carried out an unbiased screen for cellular factors that become essential when WTAs are absent. Based on the screen and a set of targeted gene deletions, we have constructed an interaction network for WTAs. Here we describe the screen, our follow up validation, the interaction network, and results showing that many genes that become essential in the absence of WTAs are dispensable when LTAs are deleted. For example, D-alanylation becomes an essential modification of LTAs when WTAs are not made; however, it is not required on WTAs when LTAs are deleted. We conclude that WTAs and LTAs act as part of distinct networks.

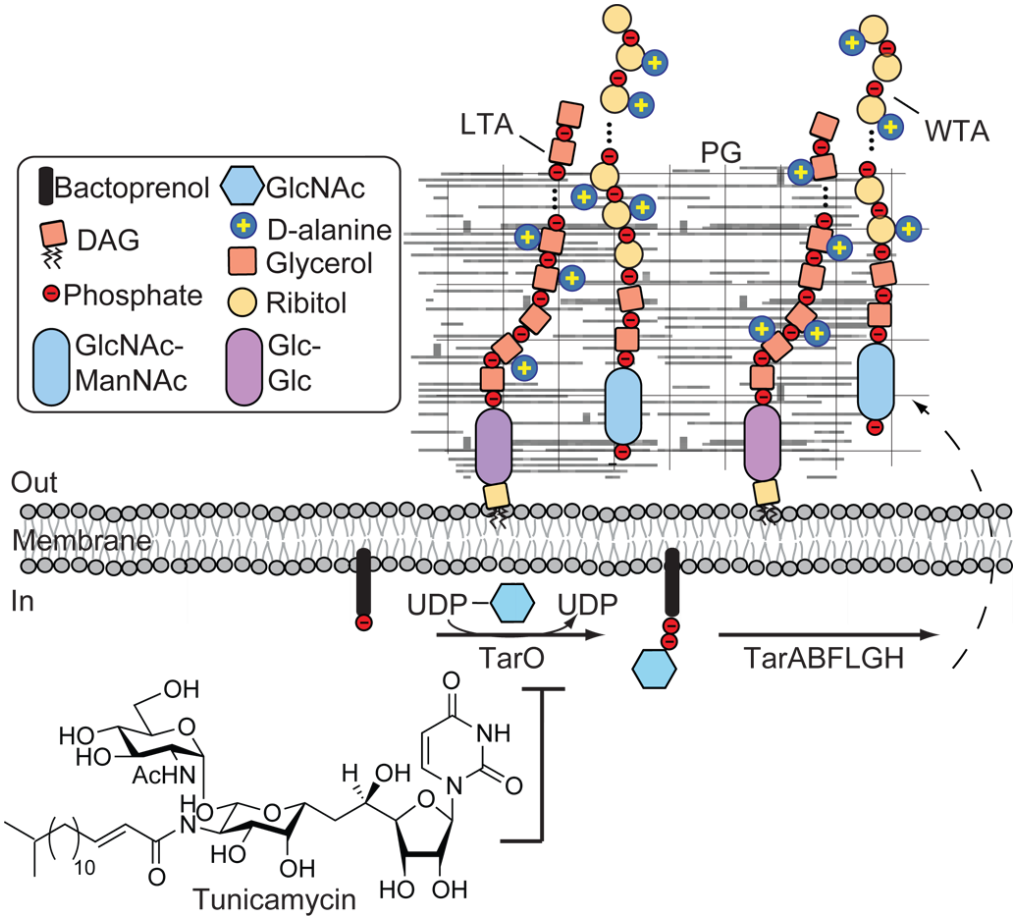

Figure 3.1: Teichoic acids are a major component of the *S. aureus* cell envelope. WTAs are attached to PG, while LTAs are linked to membrane-bound lipid carriers (diacylglycerol, DAG). Tunicamycin is a selective inhibitor of the first step of WTA biosynthesis, catalyzed by TarO(44; 181; 234)}.

3.3 Methods

3.3.1 Bacterial Strains, Reagents, and General Methods

Plasmids were constructed in *Escherichia coli* XL-1 Blue (Stratagene) or Stellar Gold (Clontech) competent cells and introduced into restriction-negative *S. aureus* strain RN4220 by electroporation(194). Plasmids were purified from *S. aureus* RN4220 by first washing cells with a 1:1 mixture of cold acetone:ethanol, then pretreating cells with lysostaphin (50 µg/ml, 10 min, 37°C) prior to isolation using a standard plasmid miniprep protocol (Qiagen).

Plasmids were then introduced into restriction-positive wild-type strains by electroporation. *S. aureus* was grown primarily in tryptic soy broth (TSB) medium at 30°C. Antibiotic markers were selected with erythromycin (Em) (10 μg/ml), tetracycline (Tet) (2.5 μg/mL), carbenicillin (Carb) (100μg/mL), a combination of kanamycin and neomycin (Km) (50μg/mL, each) and chloramphenicol (Cm) (10 μg/mL). Tunicamycin (Tm) purchased from Sigma Aldritch was dissolved in DMSO and diluted to a final concentration of 0.4μg/mL. Anhydrotetracycline was dissolved in 100% ethanol to a 1000X stock of 100μg/mL. Novagen KOD Hot Start Polymerase was used for all PCRs and all restriction enzymes were purchased from New England Biolabs. A Clontech In-Fusion HD Cloning Kit was used for isothermal assembly.

3.3.2 Transposon Library and Screen

The transposon library was constructed *in S. aureus* HG003 using the *bursa aurealis* system(15). Frozen aliquots of the library stock were thawed and diluted 1:1000 into 10 mL of BHI overnight at 37°C. This culture was then diluted 1:100 into 100mL of BHI with or without Tm, then grown at 37°C for 24 hours. Cells were pelleted and DNA was extracted using a Wizard Genomic DNA Preparation Kit. The DNA was sheared, addended with a polyC tail (TdT, Promega), amplified and barcoded via PCR, and sequenced using an Illumina Hi-Seq2000 at the Tufts Genome Sequencing Facility. Insertions were mapped to ORFs using the sequenced NCTC 8325 genome and the Galaxy webserver. The Mann-Whitney-U Test was used in combination with Fisher's Test to identify mutants in genes for which tunicamycin treatment led to significant depletion as compared to the number of identified reads for the untreated control.

3.3.3 Construction of Mutant Strains

Gene deletions were made using the pMAD and pKFC allelic replacement systems(10; 120). For plasmids pMADvraFG (P1-P4), pKFClyrA (P5-P8), pKFC965 (P9-P12), flanking arms with homology to chromosomal regions adjacent to the deletion locus were obtained via PCR. Arms were then digested and ligated together and amplified again using PCR, or spliced via overlap PCR with upFor and downRev primers, then digested, gel purified, and ligated into digested parent vector. Double crossovers were performed at 39-40.5°C and validated as Tm^S and Em^S (pMAD) or Tm^S and Cm^S (pKFC) by restreaking in the presence and absence of these antibiotics overnight, then confirmed via sequencing. Plasmids pKFCgraR (P13-P16), pKFCtarOlink (P17-P20), pKFCdltD (P21-P24), pKFClyrAkan (P39-P42), and pKFC965kan (P43-P46) were instead assembled from flanking homology arms with an intervening antibiotic marker (*aphA3* P25-P26, *tetM* P27-P28) using isothermal assembly. Double crossovers were validated as Tm^S Cm^S Tc^R or Tm^S Cm^S Km^R via restreaking and sequencing. Strain JSM061 was obtained via pMADdltA, in a manner similar to MW2 Δ*dltA*(42). Strains JSM069 and JSM061 were obtained via phage transduction of marked deletions into clean background strains. Complementation constructs pLOWgraR (P29-P30), pLOWvraFG (P31-P32), pLOWlyrA (P33-P34), pLOW965 (P35-P36), and pLOWDlt (P37-P38) were cloned into pLOW via restriction digest and ligation, using primers listed in Table 2 (141). Double mutant strains, used to construct the pathway interaction map (Figure 3.4) were created through ϕ85 transduction of a marked deletion into unmarked deletion backgrounds.

3.3.4 Linkage Analysis

Strain JSM095 was created by installing a *aphA3* (Km^R) marker approximately 4.5kb downstream of Δ*tarO::tet*^{R} in TCM011 using pKCtarOlink. Donor phage ϕ85 was prepared

from this strain and used to transduce *aphA3* into WT and mutant backgrounds. Km^R colonies were obtained at 37°C, then assayed for Tet^R and Congo Red sensitivity in 96-well format, overnight at 37°C(208).

Table 3.1: Strains used in this study

Strains	Relevant Genotype	Reference or Source
RN4220	RN450 partial *agr* defect ST8; CC8; codon in both *hsdR* and *sauUSI*	(129)
Newman	ST8; CC8 isolated in 1952 human clinical MSSA	(69)
HG003	*rsbU* and *tcaR* repaired NCTC 8325	(108)
MW2 (USA400)	Clinical isolate; community-acquired methicillin resistant (CA-MRSA)	(12)
MW2 Δ*dltA*		(42)
RN6911	Δ*agr*::*tetM* derivative of RN6390	(167)
TCM011	Δ*tarO*::*tetR* pCL25 P_{pen} *tarO* $Tet^R Em^R$	Laboratory Stock
SEJ1	RN4220Δ*spa*	(100)
4S5	SEJ1Δ*ltaS* suppressor strain	(55)
LAC*	CA-MRSA LAC strain (AH1263)	(34)
ANG2134	LAC*Δ$ltaS_N$::*erm*, Em^R	(55)
ANG2570	LAC* Δ*gdpP*::kan^R pCL55iTETr862-*gdpP*, Km^R, Cm^R	(54)
ANG1838	4S5 pCN34iTET-$gdpP_{4S5}$	(55)
JSM060	HG003 pBursa pFA545 Cm^R Em^R Tet^R	This Study
JSM065	Newman [Δ*graR*::*tetM*] by transduction, Tet^R	This Study
JSM084	Newman pLOWgraR, Em^R	This Study

JSM081	JSM065 [Δ*graR*::*tetM*] by transduction, Tet^R, Em^R	This Study
JSM061	RN4220 Δ*vraFG*	This Study
JSM111	RN4220 pLOWvraFG Em^R	This Study
JSM085	JSM061 pLOWvraFG Em^R	This Study
JSM064	Newman Δ*dltA*	This Study
JSM063	Newman Δ*dltD::aphA3*, Km^R	This Study
JSM095	TCM011 *aphA3*, Km^R Tc^R Em^R	This Study
JSM073	SM002 [Δ*dltD::aphA3*] by transduction Km^R	This Study
JSM074	SM003 [Δ*dltD::aphA3*] by transduction Km^R	This Study
JSM071	JSM064 [Δ*lyrA*::*aphA3*] by transduction Km^R	This Study
JSM072	JSM064 [Δ*SAOUHSC_00965*::*aphA3*] by transduction Km^R	This Study
JSM090	4S5 [Δ*dltD::aphA3*] by transduction Km^R	This Study
JSM104	4S5 [Δ*SAOUHSC_00965*::*aphA3*] by transduction Km^R	This Study
JSM103	4S5 [Δ*lyrA*::*aphA3*] by transduction Km^R	This Study
JSM067	JSM061 [Δ*dltD::aphA3*] by transduction Km^R	This Study
JSM096	JSM061 [Δ*lyrA::aphA3*] by transduction Km^R	This Study
JSM097	JSM061 [Δ*SAOUHSC_00965::aphA3*] by transduction Km^R	This Study
JSM098	SH002 [Δ*graR::tetM*] by transduction, Tc^R	This Study
JSM099	SH003 [Δ*graR::tetM*] by transduction, Tc^R	This Study
JSM072	JSM065 [Δ*dltD::aphA3*] by transduction Tc^R Km^R	This Study
JSM132	RN4220 pLOWDlt Em^R	This Study
JSM137	JSM061 pLOWDlt Em^R	This Study
JSM133	Newman pLOWDlt Em^R	This Study
JSM136	JSM065 pLOWDlt $Em^R Tc^R$	This Study

JSM135	4S5 pLOWDlt Em^R	This Study
JSM159	SEJ1 [Δ*gdpP::kan*^{R}] by transduction, Km^R	This Study
SHM002	HG003 Δ*lyrA*	This Study
SHM009	SM001 pLOWlyrA Em^R	This Study
SHM003	HG003 Δ*SAOUHSC_00965*	This Study
SHM010	SM003 pLOW965 Em^R	This Study
SHM037	HG003 Δ*lyrA*::*aphA3* Km^R	This Study
SHM039	HG003 Δ*SAOUHSC_00965*::*aphA3* Km^R	This Study
SHM086	JSM064 pLOWDlt Em^R	This Study
SHM091	JSM061 pLOWDlt Em^RKm^R	This Study
SHM094	SM002 pLOWDlt Em^R	This Study
SHM095	SM003 pLOWDlt Em^R	This Study

Table 3.2: Plasmids and oligonucleotide primers used in this study

Plasmid or Primer	Description or Sequence	Reference or Source
Plasmids		
pBursa	Mariner transposon plasmid*, bursa aurealis*, Em^R, rep^{TS}, Cm^R	(15)
pFA545	Transposase Plasmid Tc^Rrep^{TS}	(15)
pMAD	*E. coli*/*S. aureus* shuttle vector ori^{Ts} X-Gal colorimetric selection $Carb^R$ Em^R	(10)
pKFC	Temperature-sensitive shuttle vector; ori^{Ts} $Carb^RCm^R$	(120)
pLOW	Low-copy expression plasmid $Carb^REm^R$	(141)
pTM378	Template for *aphA-3* gene, Km^R	(232)
pCL55iTETr 862-*gdpP*	Integrative plasmid with *gdpP* under an anhydrotetracycline-inducible promoter, Cm^R	(54)

pMADvraFG	P1-P4 PCR in pMAD for deletion of *vraFG* $Carb^{R}Em^{R}$	This Study
pKFCgraR	P13-P16 PCR in pKFC for replacement of *graR* with *tetM* $Carb^{R}Tc^{R}$ Cm^{R}	This Study
pKFCdltD	P21-P24 PCR in pKFC for replacement of *dltD* with *aphA-3* $Carb^{R}Km^{R}$ Cm^{R}	This Study
pKFClyrA	P5-P8 PCR in pKFC for markerless deletion of *lyrA* $Carb^{R}Cm^{R}$	This Study
pKFClyrAkan	P39-P42 PCR in pKFC for replacement of *lyrA* with *aphA-3* $Carb^{R}Km^{R}$ Cm^{R}	This Study
pKFC965	P9-P12 PCR in pKFC for markerless deletion of *lyrA* $Carb^{R}Cm^{R}$	This Study
pKFC965kan	P43-P46 PCR in pKFC for replacement of *965* with *aphA-3* $Carb^{R}Km^{R}$ Cm^{R}	This Study
pLOWvraFG	P31-P32 PCR in pLOW for expression VraFG $Carb^{R}Em^{R}$	This Study
pLOWgraR	P29-P30 PCR in pLOW for expression of GraR $Carb^{R}Em^{R}$	This Study
pLOWlyrA	P33-P34 in pLOW for expression of LyrA $Carb^{R}Em^{R}$	This Study
pLOW965	P35-P36 in pLOW for expression of 965 $Carb^{R}Em^{R}$	This Study
pLOWDlt	P37-P38 in pLOW for expression vector of DltABCD $Carb^{R}Em^{R}$	This Study
pKFCtarOlink	P17-P20 PCR in pKFC for installation of *aphA-3* 4.3kbp downstream of *tarO::tetR* $Carb^{R}Km^{R}$ Cm^{R}	This Study
Primers		
P1. *vraFG* EcoRI upFor	taGAATTCaactcgatgctagatacaca	
P2. *vraFG* XhoI upRev	taCTCGAGttaacactcctataatttatctt	

P3. *vraFG* XhoI downFor	taCTCGAGacgagataatatttaaaaatttcc	
P4. *vraFG* BamHI downRev	taGGATCCaataaaataaacataagtgtac	
P5. *lyrA* BamHI upFor	gatctgattGGATCCaatattgagcatacgcaatatc	
P6. *lyrA* upRev	ctagcaagcgctttgtatatgtaacctccattag	
P7. *lyrA* downFor	ctaatggaggttacatatacaaagcgcttgctag	
P8. *lyrA* SalI downRev	gatctgattGTCGACcatgacgctgggaattgg	
P9. *965* BamHI upFor	gatctgattGGATCCtcagtgaatttttggaaattg	
P10. *965* upRev	cgtctaagaaaagcttattataacttaccttcttattc	
P11. *965* downFor	gaataagaaggtaagttataataagcttttcttagacg	
P12. *965* SalI downRev	gatctgattGTCGACaagttatattaatatatgaacttc	
P13. *graR* upFor	GACGGCCAGTGAATTcgaacaggttgttgc	
P14. *graR* upRev	gcgagatttgggttgttcaataccagcaac	

P15. *graR* downFor	gttatataaatatggcgtttcgagagatac	
P16. *graR* downRev	CGACTCTAGAGGATCatacctaattgatcc	
P17. *tarO* link upFor	GACGGCCAGTGAATTCctggcagatgaaaatccatt	
P18. *tarO* link upRev	acctcaaatggttcgctttacgattttcgactcgga	
P19. *tarO* link downFor	gttttagtacctaggggaagtataattgcgtattga	
P20. *tarO* link downRev	CGACTCTAGAGGATCtctgttaaatgtacagctttc	
P21. *dltD* upFor	GACGGCCAGTGAattcttcccaacgatttcat	
P22. *dltD* upRev	acctcaaatggttcgccgtaactcttctaatgcttca	
P23. *dltD* downFor	gttttagtacctaggaatacaaatagcacataactca	
P24. *dltD* downRev	CGACTCTAGAGGATCtcataatggttaaaattaaaaagc	
P25. *aphA-3* for	gcgaaccatttgaggtgat	
P26. *aphA-3* rev	cctaggtactaaaacaattcat	

P27. *TetM* for	caacccaaatctcgcaatttg	
P28. *TetM* rev	ccatatttatataacaacataaaacgc	
P29. pLOW *graR* SalI For	taGTCGACagaaaatatgaaatatactaaatg	
P30. pLOW *graR* XmaI Rev	taCCCGGGttattcatgagccatatatcc	
P31. pLOW *vraFG* SalI For	taGTCGACtaaattatagga gtgttaaagtg	
P32. pLOW *vraFG* XmaI Rev	taCCCGGGttatatggaatgtctaattgttc	
P33.pLOW lyrA For	gattGTCGACgttacctaatggagg	
P34. pLOW lyrA Rev	ttaaGGATCCttattaatggtgatggtgatggtgtttgtttttatctgaagattgttc	
P35. pLOW 965 For	gattGTCGACgttgaataagaaggtaag	
P36. pLOW 965 Rev	gattGGATCCttaagcattaaaaattaataacaatataatagctac	
P37. pLOW Dlt For	gattGTCGACtgagttctaatgagggag	
P38. pLOW Dlt Rev	ttaaGGATCCttaatttttaggtttatctacttc	

P39. lyrAkan upFor	CCTAATGGAGGTTACATATAGCGAACCATTTGAGGTGAT AGG	
P40. lyrAkan upRev	CCTATCACCTCAAATGGTTCGCTATATGTAACCTCCATTA GG	
P41. lyrAkan downFor	GATGAATTGTTTTAGTACCTAGGACAAAGCGCTTGCTAG TACCTC	
P42. lyrAkan downRev	GAGGTACTAGCAAGCGCTTTGTCCTAGGTACTAAAACAA TTCATC	
P43. 965kan upFor	GATTGTTGAATAAGAAGGTAAGTTATAGCGAACCATTTG AGGTGATAGG	
P44. 965kan upRev	CCTATCACCTCAAATGGTTCGCTATAACTTACCTTCTTAT TCAACAATC	
P45. 965kan downFor	GATGAATTGTTTTAGTACCTAGGAATAAGCTTTTCTTAG ACGTATGTG	
P46. 965kan downRev	CACATACGTCTAAGAAAAGCTTATTCCTAGGTACTAAAA CAATTCATC	

3.4 Results

3.4.1 Design of an Unbiased Screen for Cellular Factors that Interact with WTAs

To understand TA function better, we sought to design a genome-wide synthetic lethal screen for factors that interact with WTAs. Transposon mutagenesis is the standard way to generate a diverse mutant collection for genome-wide interrogations, but it is not possible to construct a transposon library in a WTA-deficient strain because bacteria lacking WTAs are temperature-sensitive as well as phage-resistant, which makes them recalcitrant to available techniques for making transposon mutant libraries(15; 46; 225; 232). In principle, it is possible to overcome this issue by constructing the transposon library in a wildtype strain and then using an inhibitor to turn off WTA expression. We have previously shown that the

natural product tunicamycin is a potent and highly selective inhibitor of *S. aureus* TarO, the first enzyme in the WTA pathway (Figure 3.1) (44; 181; 234). To use tunicamycin to comprehensively probe the *S. aureus* genome for interactions with WTAs, we needed a highly saturated transposon mutant library. Using a *mariner*-based transposon system(15), we constructed a mutant pool in *S. aureus* HG003(108). Transposon-directed insertion site sequencing (TraDIS), a PCR-based next generation sequencing technique that determines the location and abundance of transposon insertions in a population, showed that the library contained 60,000 independent insertion sites (Figure 3.2), which represents approximately twenty-fold coverage of the *S. aureus* genome (135; 221; 223). The high saturation of the transposon library enabled us to screen for genes that interact with WTAs by using tunicamycin to turn off WTA synthesis.

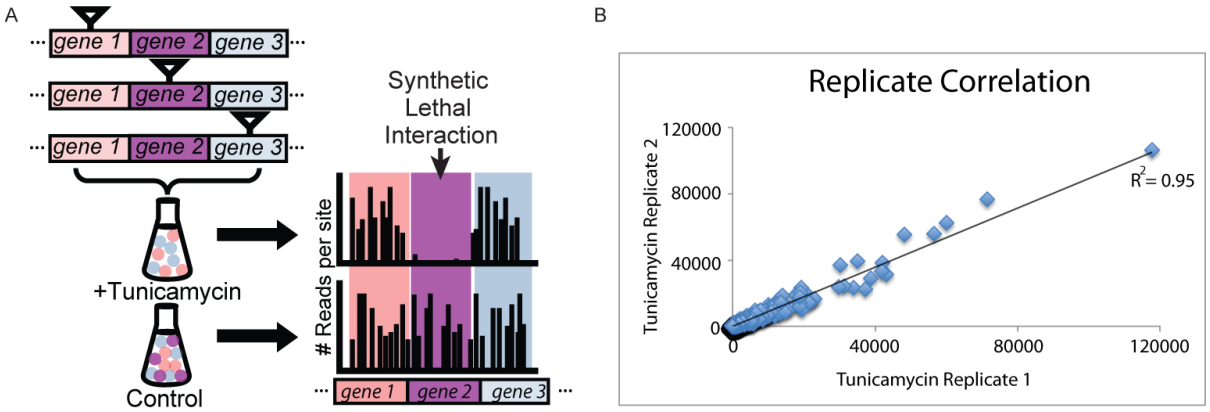

Figure 3.2: The transposon screen identified 24 genes that are synthetically lethal with WTA depletion. (*A*) Schematic showing how genes that become essential (purple) with WTA depletion (*i.e.,* TarO inhibition) are identified by comparing the reads for tunicamycin-treated and untreated transposon libraries. (*B*) Correlation between replicates of the tunicamycin-treated transposon library. Blue diamonds represent each of the 2969 ORFs assessed.

3.4.2 Identification of Transposon Mutants Sensitive to WTA Depletion

We grew replicate cultures of the pooled mutant library in the presence and absence of tunicamycin, sequenced the transposon insertion sites, and quantified PCR reads for each transposon mutant under each condition (Figure 3.2*A*, Supplementary File 1). Replicates of tunicamycin treatment strongly correlated in PCR reads for each ORF (Figure 3.2*B*). As shown in Table 3.3 and Figure 3.3, a similar number of reads were obtained for both treated conditions, yet we observed a significant reduction in the total number of insertion sites (average of 10.74% reduction after normalization). Genic insertion sites were disproportionately reduced in comparison to intergenic sites (11.31% vs. 8.9% normalized). This suggested that several mutants had been eliminated from the population, *i.e.* were synthetically lethal with WTA depletion.

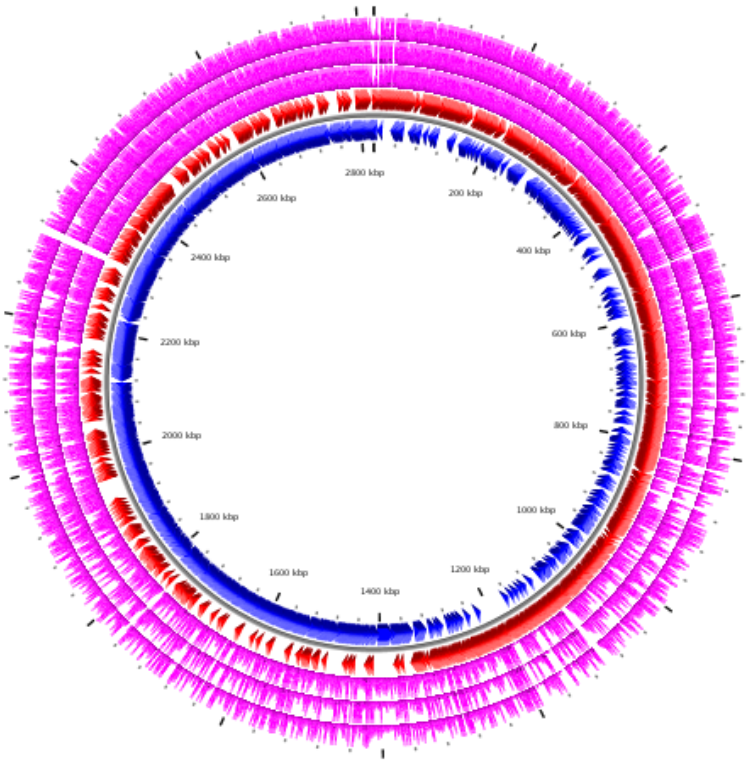

Figure 3.3: Transposon insertion map for both overnight (innermost pink circle) and tunicamycin treatments (replicate 1, middle pink circle, replicate 2, outermost pink circle).

Table 3.3: Transposon Library Statistics

	Initial Library	No Tun (24hrs)	Tun1 (24 hours)	Tun2 (24 hours)
Total Insertion Sites	72699	61061	56829	52516
Total Genic Insertion Sites	57825	48317	44698	41276
Total Intergenic Insertion Sites	14874	12744	12131	11240
Total Reads	6246137	10497679	11569611	9598001
Total +Strand	3139416	4880073	5914259	4865991
Total -Strand	3106721	5617606	5655352	4732010
Total Genic Reads	5051212	8239326	8990388	7424194
Total Intergenic Reads	1194925	2258353	2579223	2173807
Genome Size	2,821,361			
Genic Regions	2,397,907			
Intergenic Regions	423,454			
Total ORFs	2969			
Calculated Coverage	24.5	20.6	19.1	17.7

The differences in PCR reads (normalized by total reads obtained) between the two conditions, expressed as growth ratios, were assigned statistical significance based on the coverage of transposon insertions within the boundaries of a particular ORF (Mann-Whitney U test). Using this method, we were able to assess mutants in 2,535 ORFs (85% of the genome) for differential growth. We favored this analysis over calculating the Dval ratio between treatment and no drug control, as this method tends to generate false positives more for ORFs highly depleted from the no treatment condition. Nevertheless, each method of anlaysis yielded partially-overlapping results (Table 3.4). Fewer than 49 ORFs showed a difference in growth upon tunicamycin treatment (p<0.05), and of these 2 were enriched and 47 were depleted from the population. To identify genes that were synthetically lethal with WTA deletion, we established a stringent cut-off of >90% growth depletion in tunicamycin with a p value of <0.002. Only ten genes met these criteria (Fig. 3.3*A*). Decreasing the

stringency of the cutoff to 85% growth depletion with $p<0.04$ yielded fourteen additional genes (Figure 3.3*B*). Hence, a very small subset of approximately 2,500 disrupted genes in the mutant library showed a strong synthetic phenotype with WTA depletion. Notably, the majority of the genes in the list of 24, including eight of the top ten genes, were predicted to localize to the membrane or to have a cell envelope-related function. Because WTAs reside in the cell envelope, one would expect their synthetic lethal interactions to be weighted towards factors that contribute to envelope biogenesis and integrity.

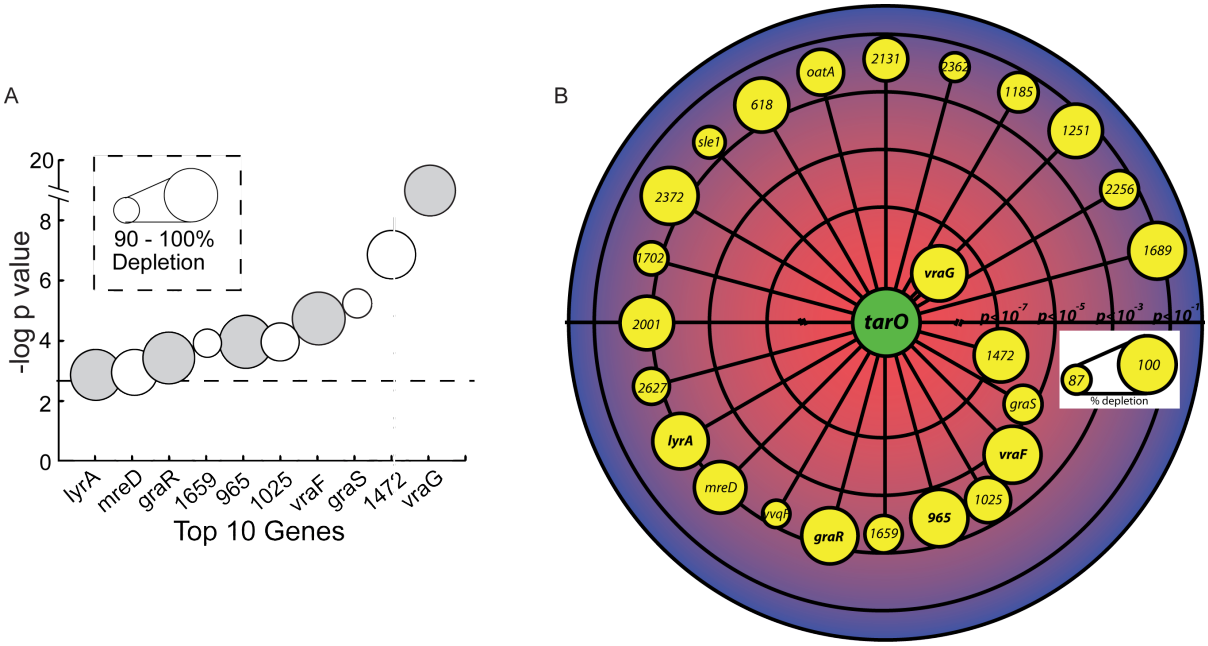

Figure 3.3: (*A*) The 10 most depleted genes are plotted by -log *p* values; the area of the circles reflects the extent of growth depletion, with the smallest circles denoting ~90% depletion. (*B*) Extended list of 24 genes with $p<0.04$ and >85% depleted from the transposon pool.

Table 3.4: Top Genes >300bp Long with Dval Ratios < 0.10 Upon Tunicamycin Treatment

Gene	DvalRatio	ProteinID	Length
SAOUHSC_00452	0.00	hypothetical protein	329
msrR	0.00	transcriptional regulator	983

dnaJ	0.00	chaperone protein DnaJ	1139
SAOUHSC_02153	0.00	hypothetical protein	680
atpI	0.00	hypothetical protein	452
yyaA	0.00	hypothetical protein	839
SAOUHSC_00965*	0.00	hypothetical protein	602
vraF	0.00	ABC transporter ATP-binding protein	761
Pnp	0.00	polynucleotide phosphorylase/polyadenylase	2096
SAOUHSC_02316	0.01	DEAD-box ATP dependent DNA helicase	1520
graR	0.01	hypothetical protein	674
SAOUHSC_02406	0.01	hypothetical protein	932
SAOUHSC_00618	0.01	hypothetical protein	716
vraG	0.01	ABC transporter permease	1889
SAOUHSC_01050	0.01	hypothetical protein	1019
SAOUHSC_02001	0.02	hypothetical protein	1043
SAOUHSC_01472	0.02	DnaQ family exonuclease/DinG family helicase	2693
SAOUHSC_02155	0.02	hypothetical protein	380
lyrA	0.02	hypothetical protein	1259
mreD	0.03	hypothetical protein	530
relQ	0.03	GTP pyrophosphokinase	635
isaA	0.04	immunodominant antigen A	701
ackA	0.04	acetate kinase	1202
SAOUHSC_02646	0.04	hypothetical protein	455
SAOUHSC_02279	0.04	hypothetical protein	662
rplS	0.04	50S ribosomal protein L19	350
SAOUHSC_01207	0.04	signal recognition particle protein	1367
SAOUHSC_01732	0.05	hypothetical protein	350
mreC	0.05	rod shape-determining protein MreC	842
SAOUHSC_01025	0.05	hypothetical protein	1295
oatA	0.05	hypothetical protein	1811
SAOUHSC_00718	0.06	hypothetical protein	584
SAOUHSC_02350	0.06	F0F1 ATP synthase subunit A	728
rsbV	0.06	STAS domain-containing protein	326
mazF	0.06	hypothetical protein	362
SAOUHSC_01655	0.07	hypothetical protein	410
SAOUHSC_01476	0.08	hypothetical protein	317
SAOUHSC_02441	0.08	alkaline shock protein 23	509
SAOUHSC_02627	0.08	hypothetical protein	902
SpdD	0.09	hypothetical protein	743
SAOUHSC_01863	0.09	hypothetical protein	311
graS	0.09	hypothetical protein	1040
SAOUHSC_02131	0.09	hypothetical protein	602
SAOUHSC_00488	0.09	hypothetical protein	932
SAOUHSC_01702	0.10	MTA/SAH nucleosidase	686

**Bolded genes were identified as top hits in both Dval and Mann-Whitney U tests*

3.4.3 Targeted Knockouts of Top Candidate Genes Confirm Sensitivity to WTA Depletion

Transposons often inactivate the ORF into which they insert, but may allow transcription of a truncated mRNA and can also have indirect effects such as polar disruption of nearby genes. Because the top genes identified in the screen were well-saturated with transposon insertions in the control cultures (no tunicamycin), but had few or no insertions across multiple sites in the treated samples, it seemed likely that they were indeed synthetically lethal with WTA depletion (Supplementary File 1). To confirm that growth depletion was the result of gene inactivation, we selected a subset of the top ten genes spanning a range of growth depletion ratios and *p* values and prepared targeted knockouts in order to confirm susceptibility to tunicamycin. Knockouts tested included Δ*graR*, Δ*vraFG*, Δ*SAOUHSC_00965* (hereafter known as Δ*965)*, and Δ*lyrA*. Because simultaneous deletion of LTAs and WTAs was predicted to be lethal, we also examined a strain that lacks LTAs ($\Delta ltaS_{4S5}$) to examine its tunicamycin susceptibility(55; 168; 198)[*]. All strains were tested in a dilution series on agar plates with and without tunicamycin. Tunicamycin had no effect on the growth of wildtype *S. aureus* colonies, but prevented growth of the $\Delta ltaS_{4S5}$ strain, consistent with a synthetic lethal interaction between the LTA and WTA pathways. The other mutant strains also exhibited tunicamycin sensitivity (Figure 3.4). Complementation with plasmid-borne copies of deleted genes restored growth in the presence of tunicamycin. These

[*] Because library preparation involved a high temperature step and strains lacking LTAs are thermosensitive, we were unable to assess the *ltaS* locus from the growth depletion analysis as it was not well-represented in the control samples.

experiments showed that the genome-wide growth depletion analysis accurately identified genes that become essential when WTA synthesis is inhibited. Because Δ*ltaS*$_{4S5}$ contains a suppressor mutation that attenuates the function of the c-di-AMP phosphodiesterase *gdpP*, we also confirmed that the observed sensitivity of this strain to WTA depletion was specifically linked to deletion of the LTA pathway. We tested strains ANG2570 and JSM030, which have marked deletions of *gdpP* and found these strains grew equivalently to wildtype controls (Figure 3.5). Note that we were unable to obtain colonies from Newman Δ*dltA* transduced with a kan^{R}-marked deletion of *gdpP*.

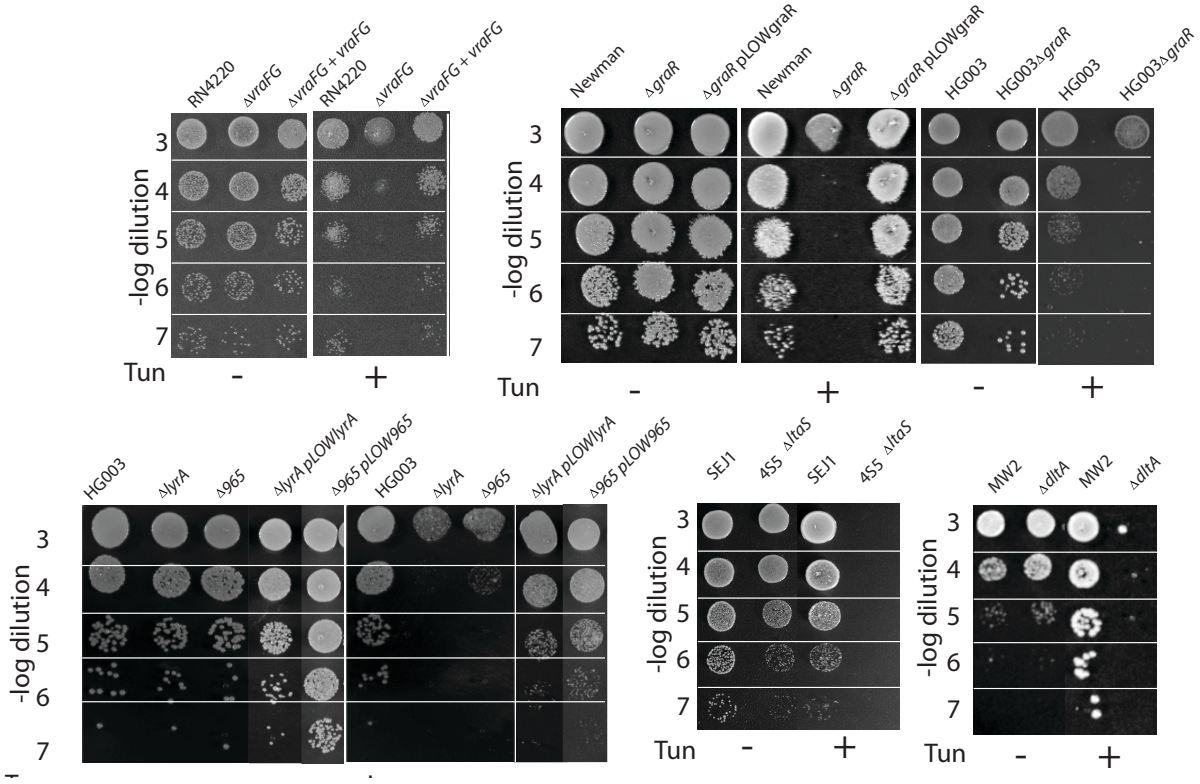

Figure 3.4: Dilution series of selected wildtype and mutant strains grown in the absence and presence of 0.4 μg/mL tunicamycin.

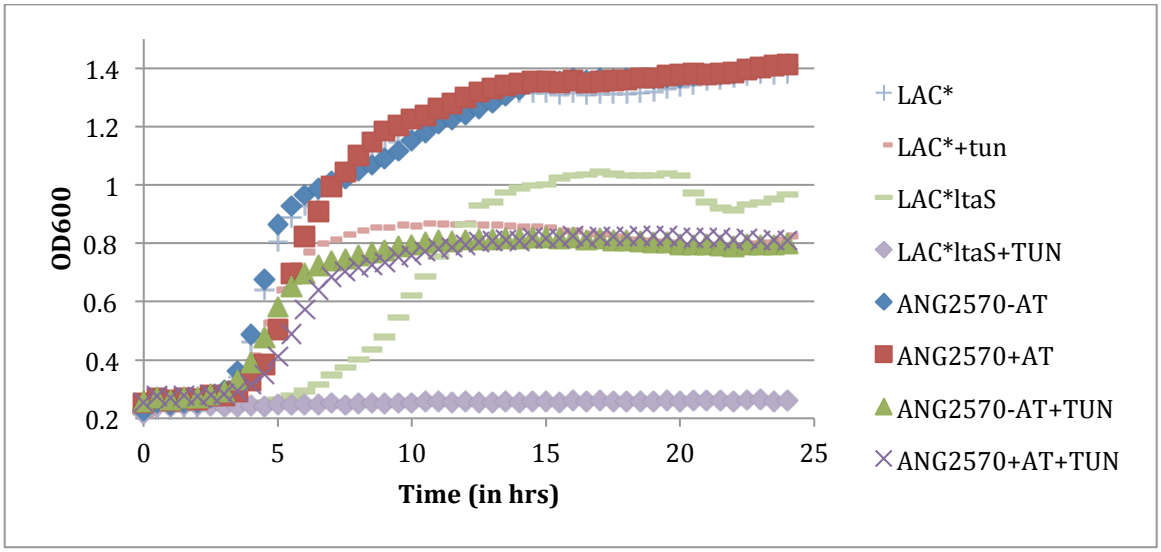

Figure 3.5: Representative growth curves of selected strains grown in the presence and absence of 0.4 µg/mL tunicamycin at 37C, overnight, in a 96 well plate. Anhydrotetracycline (AT, 100ng/mL) was used to induce expression of *gdpP* for strain ANG2570.

3.4.4 D-alanylation Becomes Essential When WTA Synthesis is Inhibited

Four of the top ten genes identified in the transposon screen, *graR*, *graS*, *vraF*, and *vraG*, encode a regulatory protein complex comprising a two component signaling system and a two component ABC transporter (78; 79; 250). The GraRSVraFG complex regulates expression of *lyrA*, also in the top ten list, but it is best known for regulating the *dltABCD* operon (Figure 3.6*A*), which encodes the machinery that installs D-alanines on both LTAs and WTAs. Because Dlt null mutants are temperature-sensitive, there were almost no insertions in the *dlt* operon in the untreated library even though this modification is not essential in a wildtype background(11; 42). Therefore, the genome-wide growth depletion analysis did not provide information about possible synthetic interactions between the *dltABCD* genes and WTAs. To assess whether the D-alanylation pathway itself becomes

essential when WTAs are depleted, we constructed two Dlt null strains, Δ*dltA* and Δ*dltD*, and tested their sensitivity to WTA-inhibitory concentrations of tunicamycin (Figure 3.6*B,C*). Neither of the knockout strains grew on plates or in liquid media containing tunicamycin, but complementation with a plasmid expressing *dltABCD* restored growth. Hence, the D-alanylation machinery is required when WTA expression is inhibited, implying that D-alanylated LTAs are essential if WTAs are not produced.

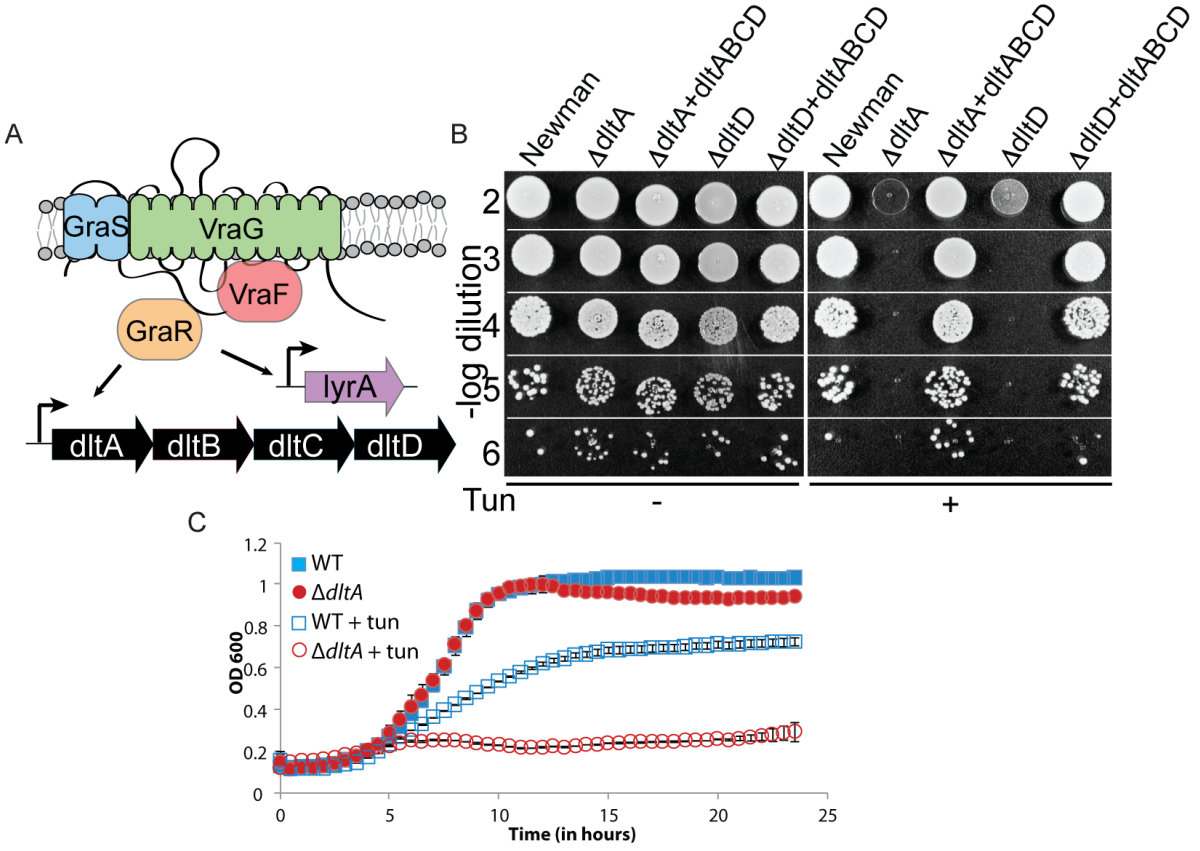

Figure 3.6: Identification and validation of Dlt⁻ mutants as synthetically lethal with WTA depletion. (*A*) Four of the 10 most depleted genes encode the GraRSVraFG complex, which regulates expression of *lyrA* (purple) and the *dlt* genes (black). (*B*) Dilution series of wildtype and *dlt* knockout strains grown in the absence and presence of 0.4 μg/mL tunicamycin shows that the *dlt* deletion is synthetically lethal with WTA depletion. Complementation with the

dltABCD operon restored viability in the presence of tunicamcyin. (*C*) Growth of MW2 wildtype and Δ*dltA* with and without tunicamycin treatment in 96 well format at 30°C.

3.4.5 Linkage Analysis Provided Gene-Gene Validation of Compound-Gene Synthetic Lethal Interactions

The primary target of tunicamycin in *S. aureus* is TarO, the first enzyme in the WTA biosynthetic pathway, but there is also a secondary target, MraY (234). Although our screen and follow up validation used tunicamycin concentrations that are two orders of magnitude below those that inhibit MraY, we wanted to confirm key results using a fully genetic approach that did not rely on a small molecule (44). This seemed necessary because some of the knockouts, including Δ*dltA*, Δ*graR*, and Δ*vraFG*, are known to have increased susceptibility to cationic antimicrobial peptides (CAMPs) and certain other antibiotics with cell envelope targets (155; 179; 180). Increased susceptibility is proposed to occur because the cell surface lacks the D-alanine modifications that normally repel positively charged toxins at the envelope interface (192). While tunicamycin is not charged at physiological pH, we wanted to rule out increased access to MraY as an explanation for the lethal phenotypes we observed. We made strains with regulated, ectopic expression of TarO, but observed leaky expression in the absence of inducer. Therefore, we used linkage analysis to test synthetic lethality of double mutant combinations. We constructed a Δ*tarO::tet*^{R} strain with a kanamycin-resistance gene installed in an intergenic region 4.3 kbp downstream. This strain contained a copy of *tarO* integrated elsewhere in the chromosome to enable the preparation of phage lysates. We then measured linkage of the two antibiotic resistance markers after

phage transduction into either the wildtype or mutant backgrounds (Figure 3.7)[†]. Transductants were selected on kanamycin plates and then scored for growth in media containing kanamycin, tetracycline, or Congo Red, an azo dye to which WTA-less *S. aureus* strains are highly sensitive (208). For the wildtype strain, approximately half the kan^R transductants were both tetracycline resistant and Congo Red sensitive, indicating that the *tarO* deletion moves in tandem with the kanR marker 50% of the time. For the mutant strains, the compound sensitivity profiles showed that none of the kan^R transductants contained the *tarO* deletion (Figure 3.7). This linkage disequilibrium confirmed synthetic lethality between Δ*tarO* and the other gene deletions, validating the screening results obtained using tunicamycin to inhibit WTA synthesis.

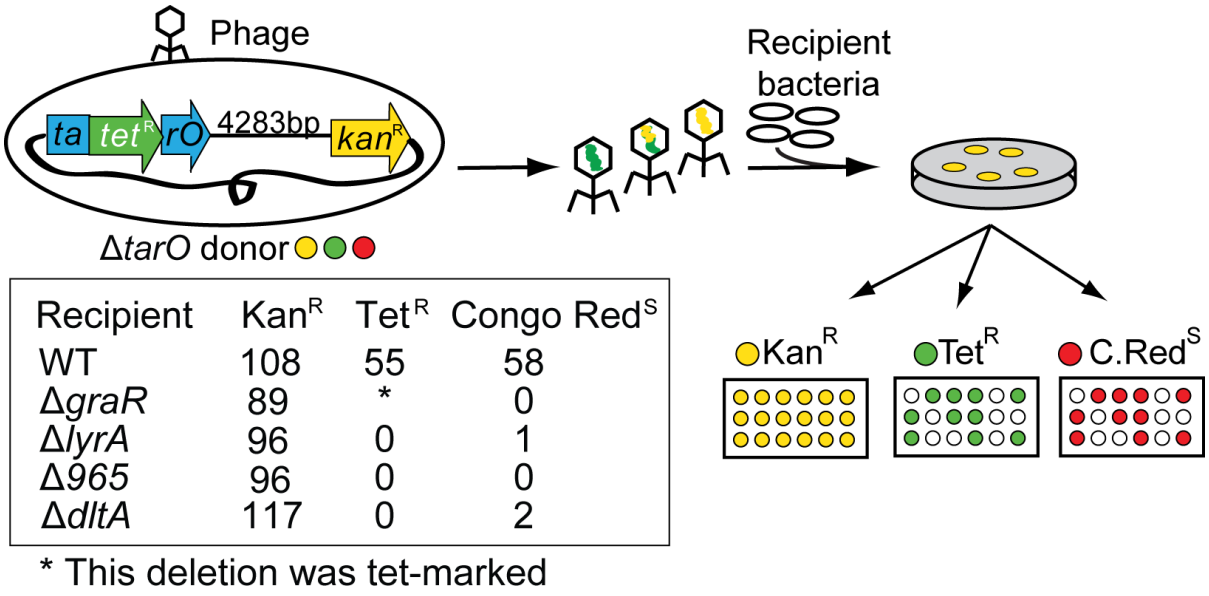

Recipient	Kan^R	Tet^R	Congo Red^S
WT	108	55	58
Δ*graR*	89	*	0
Δ*lyrA*	96	0	1
Δ*965*	96	0	0
Δ*dltA*	117	0	2

* This deletion was tet-marked

Figure 3.7: Linkage analysis confirms compound-gene synthetic lethality. The Δ*tarO*::*tetM* locus could be transduced with the kan^R gene (*aphA3*) into a wildtype background ~50% of

[†] We were unable to assess linkage in Δ*dltD* and Δ*ltaS*$_{4S5}$, as the former deletion was marked with kanamycin resistance, and *ltaS* and *tarO* are within close proximity of each other on the chromosome.

the time; it could not be transduced with the kan^R gene into any of the tested mutant strains . WTA null recipients were identified by assaying for tetracycline resistance (Tet^R) and Congo Red susceptibility (Congo Red^S). Because the Δ*graR* strain was tet-marked, it could only be tested for Congo Red susceptibility.

3.4.6 WTAs and LTAs Have Different Genetic Interactions

WTAs and LTAs are proposed to play redundant cellular roles related to their anionic backbones. Having identified and validated a number of gene knockouts that are synthetically lethal with WTA removal, we next tested several of these in combination with LTA removal to determine if LTAs and WTAs have similar genetic interactions. We were able to transduce marked deletions of Δ*dltD*, Δ*965*, Δ*lyrA*, and Δ*graR* into the $\Delta ltaS_{4S5}$ strain and each of the double mutants was viable. Because WTAs and LTAs have distinct sets of genetic interactions**,** they function as part of different cellular networks/pathways.

The network in Figure 3.8 summarizes the interactions between WTAs, LTAs, and several other genes. The WTA synthetic lethal interaction network includes, in addition to the LTA pathway, five signaling system components that regulate genes involved in modifying the cell envelope (VraFG*,* GraRS, YvqF/VraT) and two sets of genes that modify cell envelope components (*dltABCD* and *oatA*) (20; 37; 78; 79; 250). Three other genes in the WTA interaction network (*lyrA*, 965, and SAOUHSC_2256) encode structurally related membrane proteins that resemble type II CAAX prenyl endopeptidases, a family of proteins well-known in eukaryotes because key members are involved in the proteolytic processing of prenylated Ras and other lipoproteins (174). There are five genes encoding CAAX protease-like (CPL) homologs in *S. aureus*, including the three identified in the growth depletion

analysis, but only Δ*lyrA* mutants have been characterized(99). These mutants have altered crosswall structures and are deficient in a subset of surface proteins (88), but as yet there is no evidence that LyrA has a proteolytic function. While a molecular understanding of CPL homologs in prokaryotes is still lacking, the results reported here emphasize the importance of this family of proteins for *S. aureus* cell envelope physiology. The screen also identified *mreD*, which encodes a broadly conserved membrane protein implicated in regulating peptidoglycan synthesis(134), providing the first genetic connection between two pathways, PG and WTA biosynthesis, that are proposed to be functionally coupled (11; 44; 184).

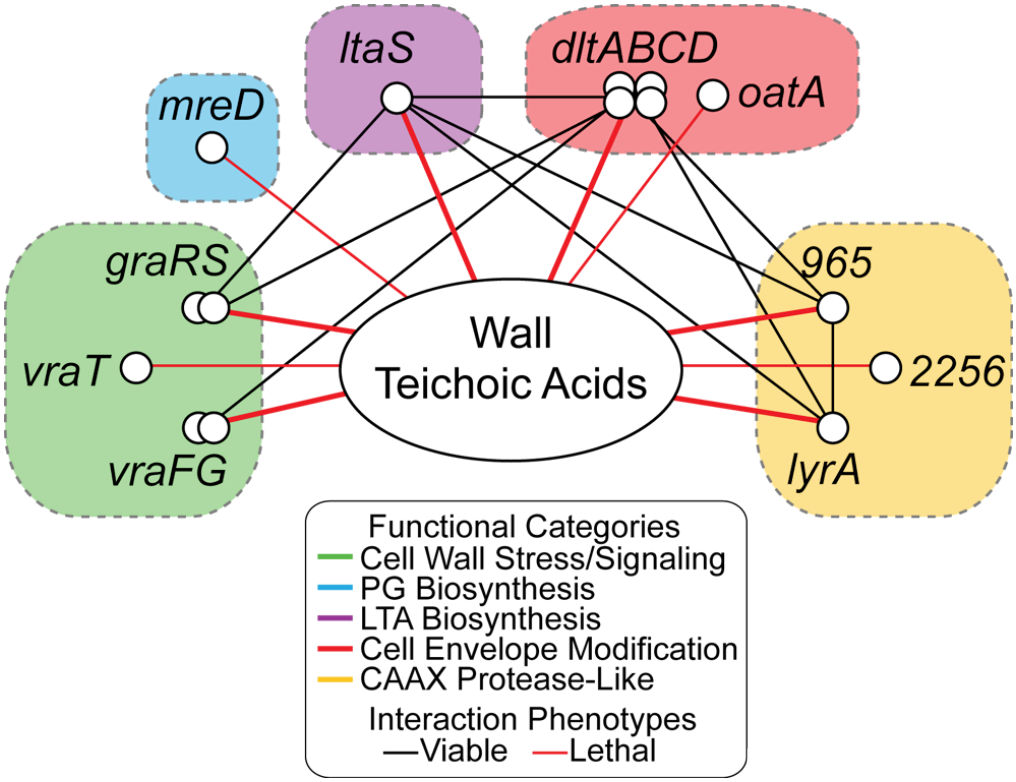

Fig. 3.8: An interaction network showing cell envelope-related genes connected to the WTA pathway. Genes (nodes) group into several distinct pathways or clusters encoding similar proteins (colored boxes). Black lines connect viable double deletion mutants. Thin red lines depict selected synthetic lethal interactions identified only from the genome-wide growth

depletion analysis (growth depletion>85%; p<0.04); thick red lines depict synthetic lethal interactions that were confirmed in one or more follow up experiments.

3.5 Discussion

Dissecting the functions of teichoic acids presents numerous challenges. These polymers play many different roles and deletion phenotypes are pleiotropic. Moreover, mutants deficient in either polymer have similar cell division defects, showing that some functions are redundant. Because lipo- and wall teichoic acids have similar, highly charged backbone structures and identical tailoring modifications, it is also difficult to identify distinct sets of physicochemical interactions for the two polymers using biochemical approaches. We thought it might be possible to gain more insight into both redundant and unique roles of TAs by mapping their synthetic lethal interactions. Using a TarO inhibitor, we carried out an unbiased screen of a large transposon mutant library for cellular factors that become essential when WTAs are depleted. Based on a growth depletion analysis, we identified approximately two-dozen genes that became essential in the absence of WTAs. We followed up on a subset of the top ten candidates, and all of them confirmed. These results are a testament to both the selectivity of the chemical probe for TarO and the high saturation of the transposon mutant library, which provided statistical power in the analysis. Because the screen gave such robust results, we were able to use the data to construct a synthetic lethal interaction network for WTAs, which will be useful for elucidating cell wall physiology. It is worth noting that while pharmacological interrogation of transposon mutant libraries has been performed previously, all earlier studies focused on screening for factors that confer resistance to compounds that have essential targets, *i.e.,* antibiotics. Our work

shows that small molecules that inhibit non-essential targets have tremendous value for elucidating pathway interactions.

The LTA synthetic lethal network has not yet been mapped, but we tested several mutants that were not viable in the absence of WTAs for synthetic lethality with LTA deletion. All double mutant strains were fully viable, showing that WTAs and LTAs have distinct genetic interactions, although they comprise a synthetic lethal pair. In *B. subtilis*, LTAs are proposed to coordinate septal cell envelope synthesis while WTAs play a role in elongation(198). *S. aureus* does not have two distinct modes of cell wall synthesis, but the network analysis described here suggests that LTAs and WTAs act in different pathways to accomplish distinct as well as redundant functions.

The work reported here highlights an important use for small molecule probes in mapping bacterial networks. In addition to revealing new biology, these interaction networks may provide target combinations for synthetically lethal antimicrobial compounds. From this study, we suggest that compound combinations that target both the WTA pathway and either D-alanylation or LTA synthesis are attractive because these factors are absent from humans and have previously been implicated in virulence/*in vivo* survival (45; 53; 59; 153; 190; 212; 233). Synthetically lethal compound combinations that target these different cell envelope components may have potential as therapeutic agents against methicillin-resistant *S. aureus* (MRSA), which continues to be a serious threat to public health.

Chapter 4: Investigation of Synthetic Lethal Interactions between the WTA, LTA, and D-alanylation Pathways

Work from this chapter is included in the article "Compound-gene interaction mapping reveals distinct roles for *Staphylococcus aureus* teichoic acids" by Santa Maria Jr., J.P., *et al.* (2014) *Submitted*.

4.1 Abstract

S. aureus mutants that lack WTAs and LTAs possess similar defects in cell division, yet have different viability and genetic interactions, suggesting that these polymers have non-overlapping roles. Furthermore, our observation that the D-alanylation pathway becomes essential only in the absence of WTAs suggests that D-alanine esters of LTAs may mediate LTA-specific functions. Examination of terminal phenotypes following WTA depletion revealed that strains lacking LTA D-alanine esters died from envelope rupture during ongoing cell division, an effect that was not suppressed by single deletion of key autolysins. In contrast, strains lacking LTAs were unable to form Z rings and stopped dividing. Hence, the presence of either LTAs or WTAs on the cell surface is required for initiation of *S. aureus* cell division, but these polymers act as part of distinct cellular networks.

4.2 Introduction

As discussed in Chapters 1 and 3, teichoic acids play fundamental roles in cell morphogenesis, PG biosynthesis, autolysis, adhesion and colonization, and susceptibility to host defenses and antibiotics. Because LTAs and WTAs possess similar structures (including D-alanyl ester modifications), lie in close physical proximity to one another in the cell envelope, and induce similar phenotypes upon deletion, it was assumed that teichoic acids have mostly redundant roles in these processes. Nevertheless, our analyses demonstrated that WTAs and LTAs have distinct genetic interactions with several pathways tested, suggesting they may also have unique or specialized functions.

Our observation that the D-alanylation pathway becomes essential only in the absence of WTAs argues that D-alanine esters of LTAs may mediate LTA-specific functions. The prior observation that GlcNAc modifications of WTAs alter MRSA beta lactam susceptibility

in a stereospecific manner provides early evidence for TA modifications in modulating specific interactions with cellular envelope factors (42). Saar-Dover and colleagues have argued that D-alanylation influences LTA conformations, changing the density and rigidity of the cell wall (192). Others have suggested that positively charged D-alanine esters on TAs negatively regulate hydrolytic enzymes, and removal of WTAs is also known to result in dysregulated autolysin activity (44; 166; 200). In order to gain insight into the nature of the synthetic lethality between WTAs and LTAs, as well as the specific function of D-alanine residues on LTAs when WTAs are depleted, we analyzed their phenotypes and raised suppressors. From our observations, we conclude that either LTAs or WTAs must be present in order for cell division to initiate.

4.3 Methods

4.3.1: Reagents and General Methods

S. aureus was grown in tryptic soy broth (TSB) medium at 37°C. Fluorescein-conjugated, amidated D-lysine was synthesized by Matthew Lebar of the Kahne lab (Figure 4.1). Bacterial viability was assessed via a Live-Dead BacTiter-Glo™ (Promega).

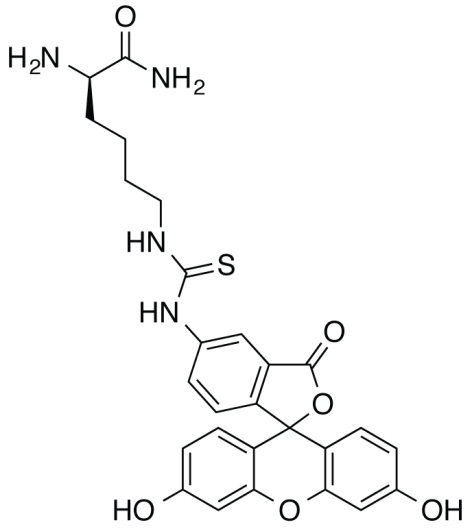

Figure 4.1: Structure of fluorescent D-amino acid probe, amidated D-lysine conjugated to fluorescein.

4.3.2 Electron Microscopy

Overnight cultures were diluted into fresh TSB and grown to early exponential phase, before addition of tunicamycin. Cells were harvested by centrifugation after 2.5 or 5hrs and fixed using a mixture of 1.25% formaldehyde, 2.5 % glutaraldehyde and 0.03% picric acid in 0.1M sodium cacodylate buffer, pH 7.4. Fixed cells were washed 3x in sodium cacodylate buffer, then incubated for 1hr in 1% OsO_4/1.5% $K_4Fe(CN)_6$ in H_2O, washed 3x in H_2O, and dehydrated in ethanol. Cells were then incubated in propyleneoxide for 1 hour, then infiltrated with 1:1 Epon:propylene oxide for 2-3hrs, embedded in Epon, sectioned via microtome, and stained using uranyl acetate.

4.3.3: Phase Contrast and Fluorescence Microscopy

Cells from exponential phase culture were pelleted and resuspended in 1X PBS. For fluorescent D-amino acid labeling, cells were resuspended in 1X PBS + 100μM D-amino acid conjugate and incubated for 1 minute, then diluted with 200μL of 1X PBS, pelleted, and resuspended in fresh 1X PBS. Cells were then mounted on slides covered with a 1% agarose in 1X PBS pad. Images were acquired with either a Hamamatsu digital camera (ORCA-ER) connected to a Nikon Eclipse TE2000-U microscope with an X-cite 120 illumination system or an Olympus BX61 microscope with a phase contrast objective UplanF1 100x and captured with a monochrome CoolSnapHQ digital camera (Photometrics). Image manipulation was limited to changing brightness and contrast via ImageJ or FIJI (197).

4.3.4: Raising and Testing Suppressors of WTA and Dlt Synthetic Lethality

Dilutions of stationary phase starter cultures were plated on TSB agar plates with (or without, for titering) 0.4μg/mL tunicamycin and grown for 24 hours at 37°C.

Table 4.1 Strains used in this study

Strains	Relevant Genotype	Reference or Source
RN4220 Δ*atl::kan*^{R}	RN4220 Δ*atl::kan*^{R}	Ting Pang, Bernhardt Lab
HG003 Δ*sle1::kan*^{R}	HG003 Δ*sle1::kan*^{R}	Ting Pang, Bernhardt Lab
Newman	ST8; CC8 isolated in 1952 human clinical MSSA	(69)
SEJ1	RN4220Δ*spa*	(100)
4S5	SEJ1Δ*ltaS* suppressor strain	(55)
JSM061	Newman Δ*dltA*	This Thesis
JSM157	SEJ1 [pLOWFtsZGFP] by transduction Em^R	This Thesis
JSM158	4S5 [pLOWFtsZGFP] by transduction Em^R	This Thesis

JSM139	JSM061 [Δ*atl::kan*^{R}] by transduction, Km^R	This Thesis
JSM138	JSM061 [Δ*sle1::kan*^{R}] by transduction, Km^R	This Thesis
JSM162	MW2 [Δ*sle1::kan*^{R}] by transduction, Km^R	This Thesis
JSM163	MW2 [Δ*atl::kan*^{R}] by transduction, Km^R	This Thesis

Table 4.2 Plasmids and oligonucleotides used in this study

pLOWFtsZGFP	pLOW for expression of FtsZ-GFP Carb^{R}Em^R	(141)

4.4 Results and Discussion

4.4.1: LTA and Dlt Null Strains Depleted of WTAs Have Distinct Terminal Phenotypes

We were surprised that D-alanylation becomes essential when WTAs, but not LTAs, are deleted because D-alanylation is a shared tailoring modification of LTAs and WTAs. As LTAs are themselves essential in the absence of WTAs, we wondered whether mutants lacking the entire LTA backbone would have a terminal phenotype upon WTA depletion similar to mutants lacking only the D-alanine modification. To address this question, we used electron microscopy to examine strains deficient in LTAs or D-alanylation after treatment with tunicamycin to deplete cells of WTAs. Compared to untreated wildtype (Figure 4.2*A*, Supplemental Folder 4), tunicamycin-treated cells have thickened crosswalls and impaired daughter cell separation. Moreover, successive division planes are frequently placed at non-orthogonal angles and duplicated septa are common (note parallel crosswalls enclosing a narrow band of cytoplasmic material in Figure 4.2*B*) (44; 200). Cells lacking LTAs due to *ltaS* deletion showed similar defects in cell separation and septal placement (Figure 4.2*C*). These phenotypes, described previously, show that WTAs and LTAs help regulate *S. aureus* cell division (44; 52; 168; 200). The *dlt* null cells resembled untreated wildtype except for

irregularities in peptidoglycan thickness and membrane contour both at crosswalls and along the cell periphery. In addition, lysed cells ("ghosts") were commonly observed (Figure 4.2*D*). These phenotypes imply that D-alanylation contributes to cell envelope integrity, either directly or through regulation of cell wall biosynthetic or hydrolytic enzymes. The Δ*dltD*Δ*ltaS*$_{4S5}$ mutant appeared identical to the Δ*ltaS*$_{4S5}$ mutant, suggesting that deleting LTAs is epistatic to removing D-alanylation (Figure 4.3*A*, Supplemental Folder 5); however, *dlt* null strains in which WTAs were depleted showed defects characteristic of deficiencies in both pathways, but exaggerated. For example, crosswalls were mispositioned and daughter cells failed to separate as in WTA-deficient cells, but there were also marked aberrations in cell envelope ultrastructure characteristic of D-alanylation deficient cells (Figure 4.3*B*). Within five hours of treatment, nearly complete cell lysis was evident in treated samples, suggesting that the combined defects so weakened the cell envelope that rupture resulted (Figure 4.3*C*). Remarkably, the Δ*ltaS*$_{4S5}$ and Δ*dltD*Δ*ltaS*$_{4S5}$ mutants depleted of WTAs did not resemble cells lacking only one type of TA. Whereas we frequently observed duplicated and misplaced crosswalls in images of cells lacking either WTAs or LTAs, we saw almost no crosswalls in fields of cells that had both polymers removed (Figure 4.3*D*). We confirmed that the lack of septa was not due to cell death - these cells were still viable as assessed by ATP production (via reaction with a luciferase kit), and plating in the absence of tunicamycin yielded colony growth. This suggested that at least one type of teichoic acid must be present in order for division to initiate and progress.

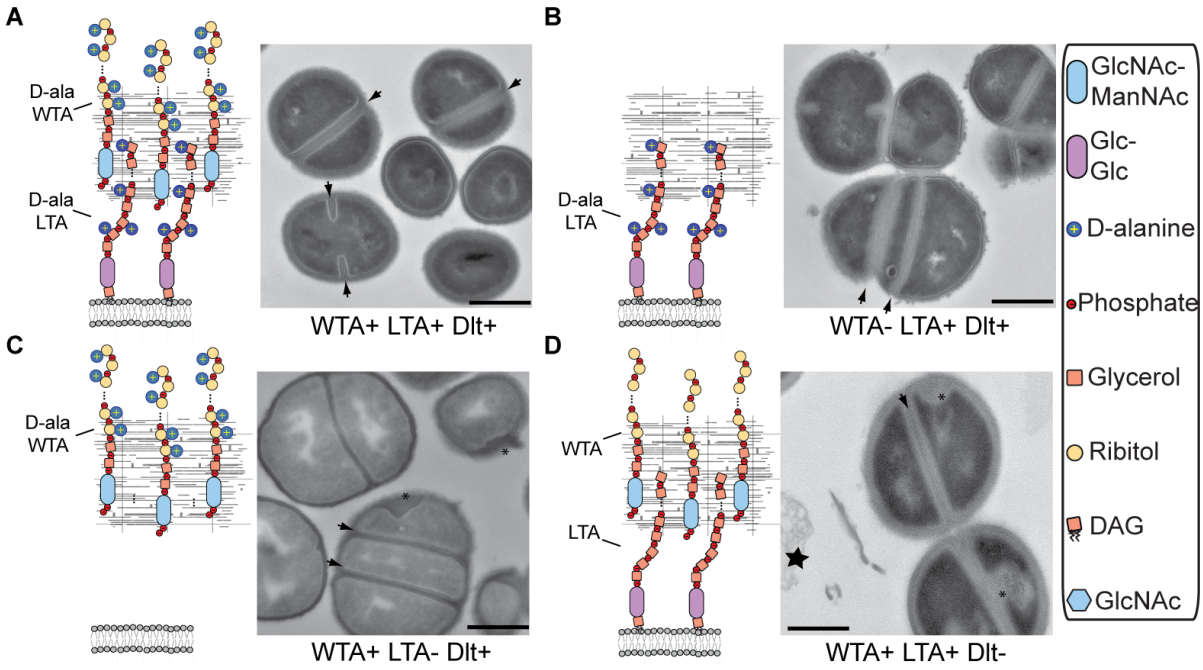

Figure 4.1: Effect of removing TAs and D-alanylation on cell morphology. Electron micrographs of *S. aureus* strains, grown in the presence and absence of 0.4µg/mL tunicamycin. To the left of each electron micrograph is a schematic showing the type of TAs present and their D-alanylation status. (A) WT cells, with division septa (black arrows); (B) WT cells treated with tunicamycin to remove WTAs. The dark line along the crosswall disappears and septal positioning is dysregulated (black arrows). Cells also fail to separate efficiently; (C) Δ*ltaS*$_{4S5}$ cells exhibit defects similar to strains lacking WTAs, with multiple septa, larger cell size, and deficiency in separation; (D) Both Δ*dltA* (shown) and Δ*dltD* (Supplemental Folder 4) mutants retain the dark midline at the crosswall (black arrow), but show several defects, including concavities in the cell membrane and irregular thickening of peptidoglycan (black asterisks) and ghost cells (black star). EM scale bars represent 500 nm. Additional fields of view are provided in Supplemental Folder 4.

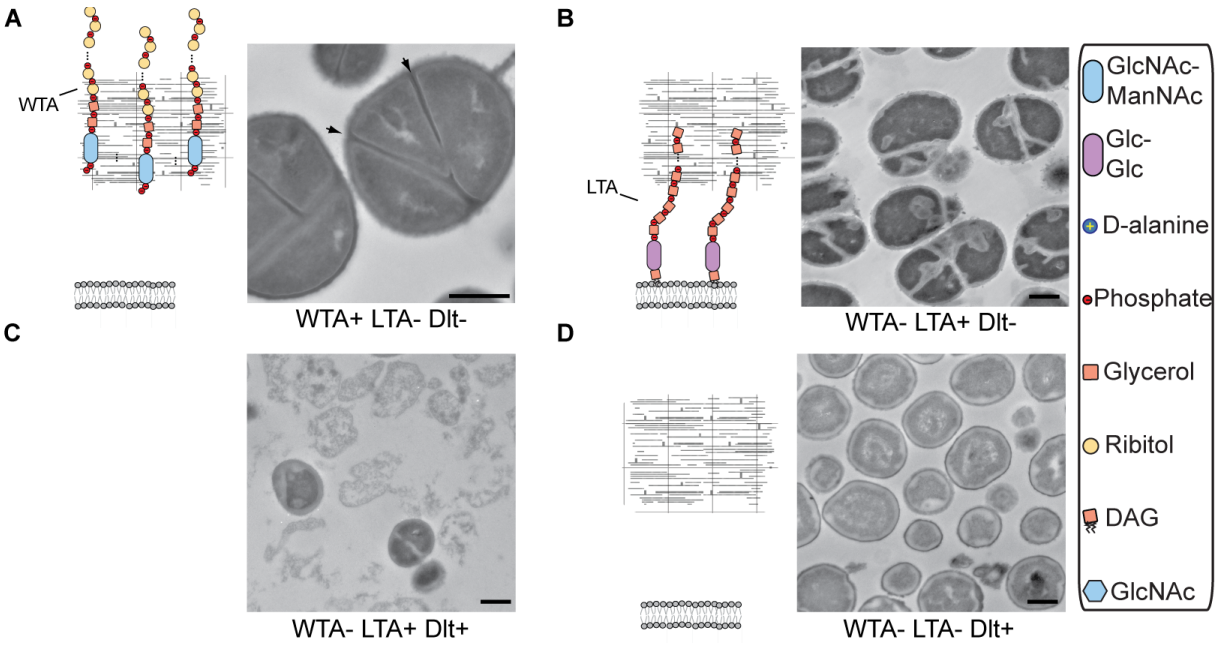

Figure 4.3: Effect of removing TAs and D-alanylation on cell morphology. Electron micrographs of S. aureus strains, grown in the presence and absence of 0.4 µg/mL tunicamycin. To the left of each electron micrograph is a schematic showing the type of TAs and their D-alanylation status. (A) The Δ*dltD*Δ*ltaS*$_{4S5}$ mutant exhibits defects similar to Δ*ltaS*$_{4S5}$, including non-orthogonal septation,larger cells, and deficiency in cell separation; Cells lacking D-alanylation and treated with tunicamycin for 2.5hrs (B) and 5hrs (C) exhibit exacerbated morphological defects, including impaired cell separation, increased incidence of membrane concavities and irregular peptidoglycan thickening, and improper placement and organization of septa; (D) Δ*ltaS*$_{4S5}$ cells treated with tunicamycin show near complete abolition of cell septation. Scale bars represent 500 nm. Additional fields of view are provided in Supplemental Folder 5.

4.4.2: LTA Null Strains Depleted of WTAs Cannot Form Z Rings

FtsZ is the first intracellular protein to move to the division site during cell division, and is essential for recruiting other components of the division machinery (1). We wondered whether mutants lacking both LTAs and WTAs were blocked at the stage of FtsZ assembly or later in the division cascade. We transduced cells with FtsZ-GFP, grew them in the absence or presence of tunicamycin to deplete WTAs, and used fluorescence microscopy to assess Z ring formation. We observed rings of fluorescent FtsZ in wildtype cells, cells lacking only one TA polymer, and in cells lacking D-alanylation, but saw no Z rings in Δ*ltaS*$_{4S5}$ cells depleted of WTAs (Figure 4.4). Thus, simultaneous removal of both types of TAs results in an inability to assemble Z rings and cells can no longer divide.

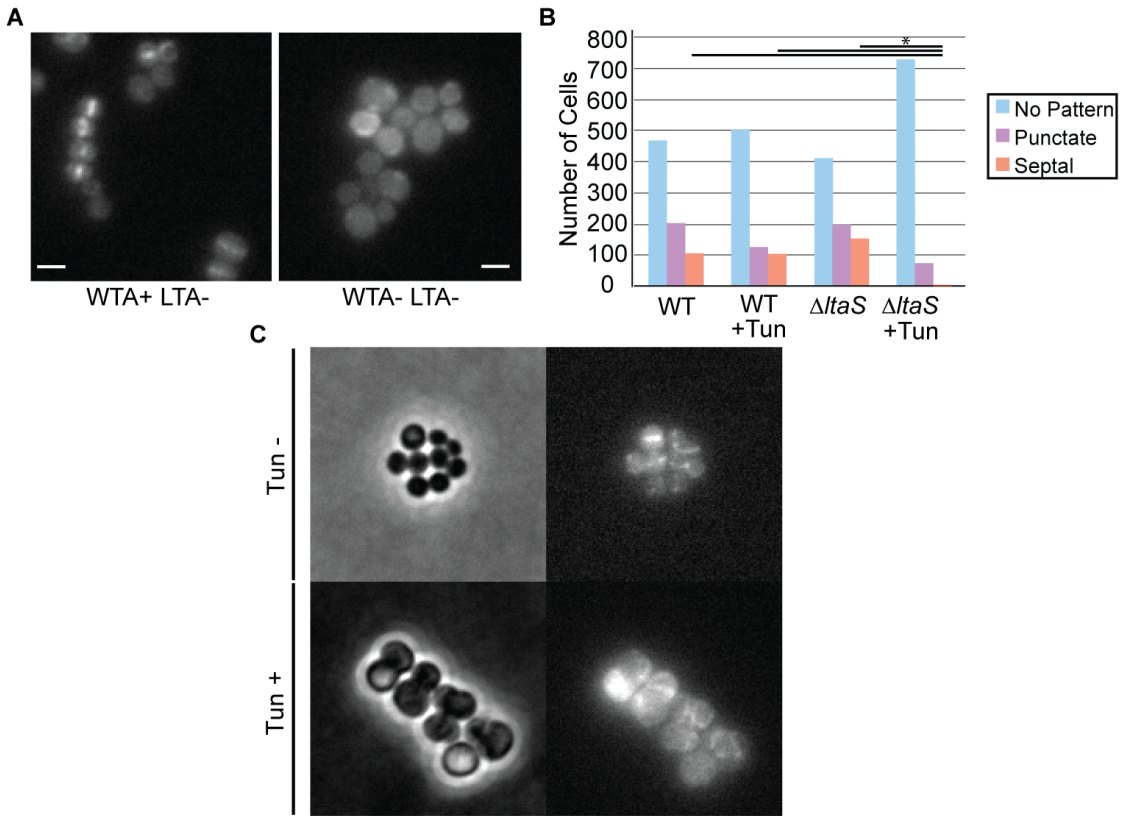

Figure 4.4: Effect of removing TAs on peptidoglycan biosynthesis and FtsZ localization. Light microscope images of S. aureus strains, grown in the presence and absence of 0.4

μg/mL tunicamycin. (A) Localization of FtsZ-GFP in untreated (left) and tunicamycin-treated (right) Δ*ltaS*$_{4S5}$ cells. Scale bars represent 1 μm; (B) Δ*ltaS*$_{4S5}$ treated with tunicamycin lacked septal fluorescence incomparison to the other conditions ($p<10$ by two-tailed t-test). (C) Newman Δ*dltA* with and without tunicamycin treatment showed localized FtsZ patterns. Additional fields of view are provided in Supplemental Folder 5.

4.4.3: Cells Lacking D-alanylated LTAs Have Altered PG Biosynthesis

Previous work from our lab has revealed a synthetic lethal relationship between WTA and PG biosynthesis, implying a functional connection between the two pathways (44). Others have shown that removing WTAs alters the localization of PBP4, and that WTA polymers physically interact with PBP2A and FmtA (11; 184). Concomitantly, strains lacking WTAs have decreased PG cross-linking by muropeptide analysis (200). In order to determine whether removal of D-alanylation and/or LTAs also affected PG biosynthesis, we treated cells with a fluorescein-conjugated D-lysine analog. This fluorescent D-amino acid is believed to be incorporated at sites of nascent PG biosynthesis in *S. aureus* via the back reaction of DD-carboxypeptidases (132).Treatment of wildtype and Δ*dltA* cells with the probe for 1 minute resulted in localized fluorescence characteristic of nascent PG biosynthesis as described by others using BODIPY-vancomycin conjugates (Figure 4.5) (219). Upon tunicamycin treatment, wildtype cells exhibited more diffuse fluorescence than untreated cells, while Δ*dltA* cells retained punctate fluorescence with a greater number of foci per cell. The mutant's altered localization pattern did not correlate with dead cells as assessed by propidium iodide staining. This suggested the observation was not an artifact of cell death, and that dysregulated PG biosynthesis precedes lysis.

These data provide further evidence for WTAs playing a role in modulating PG biosynthesis, and reveal a new role for LTAs lacking D-alanylation in directing nascent PG biosynthesis. In their transmission electron micrographs, Saar-Dover and colleagues reported that mutants lacking TA D-alanylation had increased cell wall density (192). While this was attributed primarily to the role of D-alanines in influencing LTA conformation at the membrane interface, our data suggest that D-alanines of LTAs regulate PG crosslinking. In treating Δ*ltaS*$_{4S5}$ mutants with the fluorescent probe, we observed low incorporation independent of tunicamycin treatment; however, this mutant is known to contain a suppressor mutation in the c-di-AMP phosphodiesterase GdpP attenuating its function, and Δ*gdpP* mutants exhibit a higher degree of muropeptide crosslinking, which may interfere with incorporation of the probe (55).

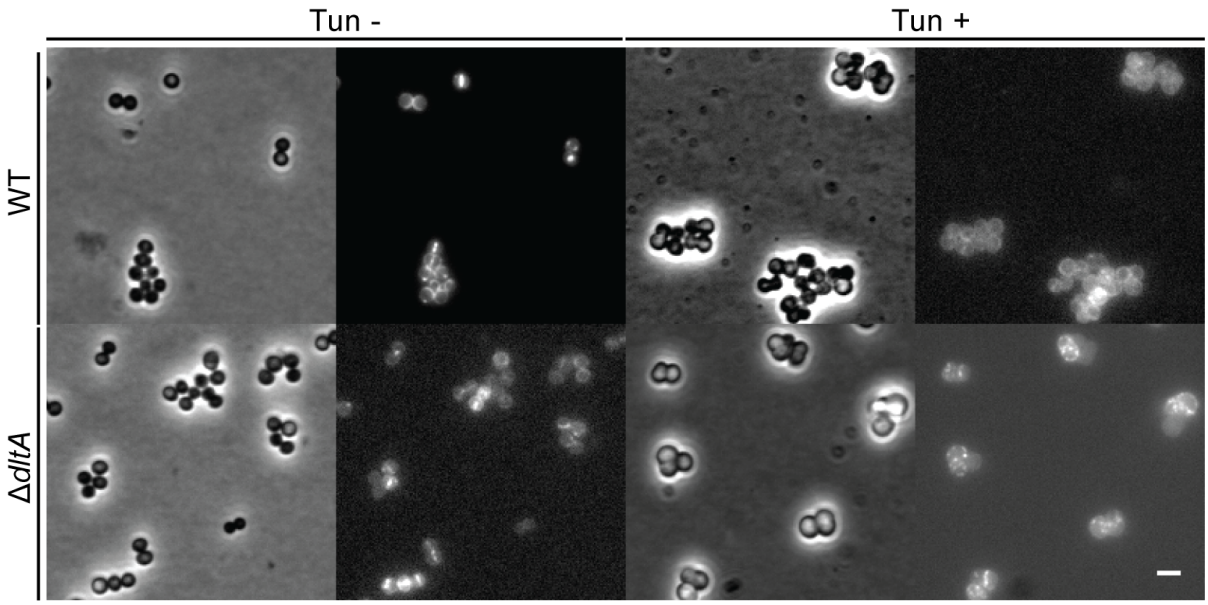

Figure 4.5: Treatment of Newman WT and Δ*dltA* with fluorescein-conjugated, amidated D-lysine to label sites of nascent PG biosynthesis. Further treatment with tunicamycin altered the localization pattern for each strain. Scale bar represents 2μm.

4.4.4: Deletion of Key Autolysins Does Not Suppress Synthetic Lethality Between the D-alanylation and WTA Pathways

Murein hydrolases serve a variety of roles in bacterial physiology by catalyzing turnover and modification of the cell wall. In *S. aureus*, PG hydrolases are required for the proper separation of daughter cells after septal PG deposition - mutants defective in Atl (bifunctional N-acetylmuramoyl-L-Ala amidase and endo-beta-*N*-acetylglucosaminidase), Sle1 (also known as Aaa, N-acetylmuramoyl-L-Ala amidase), and LytN (bifunctional *N*-acetylmuramyl-L-Ala-amidase and D-Ala-Gly endopeptidase) form characteristic aggregates of cells (87; 118; 207). Both WTAs and D-alanylation are known to regulate autolysin function. Δ*tarO* mutants exhibit elevated autolysis and lose septal localization of Atl by immunofluorescence microscopy (200). In contrast, tunicamycin enabled the septal localization of exogenously applied, fluorescent Sle1 and LytN (though this phenotype was not observed in a Δ*tarO* mutant(89). Δ*dltA* mutants also exhibit increased autolysis and it has been proposed that D-alanine esters modulate hydrolase activity by masking TA binding sites from positively-charged autolysin repeat domains (166; 256).

Previous genetic experiments have demonstrated that deletion of both Atl and Sle1 is synthetically lethal. Because WTAs and D-alanylation are known regulators of autolysins and are also synthetically lethal with each other, we wondered whether we could combine disruptions of these factors to map pathway-specific associations. We were able to construct deletion strains Δ*atl*Δ*dltA* and Δ*sle1*Δ*dltA*, which argued that TA D-alanylation is either in the same functional pathway as these autolysins, or acts independently of them. Furthermore, we found that Δ*atl* and Δ*sle1* were not killed by tunicamycin treatment. Electron microscopy revealed that strains under these conditions were mostly arrested in cell division (Figure 4.6,

Supplemental Folder 4). Δ*atl*Δ*dltA* and Δ*sle1*Δ*dltA* mutants appeared similar to both parent single mutants in possessing defects in cell separation and displaying occasional "ghost" cells due to lysis (Figure 4.7, Supplemental Folder 4). Upon tunicamycin treatment, these mutants appeared very similar to Δ*dltA* mutants treated with tunicamycin, revealing that single deletion of two major autolysins, Atl and Sle1, does not abrogate the synthetic lethality between the WTA and Dlt pathways. Additional hydrolases not associated with lysogenic phage can be found in the *S. aureus* genome (*e.g. amiC*, *lytX*, *lytY*, and *lytZ*) - though biochemical characterization of the encoded proteins has not yet been reported, it is possible that these other autolysins may become dysregulated upon removal of D-alanylation and WTAs, or that PG hydrolysis may not play a role in this synthetic lethal interaction.

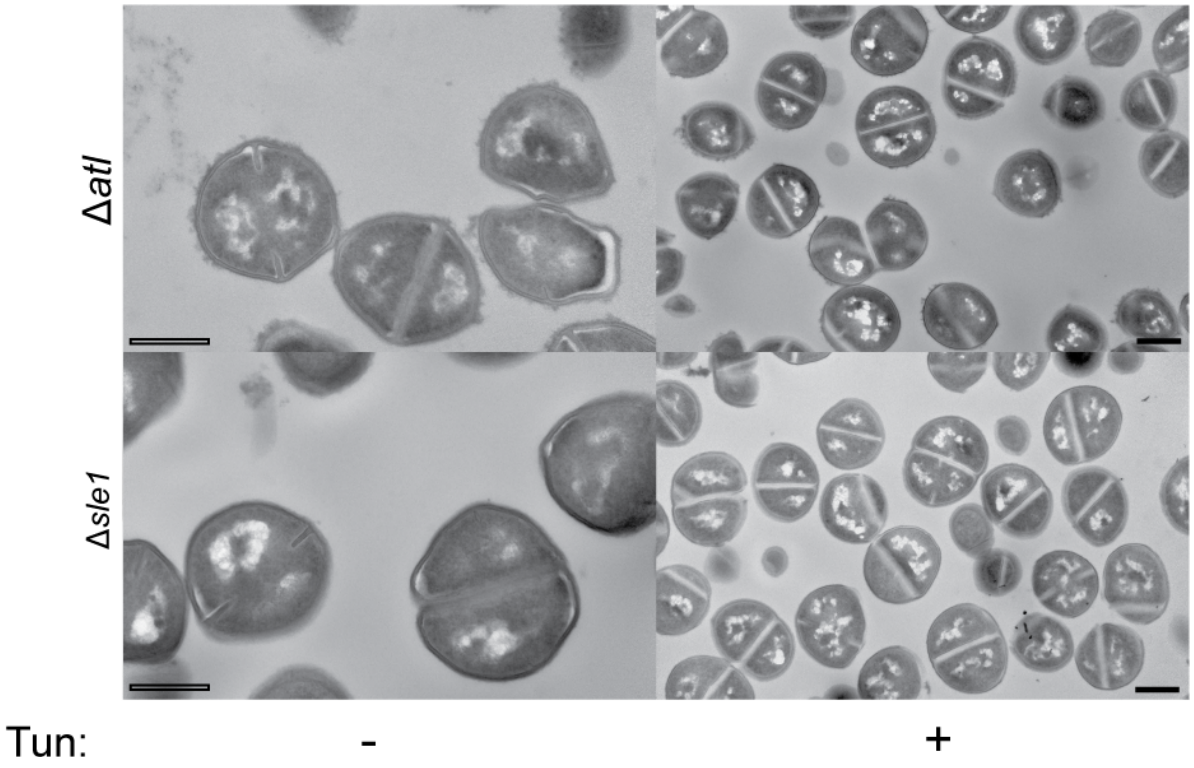

Figure 4.6: Electron micrographs of Δ*atl* and Δ*sle1* mutants with and without 0.4 μg/mL tunicamycin treatment for 1 hr. Scale bars represent 500μm.

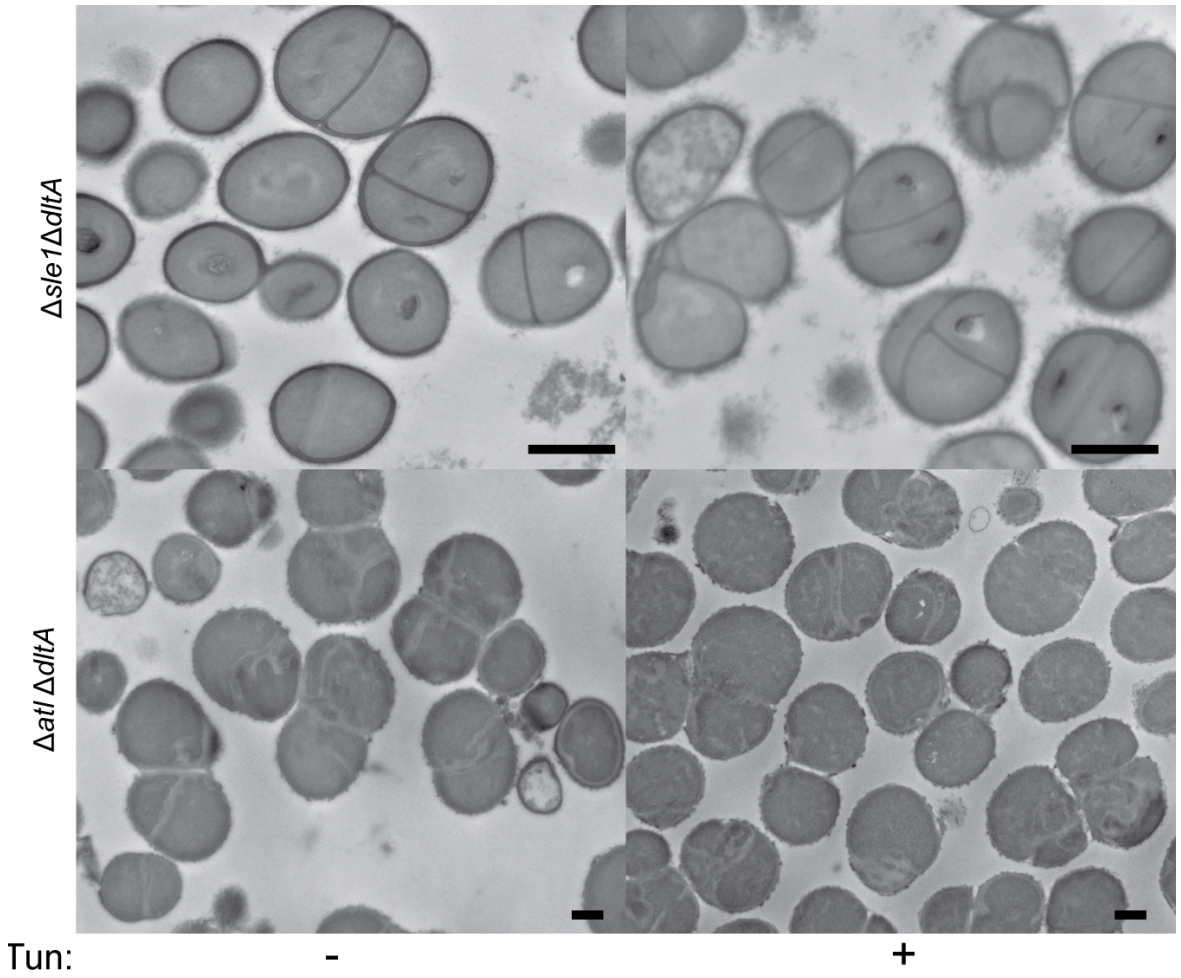

Figure 4.7: Electron micrographs of Δ*atl*Δ*dltA* and Δ*sle1*Δ*dltA* mutants with and without 0.4μg/mL tunicamycin treatment for 2.5hrs to deplete WTAs. Scale bars represent 500 nm.

4.4.5: Dlt and LTA Mutants Depleted of WTAs Have Different Suppressibility

In order to gain insight into the biological mechanism behind the observed synthetic lethality between the Dlt and LTA pathways and WTAs, we attempted to raise suppressor mutants. The frequency by which mutants arise provides insight into the nature of suppression, and assessing mutant phentoypes, in addition to sequencing, can provide information about how suppressors alter the function of their target. Attempts to raise suppressors from Δ$ltaS_{4S5}$ treated with tunicamycin proved unsuccessful, which suggested a

frequency of $<10^{-9}$. This observation argued that either synthetic lethality is unable to be suppressed, or that a combination of mutations is necessary to restore growth in the presence of tunicamycin. In contrast, we raised colonies on plates from Δ*dltA* and Δ*dltD* treated with tunicamycin at frequencies in the range of 10^{-6} to 10^{-7}. This suggested, though did not prove that loss-of-function mutations could alleviate the synthetic lethality between the Dlt and WTA pathways. Further studies to characterize suppressor mutants that remain WTA-null may identify cellular factor(s) that connect the WTA and Dlt pathways.

4.5 Conclusion

We found that D-alanylation became essential on LTAs when WTAs were removed, but was not essential on WTAs when LTAs were removed. The D-alanine deficient cells had defects in cell wall ultrastructure and displayed increased lysis, showing that the D-alanine modification on LTAs contributes to membrane integrity. The combined defects from removal of WTAs and D-alanylation evidently lead to catastrophic cell envelope damage during ongoing cell division. This lysis does not appear to be mediated by the autolysins Atl and Sle1, though we cannot rule out the activity of other autolysins not tested. Instead, it appeared by fluorescent D-amino acid incorporation that PG biosynthesis became dysregulated in Dlt^- mutants treated with tunicamycin.

An unexpected result to emerge from our studies was that simultaneous removal of LTAs and WTAs prevents FtsZ ring assembly and causes cell division to cease. FtsZ polymers serve as a scaffold for the recruitment and organization of division proteins at the septum. How extracellular TA polymers can influence the intracellular organization of division machinery remains unclear. Several proteins such as the nucleoid occlusion factor

(Noc), FtsA, and EzrA are known regulators of FtsZ polymerization, and both DNA damage and the stringent response can affect Z ring assembly (1), so it is possible that removing TAs activates these pathways. Alternatively, removing both kinds of teichoic acids may also affects membrane potential, which is known to affect FtsZ and FtsA association with the membrane (31,)

Chapter 5: High-Throughput Pathway-Directed Chemical Screens to Identify Synthetic Lethal Inhibitors

The experiments described in this chapter have been performed in collaboration with Lincoln Pasquina of the Walker Lab.

5.1 Abstract

Innovative strategies are needed to combat the imminent threat of antibiotic resistant bacterial infections. Chapter 3 described a method for identifying new synthetic lethal target pairs. Here we demonstrate that one can seamlessly transition to screen for chemical inhibitors of identified targets using strains created to validate synthetic lethal interactions. We screened ~41,000 compounds looking for inhibitors of the WTA and Dlt pathways. In addition to rapidly eliminating ineffective and toxic compounds, we found and reconfirmed several primary hits, generating new chemical matter for target identification and lead optimization. Thus, parallel, pathway-directed screening is a new and useful approach for identifying chemical inhibitors within a pathway of interest that can be used in investigation of pathway biology and for synthetic lethal compound combinations.

5.2 Introduction

The current rise in the prevalence of antibiotic-resistant infections in combination with the "discovery void" or "innovation gap" representing a lack of newly developed candidate antibiotics portends a dangerously imminent return to the pre-antibiotic era. While new governmental incentives such as the Generating Antibiotic Incentives Now (GAIN) Act hope to promote growth and development in this area, the concurrent exit of many pharmaceutical giants from the antimicrobial sector relegates the responsibility of finding promising lead compounds to academic labs. In this vein, academia has generally been afforded greater flexibility in its research pursuits, leading to the investigation of numerous alternative strategies to traditional antibiotics in order to combat the problem of drug-resistant bacteria (90).

Compound combinations have been touted as a promising new approach to targeting bacterial infections. Such cocktails may help lower the incidence of drug resistance and expand our current range of targets(230). Some combinations have already been employed clinically, such as Synercid and trimethoprim/sulfamethoxazole. Each of these combinations is composed of synergistic compounds targeting the same complex or pathway. In contrast, the combination of a beta-lactamase inhibitor and a beta-lactam, Augmentin, works by first disabling the bacteria's resistance mechanism, thus allowing the beta-lactam to more fully inhibit its intended targets, transpeptidases that construct the cell wall. Recently, it was shown that simple metabolic products, such as fumarate and mannitol, can potentiate the effects of traditional antibiotics – while the mechanism is being actively investigated, researchers have proposed that these compounds serve to perturb the metabolic state of the cell, causing them to become more susceptible to oxidative damage and increase drug uptake (3).

Because of their combinatorial nature, probing compound cocktails for efficacy in antibacterial screens can be prohibitive. Previous screens have been limited to known antibiotics in combination with previously approved drugs or bioactives (71; 213). Another approach has been to keep one drug constant, and look for compounds that potentiate its effect. We, and others have specifically applied this approach to find compounds that restore beta-lactam susceptibility to MRSA strains (80; 111; 215; 233). One major disadvantage of this approach is that there may be several underlying genetic factors that may contribute to compound sensitivity, leading to high hit rates and difficulties in target identification. For example, several genes are known to contribute to β-lactam resistance in MRSA making it difficult to immediately discern compound interactions and mechanism of action (21; 44).

Pathway-directed screening is one way to combat the target identification problem. In this method, wildtype and pathway-deficient mutants are screened in parallel, with the aim of identifying hits as differentially killing the mutant strain that act within the pathway of interest. By assaying wild-type and Δ*tarO* strains, the Walker lab employed this technique to discover 1835F03, a late-stage inhibitor of the *S. aureus* WTA biosynthetic pathway (212), and later researchers from Merck replicated this approach to identify additional inhibitors for the same target (233).

In Chapter 3, I described a method for identifying synthetic lethal gene pairs that when simultaneously disrupted lead to cell death. In the process of validating these interactions, we generated single knockout mutants for each of the gene pairs. These materials were then directly translated into parallel, pathway-specific screens to search for compounds that inhibit each half of the synthetic lethal interaction between the WTA and D-alanylation pathways (Figure 5.1). Both of these pathways are known virulence targets, yet the combination of antivirulence inhibitors targeting each factor would be predicted to have a lethal effect for *S. aureus* (45; 53; 59; 153; 190; 212; 233). We found that parallel screening improved discriminatory power, enabling rapid classification of compounds into classes and removal of undesired classes, such as generally toxic and ineffective compounds. We obtained and validated a small number of hits that we are currently investigating, in order to identify their targets and mechanisms of action.

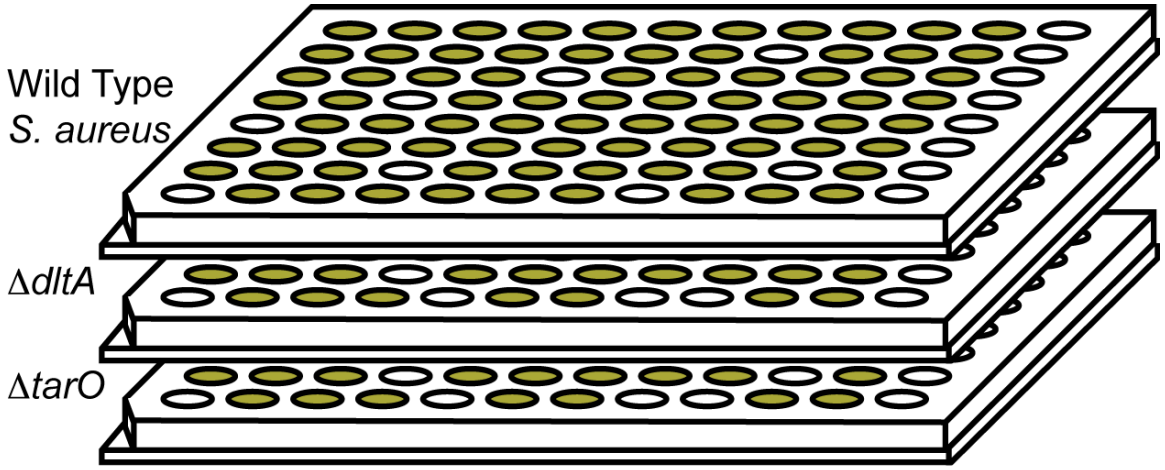

	WT	Δ*tarO*	Δ*dltA*
No Effect	High OD	High OD	High OD
Toxic	Low OD	Low OD	Low OD
TarO inhibitor	Mid OD	High OD	Low OD
DltA inhibitor	High OD	Low OD	High OD
3rd pathway?	High OD	Low OD	Low OD

Figure 5.1: Parallel, pathway-directed screening approach for the discovery of small molecules targeting the synthetic lethal interaction between the WTA and Dlt pathways. Hits were classified into subcategories based on differential killing of the screened strains

5.3 Methods

5.3.1 Screening Protocol

The night before screening, a starter culture of each strain was inoculated in tryptic soy broth (TSB) and grown until stationary phase. Thirty microliters of TSB was dispensed into all wells in lanes 1–23 of a 384-well plate (Corning® 3009) using a Matrix WellMate® plate filler and stacker. Controls were as follows: wells in lane 23 served as negative controls for full growth in the absence of any inhibitors; wells A–L in lane 24 served as positive

controls for the growth inhibitory activity of synthetic lethal inhibitors and contained final concentrations of 0.4 μg/mL tunicamycin for the Δ*dltA* strain and 10 μg/mL erythromycin for the WT and Δ*tarO* strains. DMSO stock solutions of library compounds (300 nL) were then pin-transferred into lanes 1–22 of duplicate plates. Following compound transfer, an additional 50 μL of TSB containing approximately 2 x 10^6 CFU/mL of *S. aureus* (1000-fold dilution of overnight culture) were dispensed into all wells of all of the plates. Plates were stacked five-high, covered, and incubated at 30 °C for 16 hours. Each strain was tested in duplicate for every compound (6 plates total per compound). The optical density of each well at 600 nm was read on a PerkinElmer Envision plate reader. Raw absorbance measurements were averaged across replicates and compared pairwise between the strains. Hits were determined as possessing a Z score of > 4.7 (p<.000001, by Bonferroni correction), and further classified into categories based on strain-specific killing. Compounds were classified as toxic if they gave OD_{600} measurements within one standard deviation of the mode of the death peak for each strain. Compounds were classified as having no effect on growth if it yielded OD_{600} measurements within one standard deviation of the mode of maximal bacterial growth for each strain.

5.3.2 Secondary Assay to Confirm Cherry Picks

Compounds and control diluent (DMSO) were diluted into wells of a 384-well plate to produce a series of concentrations at equivalent volumes using the Hewlett-Packard D300 Digital Dispenser. After 16 hours of growth at 30 °C, OD_{600} was measured using a Molecular Devices SpectraMax Plus 384 well plate reader.

5.3.3 Construction of a DltA Linkage Construct

PCR amplification products from P1-P2, P3-P4, and P5-P6 were cloned into BamHI/EcoRI-digested pKFC using a Clontech InFusion HD kit.

Table 5.1: Strains used in this study

Strains	Relevant Genotype	Reference or Source
Newman	ST8; CC8 isolated in 1952 human clinical MSSA	
Newman Δ*tarO*	Newman [Δ*tarO*::*tet*^{R}] by transduction, Tc^{R}	
JSM061	Newman Δ*dltA*	This Study
Newman Δ*dltC*	Newman Δ*dltC::aphA3*, Km^{R}	Leigh Matano
MW2 (USA300)	Clinical isolate; community-acquired methicillin resistant (CA-MRSA)	(12)
MW2Δ*dltA*		(42)
SA113	*Agr,* restriction-modfication-deficient derivate of NCTC8325	(179)
SA113Δ*dltA*		(179)
SEJ1	RN4220Δ*spa*	(100)
4S5	SEJ1Δ*ltaS* suppressor strain	(55)
JSM096	TCM011 with *aphA3::kan*^{R} installed upstream of the *dlt* operon	This Study

Table 5.2: Oligonucleotides and plasmids used in this study

Plasmids		
pKFC	Temperature-sensitive shuttle vector; ori^{Ts} Carb^{R}Cm^{R}	(120)
pKFCdltAlinkkan	P1-P4 PCR in pKFC for installation of *aphA-3* downstream of the dlt operon Carb^{R}Km^{R} Cm^{R}	This Study
P1. dltAlink upFor	GACGGCCAGTGAATTCattagtgcctatgcctaaag	

P2: dltAlink upRev	ACCTCAAATGGTTCGCcattaatatgacgagtttataat	
P3: dltAlink downFor	GTTTTAGTACCTAGGtgatgagtttatttgattttgac	
P4: dltAlink downRev	CGACTCTAGAGGATCaaatcgttgggaagaatgaa	
P5: aphA3 For	gcgaaccatttgaggtgat	
P6: aphA3 Rev	cctaggtactaaaacaattcat	

5.4 Results & Discussion

5.4.1 Parallel, Pathway-directed Screening Identified Compounds Selectively Killing WTA and Dlt$^-$ Mutants

We screened 41,087 compounds belonging to 3 chemical classes (commercial vendor library compounds, CVL, known bioactives, KB, and natural products, NP) (Table 5.3). As predicted, we observed innate differences in maximum OD_{600} and compound sensitivity between the strains (Figure 5.2), with Δ*tarO* having an average OD_{600} below both wildtype and Δ*dltA* strains. Therefore, we employed principal component analysis in pairwise comparison of growth measurements for each compound to identify compounds that selectively killed certain strains (Figure 5.3). We binned hits into the following categories: (i) selectively killed Δ*tarO*; (ii) selectively killed Δ*dltA*; (iii) killed both Δ*tarO* and Δ*dltA*, but not wildtype; (iv) protected Δ*dltA* or Δ*tarO*. We were able to immediately remove 34,323 compounds from consideration as generally toxic or ineffective, supporting parallel screening as an approach to quickly identify compounds potentially affecting bacterial growth by a specific mechanism of interest.

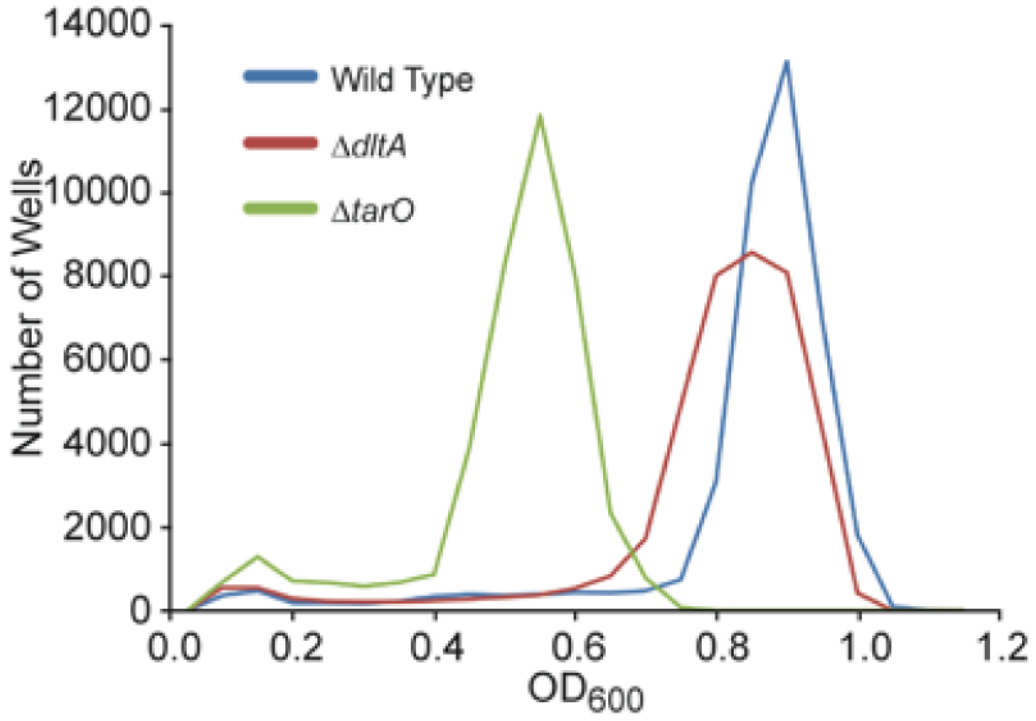

Figure 5.2: Summary of frequencies of observed bacterial growth for each of the screened strains.

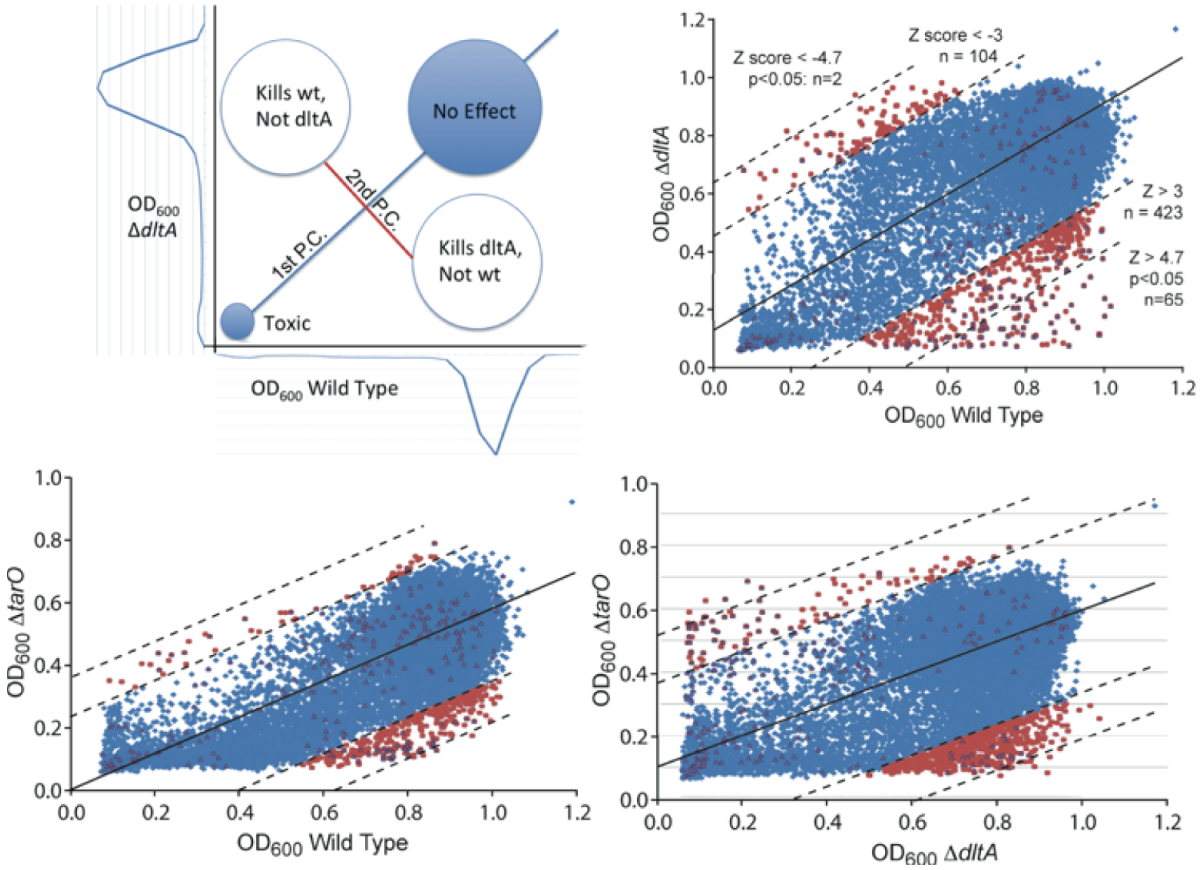

Figure 5.3: Observed distribution of compounds based on pairwise comparison of their effects on bacterial growth. Compounds in red have $Z > 4.7$.

Table 5.3 Summary of Screen Library and Hit Information

	CVL	Known Bioactives	Natural Product	Total		
Total Compounds Screened:	19418	7237	14432	41087		
Identified Hits (|Z|>4.7):	11	27	36	74		
Validated Cherry Picks:	2	15	5			
	WT	Δ*dltA*	Δ*tarO*			
Average Z-factor:	.845	.733	.683			
	WT/Δ*dltA*	WT/Δ*tarO*	Δ*dltA* Δ*tarO*			
Total Hits:	67	7	11			
CVL	9	0	2			

KB	30	3	5			
NP	28	4	4			
Validated Cherry Picks:	19	0	3			
Hit Classes	I	II	III		Generally Toxic	Ineffective
Total Hits:	4	67	3		1090	33233
CVL	0	9	0			
KB	0	30	3			
NP	4	28	0			
Validated Cherry Picks:	2	21	3			

5.4.2 Cherry Picking & Validation

We observed a low hit rate of 0.21%, with a disproportionate majority of hits identified in the known bioactives class. Overall, we found a larger number of compounds that selectively killed the Δ*dltA* strain, - however, this may be a function of library composition. Indeed, the majority of hit compounds in category II were known bioactives, and many have been previously described as compounds to which Δ*dltA* mutants are sensitized. Furthermore, strains lacking D-alanylation are known to have compromised membrane integrity, resulting in increased uptake of positively charged compounds (192). In order to confirm the observed effect of compound hits on bacterial growth, we cherry-picked a subset from each class and tested their effect on growth of a larger subset of strains in dose-dependent format. Out of 41 unique compounds retested, we validated 22 as having dose-dependent and strain-specific inhibition of bacterial growth. These compounds were tested on deletion mutants in other background strains to further corroborate killing dependent on the deleted pathway (Figure 5.4).

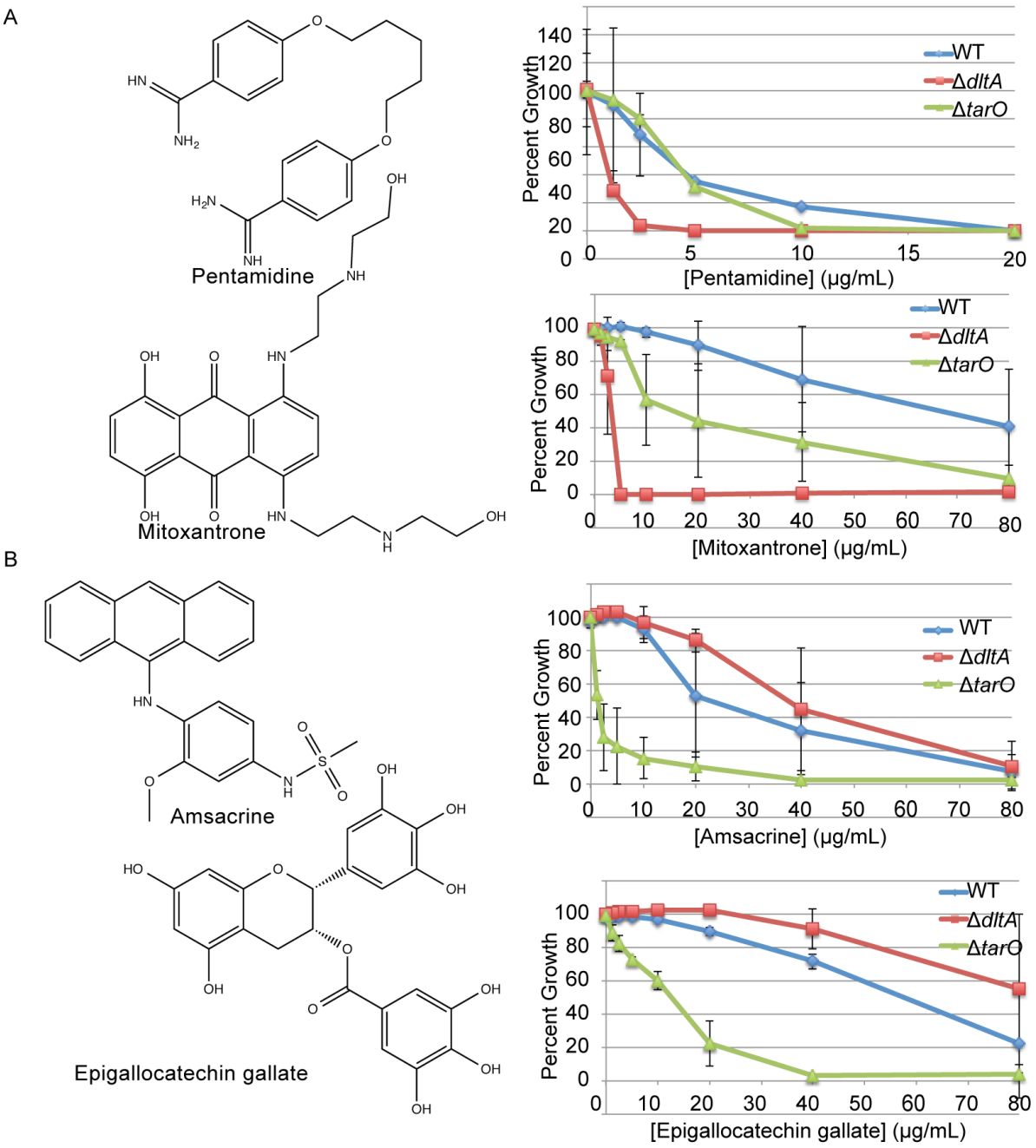

Figure 5.4: Effect of several hit compounds on the growth of wildtype, Δ*tarO* and Δ*dltA* strains.

5.4.3 Hit Analysis

Hits were filtered to remove promiscuous screen positives, *i.e.* compounds that were identified as active in multiple, orthogonal high-throughput screens through query of the ICCB Screensaver and Pubchem databases. Four hits were natural products, which await

isolation, structural characterization, and further assays for biological activity. The remaining hits were mostly known bioactives, which grouped into several classes based on shared structural similarities and/or similar targets and mechanisms of action. Four hits (diethylstilbestrol, hexestrol, toremifene, and tamoxifen) are known antagonists of the human estrogen receptor. They share a tetrasubstituted diphenyl ethylene core, and several have been previously reported as having Gram-positive specific antimicrobial activity, despite the absence of sequence (PSI-BLAST) or structural (FATCAT) homologs of the human target in *S. aureus*. While no mechanism of killing as been confirmed, these agents have exhibited synergy with other membrane actives, suggesting that it is the compromised membrane integrity of the D-alanylation mutant that sensitizes these mutants independent of interaction with the wall teichoic acid pathway (64; 67; 252). This appears to be similar for pentamidine, which has been characterized as a disruptor of the protein-protein interaction between p53 and S100B, but has been described as a promiscuous synergizer acting within the cell membrane, potentiating the activity of numerous other antibiotics in yeast (51; 140; 147). In contrast, mitoxantrone and amsacrine are structurally distinct inhibitors of human topoisomerase II. The *S. aureus* homologs Gyr/GrlAB are validated antibiotic targets of the clinical quinolone and coumerin drug classes. Interestingly, the former selectively inhibits the growth of the Δ*dltA* mutant, while the latter inhibits Δ*tarO*. This suggests that the efficacy of these compounds may be explained by their physicochemical properties and not interactions between these pathways and essential DNA replication. This hypothesis is supported by our previous observation that tunicamycin does not significantly potentiate the antibacterial activity of ciprofloxacin. We also identified several aminoglycoside antibiotics (amikacin, apramycin, bekanamycin, gentamicine) as selective killers of Δ*dltA*, and the

increased susceptibility of these mutants is attributed to a decrease in the positive charge of the cell surface, which normally serves to repel these positively charged drugs. Finally, flavonoids such as epigallocatechin gallate and epicatechin gallate have been studied extensively for their activity as beta-lactam sensitizers in staphylococci (23; 24; 206). These compounds have been found to disrupt the cell membrane, causing a reduction in d-alanylation and mislocalization of PBP2, but they are not believed to have specific interactions with Dlt or WTA machinery. Nevertheless, there are multiple cellular factors beyond the Dlt enzymes that are synthetically lethal with the WTA pathway, and compounds that show Δ*tarO*-specific killing may be exploiting these alternative targets. Similarly, identification of genes synthetically lethal with deletion of the Dlt pathway may provide insight into the targets of compounds that killed the Δ*dltA* strain.

5.5 Conclusion

We conducted a small molecule screen using three different strains in order to identify compounds that exploited the synthetic lethality between the WTA and TA D-alanylation pathways. After compound identification and validation, we now have a collection of promising small molecules that await target identification, potential SAR, and efficacy studies in alternate biochemical and phenotypic assays. Parallel screening represents a promising approach for the discovery of inhibitors that exploit identified synthetic lethal interactions.

Summary, Remaining Questions, and Future Directions

Wall teichoic acids play important roles in the biology of Gram-positives. We sought to further characterize the functions of WTAs in S. aureus by performing a synthetic lethality screen. We created a highly saturated transposon library, treated it with the TarO inhibitor tunicamycin, and identified and validated a subset of genes in multiple cell envelope pathways. Among these genes were those involved in TA D-alanylation and LTA biosynthesis. We chose to further investigate these synthetic lethal interactions and found that cells lacking WTAs and D-alanylation lyse, while cells lacking both LTAs and WTAs stop dividing. Finally, we conducted a pathway-directed, high-throughput screen to identifying compound combinations that exploit cell wall synthetic lethal interactions.

While we have discovered novel interactions with the WTA pathway of *S. aureus* and outlined a new pipeline for identifying synthetic lethal compound combinations, questions old and new remain. These include:

- *Validation of additional genes identified as synthetic lethal when deleted in the absence of WTAs*. While we validated all genes that we selected in the list of top 10 candidates, there are additional genes both within and outside of our thresholds that await further investigation. Because gene deletions remain challenging in *S. aureus*, it may be possible to verify the status of these genes using selected transposon mutants from the Nebraska library. Furthermore, we were unable to assess all ORFs for synthetic lethality due to their low coverage or absence in the transposon library. Advances in transposon delivery and alterations of transposon structure (*e.g.* incorporation of outward facing promoters and transcriptional terminators) will not only afford better coverage to other libraries; it will also enable one to assay the effect

of modulating gene dosage genome-wide on interaction with the WTA pathway. This also facilitates the query of essential genes, by enabling downregulation instead of only blunt disruption.

- *Assessment of intragenic and intergenic regions for synthetic lethality*. We primarily employed the Mann-Whitney U test to identify candidate ORFs synthetically lethal with depletion of WTAs, but this method ignores additional genomic features such as small RNAs and promoter and terminator elements. Newer methods such as Hidden Markov Modeling enable the interrogation of these regions, as well as the contribution of individual domains within a gene to mutant viability.
- *Absolute quantification of genetic interactions or fitness with depletion of WTAs*. In the first TnSeq experiment, van Opijnen & colleagues quantified genetic interactions by calculating the expansion of transposon mutants within the library. Though we used PCR reads as a surrogate for mutant abundance at a final time point, it is possible to directly calculate mutant growth rates by obtaining samples at several time points before and at stationary phase. This approach has an advantage of profiling mutant growth over time, and may serve as a better indicator of fitness in a test condition.
- *Generation of a cell wall interactome*. Our experiments, centered on the WTA pathway, were facilitated through the use of tunicamycin as a specific and nonlethal inhibitor of TarO. Similar inhibitors for other cell wall targets, or less preferably, constructing transposon libraries in deletion mutant backgrounds will generate additional networks to elucidate functional connections between cell envelope components.

- *Characterization of mechanisms of synthetic lethal interactions*. Using tunicamycin to inhibit WTA biosynthesis provided the ability to remove WTA polymers without disrupting potential protein-protein interactions of the WTA biosynthetic enzymes (though it is possible that tunicamycin binding induced an alternate conformation of TarO and had a resulting effect on its interactions). A major question that remains for each of the WTA interaction partners is whether lethality is the result of a disrupted, directed physicochemical interaction with WTA polymers, or whether it is caused indirectly, through an intermediate factor. For several factors, such as *lyrA* and *965*, we are unsure of their physiological roles, and elucidating the mechanism of synthetic lethality will first require characterizing the phenotypes of knockout mutants. Once their functions are clarified, one can then interrogate the effect of blocking WTA surface expression on this function, and design experiments to test for alterations of protein localization, abundance, enzymatic activity, or conformational change. We have also attempted to identify mechanisms by isolating resistant mutants of Δ*dltA* strains treated with tunicamycin, and identification of the genetic determinants of this resistance may shed light on the nature of the interaction between the WTA and D-alanylation pathways.
- *Elucidation of the role of D-alanylation in teichoic acid function*. We observed conditional essentiality of TA D-alanylation only when WTAs, but not LTAs were depleted. While several questions remain regarding how D-alanylation occurs (*i.e.* substrates and function of DltB and DltD, location of the alanylation reaction within the envelope, and whether D-alanines are transferred enzymatically between LTAs and WTAs), our experiments suggest a key functional role for the D-alanines of

LTAs in the cell envelope. Recent findings provide support for TA modifications mediating specific physicochemical interactions and proteomic characterization of pulldowns using WTAs isolated from wildtype and D-alanylation deficient mutants may identify proteins whose binding to TAs is modulated by TA D-alanylation state (42).

- *Illumination of the mechanism of TA control of cell division*. We provided evidence that removal of both WTAs and LTAs prevents the formation of FtsZ rings and abolishes cell division altogether. However, it remains unclear how extracellular TA polymers influence the assembly and activity of cytoplasmic divisome components, and whether TA regulation of division is mediated by specific physical interactions or by general perturbation of envelope structure. We hypothesize that *mreD*, also identified as synthetically lethal with WTA depletion, may be key in mediating interactions between WTA, PG, and division machinery.
- *Identification of the function of bacterial CAAX-like protease homologs.* Though we identified several proteins of unknown function as synthetically lethal with WTA depletion, 3 of the top candidates (2 of which we validated) possessed CAAX-like domains. While this family of enzymes is implicated in the proteolytic processing of prenylated proteins in eukaryotes, the function of these proteins is largely unknown in bacteria. In *B. subtilis*, PrsW was implicated in proteolysis of an anti-sigma factor that represses gene expression, thereby leading to activation of cell wall stress response pathways (73). However, in *S. aureus*, these proteins were implicated in the sorting of surface proteins with YSIRK signal peptides (in *S. aureus* HG003, these include SAOUHSC genes *spa*, 300, 1079, *lytN*, 1843, 1873, *sasB*, 2798, and 3006) (88). The

use of fluorescent protein fusions and the construction of transposon libraries in deletion mutant backgrounds may help determine the function of these proteins and their role in sorting proteins in the cell envelope.

- *Validation of Putative Pathway-Specific Inhibitors.* Though we have identified several compounds that specifically kill Δ*dltA* and/or Δ*tarO*, these compounds must be further validated in follow-up biochemical and phenotypic assays to confirm their action within the pathways of interest. As we have identified multiple cellular targets that are synthetically lethal with removal of WTAs, it is possible that compounds that kill Δ*tarO* may hit these factors over Dlt pathway enzymes. Alternatively, these compounds may lack specific targets, but gain increased access to the cytoplasm or membrane due to inherent defects in the Δ*dltA* and Δ*tarO* cell envelopes. We have generated multiple deletion and complemented mutants within different pathway enzymes to corroborate findings with the Δ*dltA* and Δ*tarO* strains. Furthermore, extensive characterization of Δ*tarO* strains has provided numerous orthogonal assays to test inhibition of WTA production (*e.g.* WTA PAGE, sensitization with Congo Red, synergism with β-lactams, antagonism of Congo Red). Finally, recent work by B. McKay Wood of the Walker lab has led to the reconstitution of DltA for *in vitro* inhibition assays.
- *Generate new antibiotics and new targets for cell envelope active antibiotics.* We have shown that transposon mutagenesis is a valuable tool for discovering new synthetic lethal interactions when used in combination with a nonlethal small molecule inhibitor of a pathway of interest. We also demonstrated a screening technique to find new small molecule inhibitors of identified synthetic lethal targets.

It is our hope that these compounds can be exploited both therapeutically and as probes to investigate pathway biology.

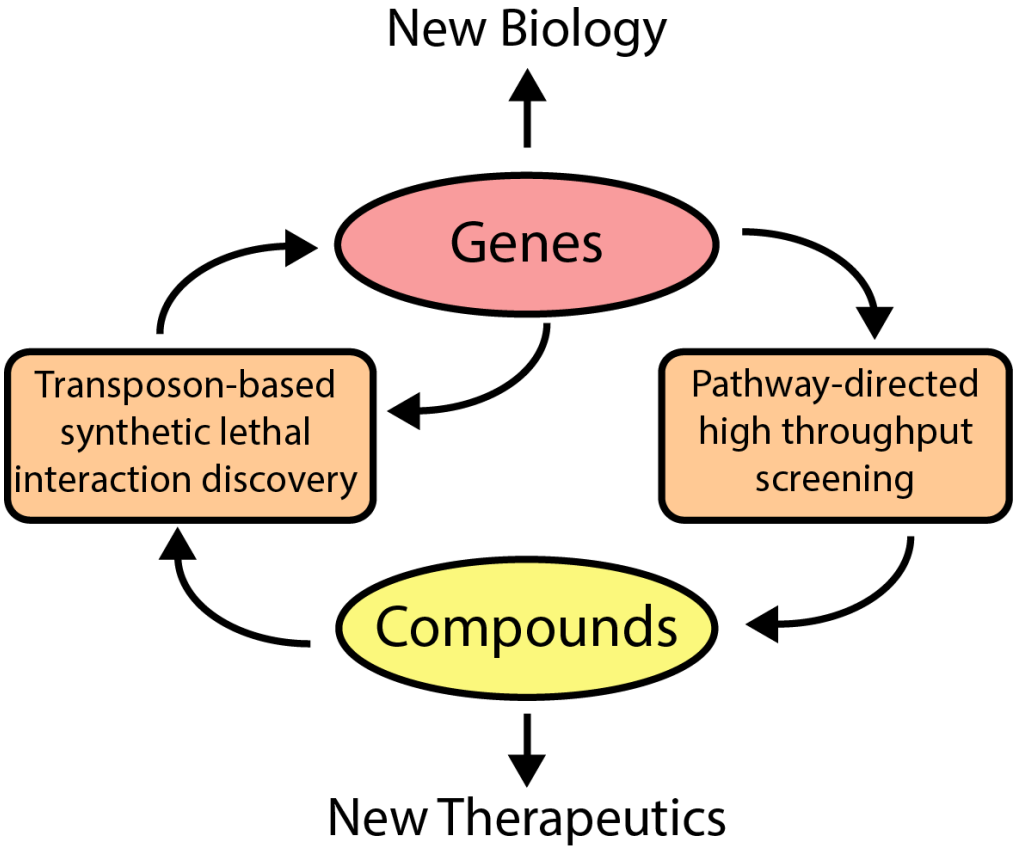

Appendix A: Electron Microscopy of Treatment with a Putative LtaS Inhibitor

A.1: Introduction

Because mutants lacking LTAs are severely compromised in fitness, inhibitors of the LTA biosynthesis pathway are attractive candidates for development as traditional antibiotics. *S. aureus* mutants lacking LTAs cannot grow at high temperatures and must be osmotically stabilized unless several suppressor mutations are present. Richter and colleagues designed a small molecule screen that exploited the temperature sensitivity of LTA mutants and surveyed compounds that only killed *S. aureus* at high temperatures. They reported Compound 1771 (2-oxo-2-(5-phenyl-1,3,4-oxadiazol-2- ylamino)ethyl 2-naphtho[2,1-b]furan-1-ylacetate) as an inhibitor of *S. aureus* LtaS (190). Treatment with this amphipathic compound caused a reduction in immunoreactivity to extracted LTAs, inhibition of recombinant LtaS *in vitro*, and inhibition of *S. aureus* growth *in vitro* and in a mouse infection model. However, compound 1771 exhibited a steep dose-response profile, none of several compound analogs tested retained activity, and they were unable to raise resistant mutants, all of which are characteristics of compounds that work non-specifically to disrupt the bacterial membrane. Nevertheless, we were interested in using compound 1771 to help elucidate the functions of LTAs and screen for genes that are synthetic lethal with LTA depletion. In order to examine the effect of compound 1771 treatment on cells, we first determined the MIC in *S. aureus* Newman to be 12.5 μM (growing overnight at 37°C), similar to that reported. We also attempted to raise resistant mutants on agar plates containing 15μM compound 1771 in wildtype, Δ*tarO*, and Δ$ltaS_{4S5}$ backgrounds over 24 hrs at 37°C, but were unable to obtain any colonies, suggesting resistance frequencies $<10^{-9}$ and similar to the results reported for wildtype strains. As the Δ$ltaS_{4S5}$ strain is missing the

putative target of compound 1771 and has a suppressor mutation enabling the growth of cells without LTAs, we hypothesized that this compound has off-target effects.

To further examine the effects of compound 1771 on cellular morphology and growth, we treated cells with 15μM compound for 2.5 hrs at 37°C and examined their phenotypes using transmission electron microscopy. In contrast to reports and observations of LTA-deficient strains, which exhibit noticeable defects in cell size, septation, and separation, the wildtype strain appeared normal in size and formed cells with single septa (Figure A.1). However, these cells exhibited a greater number of mesosomes than untreated cells, and appeared to have defects in cell membrane ultrastructure. This was less true for the Δ*dltA* mutant, which appeared similar to untreated cells and retained a small presence of ghost cells. Strikingly, treated Δ*tarO* cells exhibited increased lysis in comparison to untreated cells. It also septated in contrast to $\Delta ltaS_{4S5}$ cells treated with tunicamycin. Though these results argue that compound 1771 does not phenocopy *ltaS* deletion, it is important to consider that small molecule inhibition of LtaS would slowly deplete cells of LTAs. Though we waited approximately 5 doubling times until sample collection, it is possible that residual LTA remains. To further analyze the effect of slowly titrating out LtaS activity using a genetic approach, one could construct a strain with *ltaS* under a tightly-controlled and inducible promoter and examine phenotypes of cells collected over a time course of depletion.

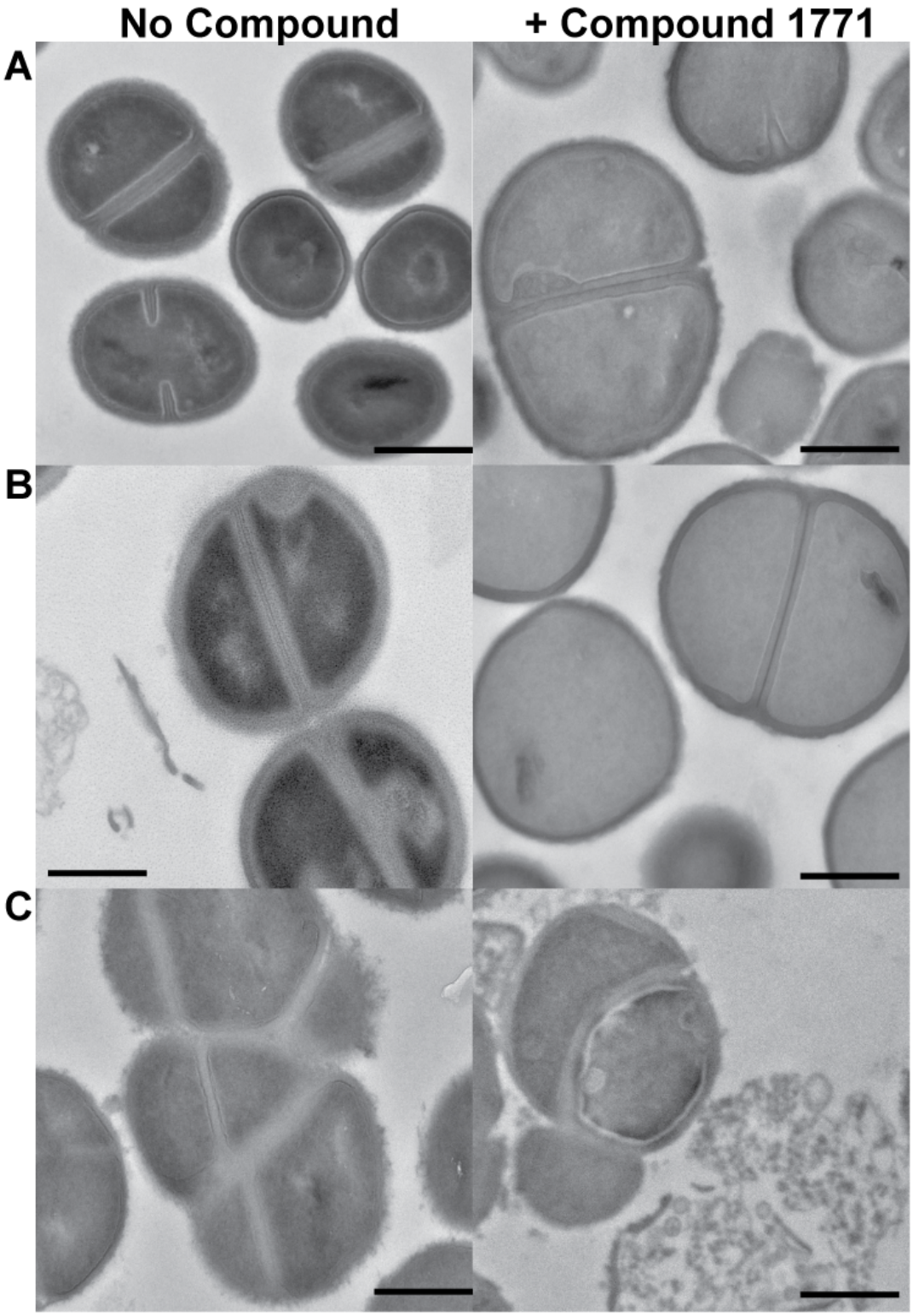

Figure A.1: Electron microscopy of cells treatd with 15μM compound 1771 and grown for 2.5 hours at 37°C. (A) Wildtype cells; (B) Δ*tarO*; (C) Δ*dltA*. Scale bars represent 500 nm.

References Cited

1. Adams D, Errington J. 2009. Bacterial cell division: assembly, maintenance and disassembly of the Z ring. *Nat Rev Microbiol* 7:642-53
2. Akerley B, Rubin E, Camilli A, Lampe D, Robertson H, Mekalanos J. 1998. Systematic identification of essential genes by *in vitro mariner* mutagenesis. *Proc Nat Sci Acad* 95:8927-32
3. Allison K, Brynildsen M, Collins J. 2011. Metabolite-enabled eradication of bacterial persisters by aminoglycosides. *Nature* 473:216-20
4. Allison SE, D'Elia MA, Arar S, Monteiro MA, Brown ED. 2011. Studies of the genetics, function, and kinetic mechanism of TagE, the wall teichoic acid glycosyltransferase in *Bacillus subtilis* 168. *J Biol Chem* 286:23708-16
5. Aly R, Shinefield HR, Litz C, Maibach HI. 1980. Role of teichoic acid in the binding of *Staphylococcus aureus* to nasal epithelial cells. *J Infect Dis* 141:463-5
6. Anderson AJ, Green RS, Sturman AJ, Archibald AR. 1978. Cell wall assembly in *Bacillus subtilis*: location of wall material incorporated during pulsed release of phosphate limitation, its accessibility to bacteriophages and concanavalin A, and its susceptibility to turnover. *J Bacteriol* 136:886-99
7. Andre G, Deghorain M, Bron PA, van S, II, Kleerebezem M, et al. 2011. Fluorescence and atomic force microscopy imaging of wall teichoic acids in *Lactobacillus plantarum*. *ACS Chem Biol* 6:366-76
8. Araki Y, Ito E. 1989. Linkage units in cell walls of gram-positive bacteria. *Crit Rev Microbiol* 17:121-35

9. Armstrong JJ, Baddiley J, Buchanan JG, Carss B, Greenberg GR. 1958. Isolation and structure of ribitol phosphate derivatives (teichoic acids) from bacterial cell walls. *Journal of the Chemical Society*:4344-54

10. Arnaud M, Chastanet A, Debarbouille M. 2004. New vector for efficient allelic replacement in naturally nontransformable, low-GC-content, gram-positive bacteria. *Appl Environ Microbiol* 70:6887-91

11. Atilano ML, Pereira PM, Yates J, Reed P, Veiga H, et al. 2010. Teichoic acids are temporal and spatial regulators of peptidoglycan cross-linking in *Staphylococcus aureus*. *Proceedings of the National Academy of Sciences* 107:18991-6

12. Baba T, Takeuchi F, Kuroda M, Yuzawa H, Aoki K, et al. 2002. Genome and virulence determinants of high virulence community-acquired MRSA. *Lancet* 359:1819-27

13. Baddiley J. 1970. Structure, biosynthesis, and function of teichoic acids. *Accounts of Chemical Research* 3:98-105

14. Badurina DS, Zolli-Juran M, Brown ED. 2003. CTP:glycerol 3-phosphate cytidylyltransferase (TarD) from *Staphylococcus aureus* catalyzes the cytidylyl transfer via an ordered Bi-Bi reaction mechanism with micromolar K_m values. *Biochim Biophys Acta* 1646:196-206

15. Bae T, Banger AK, Wallace A, Glass EM, Aslund F, et al. 2004. *Staphylococcus aureus* virulence genes identified by bursa aurealis mutagenesis and nematode killing. *Proc Natl Acad Sci U S A* 101:12312-7

16. Bae T, Glass E, Schneewind O, Missiakas D. 2007. Generating a collection of insertion mutations in the *Staphylococcus aureus* genome using *bursa aurealis*. *Meth Mol Biol* 416:103-16.

17. Baptista C, Santos MA, São-José C. 2008. Phage SPP1 reversible adsorption to *Bacillus subtilis* cell wall teichoic acids accelerates virus recognition of membrane receptor YueB. *J Bacteriol* 190:4989-96

18. Baur S, Marles-Wright J, Buckenmaier S, Lewis RJ, Vollmer W. 2009. Synthesis of CDP-activated ribitol for teichoic acid precursors in *Streptococcus pneumoniae*. *J Bacteriol* 191:1200-10

19. Begun J, Sifri CD, Goldman S, Calderwood SB, Ausubel FM. 2005. *Staphylococcus aureus* virulence factors identified by using a high-throughput *Caenorhabditis elegans*-killing model. *Infec Immun* 73:872-7

20. Bera A, Biswas R, Herbert S, Kulauzovic E, Weidenmaier C, et al. 2007. Influence of wall teichoic acid on lysozyme resistance in Staphylococcus aureus. *J Bacteriol* 189:280-3

21. Berger-Bachi B, Rohrer S. 2002. Factors influencing methicillin resistance in staphylococci. *Arch Microbiol* 178:165-71

22. Berger-Bachi B, Strassle A, Gustafson J, Kayser F. 1992. Mapping and characterization of multiple chromosomal factors Involved in methicillin resistance in *Staphylococcus aureus*. *Antimicrob Agents Chemother* 36:1367-73

23. Bernal P, Lemaire S, Pinho M, Mobashery S, Hinds J, Taylor P. 2010. Insertion of epicatechin gallate into the cytoplasmic membrane of methicillin-resistant

Staphylococcus aureus disrupts penicillin-binding protein (PBP) 2a-mediated beta-lactam resistance by delocalizing PBP2. *J Biol Chem* 285:24055-65

24. Bernal P, Zloh M, Taylor PW. 2009. Disruption of D-alanyl esterification of *Staphylococcus aureus* cell wall teichoic acid by the β-lactam resistance modifier (-)-epicatechin gallate. *The Journal of antimicrobial chemotherapy* 63:1156-62

25. Bhavsar AP, Beveridge TJ, Brown ED. 2001. Precise deletion of tagD and controlled depletion of its product, glycerol 3-phosphate cytidylyltransferase, leads to irregular morphology and lysis of *Bacillus subtilis* grown at physiological temperature. *J Bacteriol* 183:6688-93

26. Bhavsar AP, Erdman LK, Schertzer JW, Brown ED. 2004. Teichoic acid is an essential polymer in *Bacillus subtilis* that is functionally distinct from teichuronic acid. *J Bacteriol* 186:7865-73

27. Bhavsar AP, Truant R, Brown ED. 2005. The TagB protein in *Bacillus subtilis* 168 is an intracellular peripheral membrane protein that can incorporate glycerol phosphate onto a membrane-bound acceptor in vitro. *J Biol Chem* 280:36691-700

28. Bhaya D, Davison M, Barrangou R. 2011. CRISPR-Cas systems in bacteria nad archaea: versatile small RNAs for adaptive defense and regulation. *Annu Rev Genet* 45:273-97.

29. Bierbaum G, Sahl HG. 1985. Induction of autolysis of staphylococci by the basic peptide antibiotics Pep 5 and nisin and their influence on the activity of autolytic enzymes. *Arch Microbiol* 141:249-54

30. Bijlsma J, Bourghout P, Kloosterman T, Bootsma H, De J, al. e. 2007. Development of genomic array footprinting for identification of conditionally essential genes in *Streptococcus pneumoniae*. *Appl Environ Microbiol* 73:1514-24

31. Biswas R, Martinez RE, Gohring N, Schlag M, Josten M, et al. 2012. Proton-binding capacity of *Staphylococcus aureus* wall teichoic acid and its role in controlling autolysin activity. *PLoS One* 7:e41415

32. Blades N, Broman K. 2002. Estimating the number of essential genes in a genome by random transposon mutagenesis. *Technical report, Johns Hopkins University, Department of Biostatistics*

33. Blankenberg D, Von Kuster G, Coraor N, Ananda G, Lazarus R, et al. 2010. Galaxy: a web-based genome analysis tool for experimentalists. *Current Protocols in Molecular Biology* Chapter 19:10.1-21

34. Boles B, Thoendel M, Roth A, Horswill A. 2010. Identification of Genes Involved in Polysaccharide- Independent *Staphylococcus aureus* Biofilm Formation. *PLoS ONE* 5:e10146

35. Bose J, Fey P, Bayles K. 2013. Genetic tools to enhance the study of gene function and regulation in *Staphylococcus aureus*. *Appl Environ Microbiol* 79:2218.

36. Boylan RJ, Mendelson NH, Brooks D, Young FE. 1972. Regulation of the bacterial cell wall: analysis of a mutant of *Bacillus subtilis* defective in biosynthesis of teichoic acid. *J Bacteriol* 110:281-90

37. Boyle-Vavra S, Yin S, Jo D, Montgomery C, Daum R. 2013. VraT/YvqF is required for methicillin resistance and activation of the VraSR regulon in *Staphylococcus aureus*. *Antimicrob Agents Chemother* 57:83-95.

38. Bracha R, Davidson R, Mirelman D. 1978. Defect in biosynthesis of the linkage unit between peptidoglycan and teichoic acid in a bacteriophage-resistant mutant of *Staphylococcus aureus*. *J Bacteriol* 134:412-7

39. Bron PA, Tomita S, van S, II, Remus DM, Meijerink M, et al. 2012. *Lactobacillus plantarum* possesses the capability for wall teichoic acid backbone alditol switching. *Microb Cell Fact* 11:123

40. Brown S, Meredith T, Swoboda J, Walker S. 2010. *Staphylococcus aureus* and *Bacillus subtilis* W23 make polyribitol wall teichoic acids using different enzymatic pathways. *Chemistry & biology* 17:1101-10

41. Brown S, Santa Maria J, Walker S. 2013. Wall teichoic acids of Gram-positive bacteria. *Annu Rev Microbiol* 67:313-36.

42. Brown S, Xia G, Luhachack LG, Campbell J, Meredith TC, et al. 2012. Methicillin resistance in *Staphylococcus aureus* requires glycosylated wall teichoic acids. *Proc Natl Acad Sci U S A* 109:18909-14

43. Brown S, Zhang Y-H, Walker S. 2008. A revised pathway proposed for Staphylococcus aureus wall teichoic acid biosynthesis based on *in vitro* reconstitution of the intracellular steps. *Chemistry & biology* 15:12-21

44. Campbell J, Singh AK, Santa Maria JP, Kim Y, Brown S, et al. 2011. Synthetic Lethal Compound Combinations Reveal a Fundamental Connection between Wall Teichoic Acid and Peptidoglycan Biosyntheses in *Staphylococcus aureus*. *ACS Chem. Biol.* 6:106-16

45. Campbell J, Singh AK, Swoboda JG, Gilmore MS, Wilkinson BJ, Walker S. 2012. An antibiotic that inhibits a late step in wall teichoic acid biosynthesis induces the cell

wall stress stimulon in *Staphylococcus aureus*. *Antimicrob Agents Chemother* 56:1810-20

46. Chatterjee AN, Mirelman D, Singer HJ, Park JT. 1969. Properties of a novel pleiotropic bacteriophage-resistant mutant of *Staphylococcus aureus* H. *J Bacteriol* 100:846-53

47. Chaudhuri R, Allen A, Owen P, Shalom G, Stone K, et al. 2009. Comprehensive identification of essential *Staphylococcus aureus* genes using Transposon-Mediated Differential Hybridisation (TMDH). *BMC Genomics* 10:291

48. Childs WC, 3rd, Taron DJ, Neuhaus FC. 1985. Biosynthesis of D-alanyl-lipoteichoic acid by *Lactobacillus casei*: interchain transacylation of D-alanyl ester residues. *J Bacteriol* 162:1191-5

49. Chin T, Burger MM, Glaser L. 1966. Synthesis of teichoic acids. VI. The formation of multiple wall polymers in *Bacillus subtilis* W-23. *Arch Biochem Biophys* 116:358-67

50. Clatworthy AE, Pierson E, Hung DT. 2007. Targeting virulence: a new paradigm for antimicrobial therapy. *Nat Chem Biol* 3:541-8

51. Cokol M, al. e. 2011. Systematic exploration of synergistic drug pairs. *Mol Sys Biol* 7:1-9

52. Cole RM, Popkin TJ, Boylan RJ, Mendelson NH. 1970. Ultrastructure of a temperature-sensitive rod- mutant of *Bacillus subtilis*. *J Bacteriol* 103:793-810

53. Collins LV, Kristian SA, Weidenmaier C, Faigle M, Van Kessel KPM, et al. 2002. Staphylococcus aureus strains lacking D-alanine modifications of teichoic acids are

highly susceptible to human neutrophil killing and are virulence attenuated in mice. *J Infect Dis* 186:214-9

54. Corrigan R, al. e. 2013. Systematic identification of conserved bacterial c-di-AMP receptor Proteins. *Proc Nat Sci Acad* In Press

55. Corrigan RM, Abbott JC, Burhenne H, Kaever V, Grundling A. 2011. c-di-AMP is a new second messenger in *Staphylococcus aureus* with a role in controlling cell size and envelope stress. *PLoS Pathog* 7:e1002217.

56. Corvaglia A, Francois P, Hernandez D, Perron K, Linder P, Schrenzel J. 2010. A type II-like restriction endonuclease functions as a major barrier to horizontal gene transfer in clinical *Staphylococcus aureus* strains. *Proc Nat Sci Acad* 107:11954-8.

57. D Elia MA, Henderson JA, Beveridge TJ, Heinrichs DE, Brown ED. 2009. The N-acetylmannosamine transferase catalyzes the first committed step of teichoic acid assembly in *Bacillus subtilis* and *Staphylococcus aureus*. *J Bacteriol* 191:4030-4

58. D Elia MA, Millar KE, Beveridge TJ, Brown ED. 2006. Wall teichoic acid polymers are dispensable for cell viability in *Bacillus subtilis*. *J Bacteriol* 188:8313-6

59. D Elia MA, Pereira MP, Chung YS, Zhao W, Chau A, et al. 2006. Lesions in teichoic acid biosynthesis in *Staphylococcus aureus* lead to a lethal gain of function in the otherwise dispensable pathway. *J Bacteriol* 188:4183-9

60. Davison AL, Baddiley J. 1964. Glycerol teichoic acids in walls of *Staphylococcus epidermidis*. *Nature* 202:874

61. Debabov DV, Kiriukhin MY, Neuhaus FC. 2000. Biosynthesis of lipoteichoic acid in *Lactobacillus rhamnosus*: role of DltD in D-alanylation. *J Bacteriol* 182:2855-64

62. DeJesus M, Ioerger T. 2013. A Hidden Markov Model for identifying essential and growth-defect regiosn in bacterial genomes from transposon insertion sequencing data. *BMC Bioinformatics* 14:303

63. DeJesus M, Zhang Y, Sassetti C, Rubin E, Sacchettini J, Ioerger T. 2013. Bayesian analysis of gene essentiality based on sequencing of transposon insertion libraries. *Bioinformatics* 29:695-703

64. Delattin N, al. e. 2014. Repurposing as a means to increase the activity of amphotericin B and caspofungin against *Candida albicans* biofilms. *The Journal of antimicrobial chemotherapy* 69:1035-44

65. Denapaite D, Bruckner R, Hakenbeck R, Vollmer W. 2012. Biosynthesis of teichoic acids in *Streptococcus pneumoniae* and closely related species: lessons from genomes. *Microb Drug Resist* 18:344-58

66. Dengler V, Meier PS, Heusser R, Kupferschmied P, Fazekas J, et al. 2012. Deletion of hypothetical wall teichoic acid ligases in *Staphylococcus aureus* activates the cell wall stress response. *FEMS Microbiol Lett* 333:109-20

67. Dolan K, Buchheit B, DiDone L, Wellington M, DJ K. 2009. Antifungal activity of tamoxifen: *in vitro* and *in vivo* activities and mechanistic characterization. *Antimicrob Agents Chemother* 53:3337-46.

68. Dreisbach A, van Dijl JM, Buist G. 2011. The cell surface proteome of *Staphylococcus aureus*. *Proteomics* 11:3154-68

69. Duthie E. 1952. Variation in the antigenic composition of *Staphylococcal* coagulase. *J Gen Microbiol* 7:320-6.

70. Eberhardt A, Hoyland CN, Vollmer D, Bisle S, Cleverley RM, et al. 2012. Attachment of capsular polysaccharide to the cell wall in *Streptococcus pneumoniae*. *Microb Drug Resist* 18:240-55

71. Ejim L, Farha M, Falconer S, Wildenahin J, Coombes B, al. e. 2011. Combinations of antibiotics and nonantibiotic drugs enhance antimicrobial efficacy. *Nat Chem BIol* 7:348-50

72. Elbaz M, Ben-Yehuda S. 2010. The metabolic enzyme ManA reveals a link between cell wall integrity and chromosome morphology. *PLoS Genet* 6

73. Ellermeier C, Losick R. 2006. Evidence for a novel protease governing regulated intramembrane proteolysis and resistance to antimicrobial peptides in *Bacillus subtilis*. *Genes Dev* 20:1911-22

74. Ellwood DC. 1970. The wall content and composition of *Bacillus subtilis* var. niger grown in a chemostat. *Biochem J* 118:367-73

75. Endl J, Seidl HP, Fiedler F, Schleifer KH. 1983. Chemical composition and structure of cell wall teichoic acids of staphylococci. *Arch Microbiol* 135:215-23

76. Endl J, Seidl PH, Fiedler F, Schleifer KH. 1984. Determination of cell wall teichoic acid structure of staphylococci by rapid chemical and serological screening methods. *Arch Microbiol* 137:272-80

77. Eugster MR, Loessner MJ. 2012. Wall Teichoic Acids Restrict Access of Bacteriophage Endolysin Ply118, Ply511, and PlyP40 Cell Wall Binding Domains to the *Listeria monocytogenes* Peptidoglycan. *J Bacteriol* 194:6498-506

78. Falord M, Karimova G, Hiron A, Msadek T. 2012. GraXSR proteins interact with the VraFG ABC transporter to form a five-component system required for cationic

antimicrobial peptide sensing and resistance in *Staphylococcus aureus*. *Antimicrob Agents Chemother* 56:1047

79. Falord M, Mader U, Hiron A, Debarbouille M, Msadek T. 2011. Investigation of the *Staphylococcus aureus* GraSR regulon reveals novel links to virulence, stress response, and cell wall signal transduction pathways. *PLoS ONE* 6:e21323.

80. Farha M, Leung A, Sewell E, D'Elia M, Allison S, *et al.* 2013. Inhibition of WTA synthesis blocks the cooperative action of PBPs and sensitizes MRSA to β-lactams. *ACS Chem Biol* 8:226-33

81. Strahl H & Hamoen LW. 2012 Membrane potential is important for bacterial cell division. *Proc Nat Sci Acad* 107(27):12281-12286.

82. Fey P, Endres J, Yajjala V, Widhelm T, Boissy R, *et al*. 2013. A genetic resource for rapid and comprehensive phenotype screening of nonessential *Staphylococcus aureus* genes. *mBio* 4:E00537-12.

83. Fischer W. 1994. Lipoteichoic acid and lipids in the membrane of *Staphylococcus aureus*. *Med Microbiol Immunol* 183:61-76.

84. Fischer W, Rosel P, Koch HU. 1981. Effect of alanine ester substitution and other structural features of lipoteichoic acids on their inhibitory activity against autolysins of *Staphylococcus aureus*. *J Bacteriol* 146:467-75

85. Fitzgerald SN, Foster TJ. 2000. Molecular analysis of the tagF gene, encoding CDP-Glycerol:Poly(glycerophosphate) glycerophosphotransferase of *Staphylococcus epidermidis* ATCC 14990. *J Bacteriol* 182:1046-52

86. Formstone A, Carballido-López R, Noirot P, Errington J, Scheffers D-J. 2008. Localization and interactions of teichoic acid synthetic enzymes in *Bacillus subtilis*. *J Bacteriol* 190:1812-21

87. Frankel M, al. e. 2011. LytN, a murein hydrolase in the cross wall compartment of *Staphylococcus aureus,* is involved in proper bacterial growth and envelope assembly. *J Biol Chem* 286:32593-605

88. Frankel M, Wojcik B, DeDent A, Missiakas D, Schneewind O. 2010. ABI domain-containing proteins contribute to surface protein display and cell division in *Staphylococcus aureus*. *Mol Microbiol* 78:238-52

89. Frankel MB, Schneewind O. 2012. Determinants of murein hydrolase targeting to cross-wall of *Staphylococcus aureus* peptidoglycan. *J Biol Chem* 287:10460-71

90. Frye S, Crosby M, Edwards T, Juliano R. 2011. US academic drug discovery. *Nat Rev Drug Disc* 10:409-10

91. Geddes AM, Klugman KP, Rolinson GN. 2007. Introduction: historical perspective and development of amoxicillin/clavulanate. *Int J Antimicrob Agents* 30 Suppl 2:S109-12

92. Giardine B, Riemer C, Hardison R, Burhans R, Elnitski L, et al. 2005. Galaxy: a platform for interactive large-scale genome analysis. *Genome Research* 15:1451-5.

93. Ginsberg C, Zhang Y-H, Yuan Y, Walker S. 2006. In vitro reconstitution of two essential steps in wall teichoic acid biosynthesis. *ACS Chem. Biol.* 1:25-8

94. Goecks J, Nekrutenko A, Taylor J, Team TG. 2010. Galaxy: a comprehensive approach for supporting accessible, reproducible, and transparent computational research in the life sciences. *Genome Biol* 11:R86.

95. Goodman AL, *al. e*. 2009. Identifying genetic determinants needed to establish a human gut symbiont in its habitat. *Cell Host Microbe* 6:279-89

96. Griffin J, al. e. 2011. High-resolution phenotypic profiling defines genes essential for mycobacterial growth and cholesterol catabolism. *PLoS Pathog* 7:e1002251

97. Reference Removed.

98. Gross M, Cramton SE, Götz F, Peschel A. 2001. Key role of teichoic acid net charge in Staphylococcus aureus colonization of artificial surfaces. *Infect Immun* 69:3423-6

99. Grundling A, Missiakas D, Schneewind O. 2006. *Staphylococcus aureus* mutants within increased lysostaphin resistance. *J Bacteriol* 188:6286-97.

100. Grundling A, Schneewind O. 2007. Genes required for glycolipid synthesis and lipoteichoic acid anchoring in *Staphylococcus aureus*. *J Bacteriol* 189:2521-30.

101. Haas R, Koch HU, Fischer W. 1984. Alanyl turnover from lipoteichoic acid to teichoic acid in *Staphylococcus aureus*. *FEMS Microbiology Letters* 21:27-31

102. Hancock IC, Wiseman G, Baddiley J. 1976. Biosynthesis of the unit that links teichoic acid to the bacterial wall: inhibition by tunicamycin. *FEBS letters* 69:75-80

103. Hankins J, Madsen J, Giles D, Brodbelt J, Trent M. 2012. Amino acid addition to *Vibrio cholerae* LPS establishes a link between surface remodeling in Gram-positive and Gram-negative bacteria. *Proc Nat Sci Acad* 109:8722-7.

104. Heaton MP, Neuhaus FC. 1992. Biosynthesis of D-alanyl-lipoteichoic acid: cloning, nucleotide sequence, and expression of the *Lactobacillus casei* gene for the D-alanine-activating enzyme. *J Bacteriol* 174:4707-17

105. Heaton MP, Neuhaus FC. 1994. Role of the D-alanyl carrier protein in the biosynthesis of D-alanyl-lipoteichoic acid. *J Bacteriol* 176:681-90

106. Hensel M, Shea J, Gleeson C, Jones M, Dalton E, al. e. 1995. Simultaneous identification of bacterial virulence genes by negative selection. *Science* 269:400-3.

107. Heptinstall S, Archibald AR, Baddiley J. 1970. Teichoic acids and membrane function in bacteria. *Nature* 225:519-21

108. Herbert S, Ziebandt A, Ohlsen K, Schafer T, Hecker M, et al. 2010. Repair of global regulators in *Staphylococcus aureus* 8325 and comparative analysis with other clinical isolates. *Infec Immun* 78:2877-89.

109. Holland L, Conlon B, O'Gara JP. 2010. Mutation of *tagO* reveals an essential role for wall teichoic acids in *Staphylococcus epidermidis* biofilm development. *Microbiology* 157 (Pt 2):408-18

110. Hollister J, Gaut B. 2009. Epigenetic silencing of transposable elements: A trade-off between reduced transposition and deleterious effects on neighboring gene expression. *Genome Res* 19:1419-28.

111. Huber J, Donald RG, Lee SH, Jarantow LW, Salvatore MJ, et al. 2009. Chemical genetic identification of peptidoglycan inhibitors potentiating carbapenem activity against methicillin-resistant *Staphylococcus aureus*. *Chemistry & biology* 16:837-48

112. Hubscher J, McCallum N, Sifri CD, Majcherczyk PA, Entenza JM, et al. 2009. MsrR contributes to cell surface characteristics and virulence in *Staphylococcus aureus*. *FEMS Microbiol Lett* 295:251-60

113. Hyyrylainen H, Pietiainen M, Lunden T, Ekman A, Gardemeister M, et al. 2007. The density of negative charge in the cell wall influences two-componentn signal transduction in *Bacillus subtilis*. *Microbiology* 153:2126-36.

114. Hyyrylainen HL, Vitikainen M, Thwaite J, Wu H, Sarvas M, et al. 2000. D-Alanine substitution of teichoic acids as a modulator of protein folding and stability at the cytoplasmic membrane/cell wall interface of Bacillus subtilis. *J Biol Chem* 275:26696-703

115. Jacobs M, Alwood A, Thaipisuttikul I, Spencer D, Haugen E, al. e. 2003. Comprehensive transposon mutant library of *Pseudomonas aeruginosa*. *Proc Nat Sci Acad* 100:14339-44.

116. James DB, Yother J. 2012. Genetic and Biochemical Characterizations of Enzymes Involved in *Streptococcus pneumoniae* Serotype 2 Capsule Synthesis Demonstrate that Cps2T (WchF) Catalyzes the Committed Step by Addition of beta1-4 Rhamnose, the Second Sugar Residue in the Repeat Unit. *J Bacteriol* 194:6479-89

117. Jenni R, Berger-Bächi B. 1998. Teichoic acid content in different lineages of *Staphylococcus aureus* NCTC8325. *Arch Microbiol* 170:171-8

118. Kajimura J, al. e. 2005. Identification and molecular characterization of an N-acetylmuramyl-L-alanine amidase Sle1 involved in separation of *Staphylococcus aureus*. *Mol Microbiol* 58:1087-101

119. Karamata D, Pooley HM, Monod M. 1987. Expression of heterologous genes for wall teichoic acid in Bacillus subtilis 168. *Mol Gen Genet* 207:73-81

120. Kato F, Sugai M. 2011. A simple method of markerless gene deletion in *Staphylococcus aureus*. *J Microbiol Methods* 87:76-81

121. Kawai Y, Marles-Wright J, Cleverley RM, Emmins R, Ishikawa S, et al. 2011. A widespread family of bacterial cell wall assembly proteins. *EMBO J* 30:4931-41

122. Kern T, Giffard M, Hediger S, Amoroso A, Giustini C, et al. 2010. Dynamics characterization of fully hydrated bacterial cell walls by solid-state NMR: evidence for cooperative binding of metal ions. *J Am Chem Soc* 132:10911-9

123. Kiriukhin MY, Neuhaus FC. 2001. D-alanylation of lipoteichoic acid: role of the D-alanyl carrier protein in acylation. *J Bacteriol* 183:2051-8

124. Kleckner N. 1981. Transposable elements in prokaryotes. *Annu Rev Genet* 15:341-404.

125. Kobayashi K, Ehrlich SD, Albertini A, Amati G, Andersen KK, et al. 2003. Essential *Bacillus subtilis* genes. *Proc Natl Acad Sci U S A* 100:4678-83

126. Kohler T, Weidenmaier C, Peschel A. 2009. Wall teichoic acid protects *Staphylococcus aureus* against antimicrobial fatty acids from human skin. *J Bacteriol* 191:4482-4

127. Kojima N, Araki Y, Ito E. 1985. Structure of the linkage units between ribitol teichoic acids and peptidoglycan. *J Bacteriol* 161:299-306

128. Kovács M, Halfmann A, Fedtke I, Heintz M, Peschel A, et al. 2006. A functional dlt operon, encoding proteins required for incorporation of d-alanine in teichoic acids in gram-positive bacteria, confers resistance to cationic antimicrobial peptides in *Streptococcus pneumoniae*. *J Bacteriol* 188:5797-805

129. Kreiswirth BN, Lofdahl S, Betley MJ, O'Reilly M, Schlievert PM, et al. 1983. The toxic shock syndrome exotoxin structural gene is not detectably transmitted by a prophage. *Nature* 305:709-12

130. Kristian S, Lauth X, Nizet V, Goetz F, Neumeister B. 2003. Alanylation of teichoic acids protects *Staphylococcus aureus* against Toll-like receptor 2-dependent host defense in a mouse tissue cage infection model. *J Infect Dis* 188:414-23.

131. Kristian SA, Lauth X, Nizet V, Goetz F, Neumeister B, et al. 2003. Alanylation of teichoic acids protects *Staphylococcus aureus* against Toll-like receptor 2-dependent host defense in a mouse tissue cage infection model. *J Infect Dis* 188:414-23

132. Kuru E, al. e. 2013. In Situ Probing of Newly Synthesized Peptidoglycan in Live Bacteria with Fluorescent d-Amino Acids. *Angew. Chem. Int. Ed.* 51:12519-23

133. Lampe D, Grant T, Robertson H. 1998. Factors Affecting Transposition of the *Himar1 mariner* Transposon *in Vitro*. *Genetics* 149:179-87.

134. Land A, Winkler M. 2011. The requirement for *Pneumococcal* MreC and MreD is relieved by inactivation of the gene encoding PBP1a. *J Bacteriol* 193:4166-79.

135. Langridge GC, Phan M-D, Turner DJ, Perkins TT, Parts L, *al. e*. 2009. Simultaneous assay of every *Salmonella Typhi* gene using one million transposon mutants. *Gen. Res.* 19:2308-16.

136. Lazarevic V, Abellan F-X, Möller SB, Karamata D, Mauël C. 2002. Comparison of ribitol and glycerol teichoic acid genes in *Bacillus subtilis* W23 and 168: identical function, similar divergent organization, but different regulation. *Microbiology (Reading, Engl)* 148:815-24

137. Lazarevic V, Karamata D. 1995. The *tagGH* operon of *Bacillus subtilis* 168 encodes a two-component ABC transporter involved in the metabolism of two wall teichoic acids. *Mol Microbiol* 16:345-55

138. Lee K, Campbell J, Swoboda JG, Cuny GD, Walker S. 2010. Development of improved inhibitors of wall teichoic acid biosynthesis with potent activity against *Staphylococcus aureus*. *Bioorganic & Medicinal Chemistry Letters* 20:1767-70

139. Li M, Rigby K, Lai Y, Nair V, Peschel A, *al. e*. 2009. *Staphylococcus aureus* mutant screen reveals interaction of the human antimicrobial peptide dermcidin with membrane phospholipids. *Antimicrob Agents Chemother* 53:4200-10

140. Libman M, Miller M, Richards G. 1990. Antistaphylococcal activity of pentamidine. *Antimicrob Agents Chemother* 34:1795-6

141. Liew A, Theis T, Jensen S, Garca-Lara J, Foster S, et al. 2011. A simple plasmid-based system that allows rapid generation of tightly controlled gene expression in *Staphylococcus aureus*. *Microbiology* 157:666-76.

142. Lofblom J, Kronqvist N, Uhlen M, Stahl S, Wernerus H. 2007. Optimization of electroporation-mediated transformation:
Staphylococcus carnosus as model organism. *J Appl Microbiol* 102

143. Lohe A, De Aguiar D, Hartl D. 1997. Mutations in the *mariner* transposase: The D,D(35)E consensus sequence is nonfunctional. *Proc Natl Acad Sci* 94:1293-7.

144. Lohe A, Hartl D. 1996. Autoregulation of *mariner* transposase activity by overproduction and dominant-negative complementation. *Mol Biol Evol* 13:549-55.

145. Lovering AL, Lin LY-C, Sewell EW, Spreter T, Brown ED, Strynadka NCJ. 2010. Structure of the bacterial teichoic acid polymerase TagF provides insights into membrane association and catalysis. *Nat Struct Mol Biol* 17:582-9

146. Maki H, Yamaguchi T, Murakami K. 1994. Cloning and characterization of a gene affecting the methicillin resistance level and the autolysis rate in *Staphylococcus aureus*. *J Bacteriol* 176:4993-5000

147. Markowitz J, al. e. 2004. Identification and characterization of small molecule inhibitors of the calcium-dependent S100B-p53 tumor suppressor interaction. *J Med Chem* 47:5085-93

148. Marraffini L, Sontheimer E. 2010. CRISPR interference: RNA-directed adaptive immunity in bacteria and archaea. *Nat Rev Genet* 11:181-90.

149. Matias VR, Beveridge TJ. 2005. Cryo-electron microscopy reveals native polymeric cell wall structure in *Bacillus subtilis* 168 and the existence of a periplasmic space. *Mol Microbiol* 56:240-51

150. Matias VR, Beveridge TJ. 2006. Native cell wall organization shown by cryo-electron microscopy confirms the existence of a periplasmic space in *Staphylococcus aureus*. *J Bacteriol* 188:1011-21

151. Matias VR, Beveridge TJ. 2007. Cryo-electron microscopy of cell division in *Staphylococcus aureus* reveals a mid-zone between nascent cross walls. *Mol Microbiol* 64:195-206

152. Mauck J, Glaser L. 1972. On the mode of in vivo assembly of the cell wall of *Bacillus subtilis*. *J Biol Chem* 247:1180-7

153. May JJ, Finking R, Wiegeshoff F, Weber TT, Bandur N, et al. 2005. Inhibition of the D-alanine:D-alanyl carrier protein ligase from *Bacillus subtilis* increases the bacterium's susceptibility to antibiotics that target the cell wall. *FEBS J* 272:2993-3003

154. McClintock B. 1951. Chromosome organization and genic expression. *Cold Spring Harb Symp Quant Biol* 16:13-47.

155. Meehl M, Herbert S, Gotz F, Cheung A. 2007. Interaction of the GraRS two-component systme with the VraFG ABC transporter to support vancomycin-intermediate resistance in *Staphylococcus aureus*. *Antimicrob Agents Chemother* 51:2679-89.

156. Mei JM, Nourbakhsh F, Ford CW, Holden DW. 1997. Identification of *Staphylococcus aureus* virulence genes in a murine model of bacteraemia using signature-tagged mutagenesis. *Mol Microbiol* 26:399-407

157. Meredith TC, Swoboda JG, Walker S. 2008. Late-stage polyribitol phosphate wall teichoic acid biosynthesis in *Staphylococcus aureus*. *J Bacteriol* 190:3046-56

158. Mericl AN, Friesen JA. 2012. Comparative kinetic analysis of glycerol 3-phosphate cytidylyltransferase from *Enterococcus faecalis* and *Listeria monocytogenes*. *Med Sci Monit* 18:BR427-34

159. Minnig K, Lazarevic V, Soldo B, Mauel C. 2005. Analysis of teichoic acid biosynthesis regulation reveals that the extracytoplasmic function sigma factor sigmaM is induced by phosphate depletion in *Bacillus subtilis* W23. *Microbiology* 151:3041-9

160. Muñoz-López M, García-Pérez J. 2010. DNA Transposons: Nature and Applications in Genomics. *Curr Genom* 11:115-28.

161. Nair D, Memmi G, Hernandez D, Bard J, Beaume M, et al. 2011. Whole-genome sequencing of *Staphylococcus aureus* strain RN4220, a key laboratory strain used in

virulence research, identifies mutations that affect not only virulence factors, but also the fitness of the strain. *J Bacteriol* 193:2332-5.

162. Nakao A, Imai S, Takano T. 2000. Transposon-mediated insertional mutagenesis of the D-alanyl-lipoteichoic acid (dlt) operon raises methcillin resistance in *Staphylococcus aureus*. *Res Microbiol* 151:823-9.

163. Nathenson SG, Ishimoto N, Anderson JS, Strominger JL. 1966. Enzymatic synthesis and immunochemistry of alpha- and beta-N-acetylglucosaminylribitol linkages in teichoic acids from several strains of *Staphylococcus aureus*. *J Biol Chem* 241:651-8

164. Naumova IB, Kuznetsov VD, Kudrina KS, Bezzubenkova AP. 1980. The occurrence of teichoic acids in streptomycetes. *Arch Microbiol* 126:71-5

165. Naumova IB, Shashkov AS, Tul'skaya EM, Streshinskaya GM, Kozlova YI, et al. 2001. Cell wall teichoic acids: structural diversity, species specificity in the genus *Nocardiopsis*, and chemotaxonomic perspective. *FEMS Microbiol Rev* 25:269-84

166. Neuhaus FC, Baddiley J. 2003. A continuum of anionic charge: structures and functions of D-alanyl-teichoic acids in Gram-positive bacteria. *Microbiol Mol Biol Rev* 67:686-723

167. Novick R, Ross H, Projan S, Kornblum J, Kreiswirth B, Moghazeh S. 1993. Synthesis of *Staphylococcal* virulence factors is controlled by a regulatory RNA molecule. *EMBO J* 12:3967-75.

168. Oku Y, Kurokawa K, Matsuo M, Yamada S, Lee B-L, Sekimizu K. 2009. Pleiotropic roles of polyglycerolphosphate synthase of lipoteichoic acid in growth of *Staphylococcus aureus* cells. *J Bacteriol* 191:141-51

169. Over B, Heusser R, McCallum N, Schulthess B, Kupferschmied P, et al. 2011. LytR-CpsA-Psr proteins in *Staphylococcus aureus* display partial functional redundancy and the deletion of all three severely impairs septum placement and cell separation. *FEMS Microbiol Lett* 320:142-51

170. Pajnunen M, Pulliainen A, Finne J, Savilahti H. 2005. Generation of transposon insertion mutant libraries for Gram-positive bacteria by electroporation of phage Mu DNA transposition complexes. *Microbiology* 151:1209-15.

171. Park JT, Shaw DR, Chatterjee AN, Mirelman D, Wu T. 1974. Mutants of staphylococci with altered cell walls. *Ann N Y Acad Sci* 236:54-62

172. Park YS, Sweitzer TD, Dixon JE, Kent C. 1993. Expression, purification, and characterization of CTP:glycerol-3-phosphate cytidylyltransferase from *Bacillus subtilis*. *J Biol Chem* 268:16648-54

173. Pasquina LW, Santa Maria JP, Walker S. 2013. Teichoic acid biosynthesis as an antibiotic target. *Curr Opin Microbiol* 16:531-7.

174. Pei J, Mitchell D, Dixon J, Grishin N. 2011. Expansion of type II CAAX proteases reveals evolutionary origin of γ-secretase subunit APH-1. *J Mol Biol* 410:18-26.

175. Perego M, Glaser P, Minutello A, Strauch MA, Leopold K, Fischer W. 1995. Incorporation of D-alanine into lipoteichoic acid and wall teichoic acid in *Bacillus subtilis*. Identification of genes and regulation. *J Biol Chem* 270:15598-606

176. Pereira MP, Brown ED. 2004. Bifunctional catalysis by CDP-ribitol synthase: convergent recruitment of reductase and cytidylyltransferase activities in *Haemophilus influenzae* and *Staphylococcus aureus*. *Biochemistry* 43:11802-12

177. Pereira MP, D'elia MA, Troczynska J, Brown ED. 2008. Duplication of teichoic acid biosynthetic genes in *Staphylococcus aureus* leads to functionally redundant poly(ribitol phosphate) polymerases. *J Bacteriol* 190:5642-9

178. Pereira MP, Schertzer JW, D'elia MA, Koteva KP, Hughes DW, et al. 2008. The wall teichoic acid polymerase TagF efficiently synthesizes poly(glycerol phosphate) on the TagB product lipid III. *ChemBioChem* 9:1385-90

179. Peschel A, Otto M, Jack RW, Kalbacher H, Jung G, Götz F. 1999. Inactivation of the dlt operon in *Staphylococcus aureus* confers sensitivity to defensins, protegrins, and other antimicrobial peptides. *J Biol Chem* 274:8405-10

180. Peschel A, Vuong C, Otto M, Götz F. 2000. The D-alanine residues of *Staphylococcus aureus* teichoic acids alter the susceptibility to vancomycin and the activity of autolytic enzymes. *Antimicrob Agents Chemother* 44:2845-7

181. Pooley HM, Karamata D. 2000. Incorporation of [2-3H]glycerol into cell surface components of *Bacillus subtilis* 168 and thermosensitive mutants affected in wall teichoic acid synthesis: effect of tunicamycin. *Microbiology (Reading, Engl)* 146 (Pt 4):797-805

182. Potekhina N, Streshinskaya G, Tul'skaya E, Kozlova Y, Senchenkova S, Shashkov A. 2011. Phosphate-containing cell wall polymers of bacilli. *Biochemsitry (Moscow)* 76:745-54.

183. Price NP, Tsvetanova B. 2007. Biosynthesis of the tunicamycins: a review. *The Journal of antibiotics* 60:485-91

184. Qamar A, Golemi-Kotra D. 2012. Dual Roles of FmtA in *Staphylococcus aureus* Cell Wall Biosynthesis and Autolysis. *Antimicrob Agents Chemother* 56:3797-805

185. Qian Z, Yin Y, Zhang Y, Lu L, Li Y, Jiang Y. 2006. Genomic characterization of ribitol teichoic acid synthesis in *Staphylococcus aureus*: genes, genomic organization and gene duplication. *BMC Genomics* 7:74

186. Rebollo R, Romanish M, Mager D. 2012. Transposable Elements: An Abundant and Natural Source of Regulatory Sequences for Host Genes. *Annu Rev Genet* 46:21-42.

187. Reichmann N, al. e. 2014. Differential localization of LTA synthesis proteins and their interaction with the cell division machinery in *Staphylococcus aureus*. *Mol Microbiol* In Press

188. Reichmann N, Cassona C, Grundling A. 2013. Revised mechanism of D-alanine incorporation into cell wall polymers in Gram-positive bacteria. *Microbiology* In Press

189. Reichmann NT, Grundling A. 2011. Location, synthesis and function of glycolipids and polyglycerolphosphate lipoteichoic acid in Gram-positive bacteria of the phylum Firmicutes. *FEMS Microbiol Lett* 319:97-105

190. Richter S, al. e. 2013. Small molecule inhibitor of lipoteichoic acid synthesis is an antibiotic for Gram-positive bacteria. *Proc Natl Sci Acad* 110:3531-6.

191. Rubinchik E, Schneider T, Elliott M, Scott WR, Pan J, et al. 2011. Mechanism of action and limited cross-resistance of new lipopeptide MX-2401. *Antimicrob Agents Chemother* 55:2743-54

192. Saar-Dover R, Bitler A, Nezer R, Shmuel-Galia L, Firon A, et al. 2012. D-alanylation of lipoteichoic acids confers resistance to cationic peptides in group B streptococcus by increasing the cell wall density. *PLoS Pathog* 8:e1002891

193. Sassetti C, Boyd D, Rubin E. 2003. Genes required for mycobacterial growth defined by high density mutagenesis. *Mol Microbiol* 48:77-84.

194. Schenk S, Laddaga RA. 1992. Improved method for electroporation of *Staphylococcus aureus*. *FEMS Microbiol Lett* 73:133-8

195. Schertzer JW, Brown ED. 2003. Purified, recombinant TagF protein from *Bacillus subtilis* 168 catalyzes the polymerization of glycerol phosphate onto a membrane acceptor in vitro. *J Biol Chem* 278:18002-7

196. Schertzer JW, Brown ED. 2008. Use of CDP-glycerol as an alternate acceptor for the teichoic acid polymerase reveals that membrane association regulates polymer length. *J Bacteriol* 190:6940-7

197. Schindelin J, al. e. 2012. Fiji: an open-source platform for biological-image analysis. *Nat Methods* 9:676-82

198. Schirner K, Marles-Wright J, Lewis RJ, Errington J. 2009. Distinct and essential morphogenic functions for wall- and lipo-teichoic acids in *Bacillus subtilis*. *EMBO J* 28:830-42

199. Schirner K, Stone LK, Walker S. 2011. ABC transporters required for export of wall teichoic acids do not discriminate between different main chain polymers. *ACS Chem Biol* 6:407-12

200. Schlag M, Biswas R, Krismer B, Kohler T, Zoll S, et al. 2010. Role of staphylococcal wall teichoic acid in targeting the major autolysin Atl. *Molecular Microbiology* 75:864-73

201. Sewell EWC, Pereira MP, Brown ED. 2009. The wall teichoic acid polymerase TagF is non-processive *in vitro* and amenable to study using steady state kinetic analysis. *J Biol Chem* 284:21132-8

202. Silhavy TJ, Kahne D, Walker S. 2010. The bacterial cell envelope. *Cold Spring Harb Perspect Biol* 2:a000414

203. Slavetinsky C, Peschel A, Ernst C. 2012. Alanyl-Phosphatidylglycerol and Lysyl-Phosphatidylglycerol Are Translocated by the Same MprF Flippases and Have Similar Capacities To Protect against the Antibiotic Daptomycin in *Staphylococcus aureus*. *Antimicrob Agents Chemother* 56:3492-7.

204. Soldo B, Lazarevic V, Karamata D. 2002. *tagO* is involved in the synthesis of all anionic cell-wall polymers in *Bacillus subtilis* 168. *Microbiology (Reading, Engl)* 148:2079-87

205. Soldo B, Lazarevic V, Pooley HM, Karamata D. 2002. Characterization of a *Bacillus subtilis* thermosensitive teichoic acid-deficient mutant: gene *mnaA* (*yvyH*) encodes the UDP-*N*-acetylglucosamine 2-epimerase. *J Bacteriol* 184:4316-20

206. Stapleton P, Shah S, Ehlert K, Hara Y, Taylor P. 2007. The β-lactam-resistance modifier (–)-epicatechin gallate alters the architecture of the cell wall of *Staphylococcus aureus*. *Microbiology* 153:2093-103

207. Sugai M, *et al*. 1995. Identification of endo-beta-N-acetylglucosaminidase and N-acetylmuramyl-L-alanine amidase as cluster-dispersing enzymes in *Staphylococcus aureus*. *J Bacteriol* 177:1491-6

208. Suzuki T, Campbell J, Kim Y, Swoboda JG, Mylonakis E, et al. 2012. Wall teichoic acid protects *Staphylococcus aureus* from inhibition by Congo red and other dyes. *The Journal of antimicrobial chemotherapy* 67:2143-51

209. Suzuki T, Campbell J, Swoboda JG, Walker S, Gilmore MS. 2011. Role of wall teichoic acids in *Staphylococcus aureus* endophthalmitis. *Invest Ophthalmol Vis Sci* 52:3187-92

210. Suzuki T, Swoboda JG, Campbell J, Walker S, Gilmore MS. 2011. In Vitro Antimicrobial Activity of Wall Teichoic Acid Biosynthesis Inhibitors against *Staphylococcus aureus* Isolates. *Antimicrobial Agents and Chemotherapy* 55:767-74

211. Swoboda JG, Campbell J, Meredith TC, Walker S. 2010. Wall teichoic acid function, biosynthesis, and inhibition. *Chembiochem* 11:35-45

212. Swoboda JG, Meredith TC, Campbell J, Brown S, Suzuki T, et al. 2009. Discovery of a small molecule that blocks wall teichoic acid biosynthesis in *Staphylococcus aureus*. *ACS Chem Biol* 4:875-83

213. Taylor P, Rossi L, De Pascale G, Wright G. 2012. A forward chemical genetics screen identifies antibiotic adjuvants in *Escherichia coli*. *ACS Chem Biol* 7:1547-55

214. Theilacker C, Holst O, Lindner B, Huebner J, Kaczynski Z. 2012. The structure of the wall teichoic acid isolated from *Enterococcus faecalis* strain 12030. *Carbohydr Res* 354:106-9

215. Therien A, Huber J, Wilson K, Beaulieu P, Caron A, al. e. 2012. Broadening the spectrum of β-lactam antibiotics through inhibition of signal peptidase type I. *Antimicrob Agents Chemother* 56:4662-70

216. Tomasz A, McDonnell M, Westphal M, Zanati E. 1975. Coordinated incorporation of nascent peptidoglycan and teichoic acid into pneumococcal cell walls and conservation of peptidoglycan during growth. *J Biol Chem* 250:337-41

217. Tomita S, Irisawa T, Tanaka N, Nukada T, Satoh E, et al. 2010. Comparison of components and synthesis genes of cell wall teichoic acid among *Lactobacillus plantarum* strains. *Biosci Biotechnol Biochem* 74:928-33

218. Torii M, Kabat E, Bezer A. 1964. Separation of teichoic acid of *Staphylococcus aureus* into two immunologically distinct specific polysaccharides with α- and β-N-acetylglucosaminyl linkages respectively. Antigenticity of teichoic acids in man. *J Exp Med* 120:13-29

219. Turner R, al. e. 2010. Peptidoglycan architecture can specificy division planes in *Staphylococcus aureus*. *Nat Commun* 1:1-9

220. Vadyvaloo V, Arous S, Gravesen A, Héchard Y, Chauhan-Haubrock R, et al. 2004. Cell-surface alterations in class IIa bacteriocin-resistant *Listeria monocytogenes* strains. *Microbiology (Reading, Engl)* 150:3025-33

221. Valentino MD, Kos V, Sadaka A, Santa Maria J, Lazinski D, et al. 2014. Genes contributing to *Staphylococcus aureus* success in infection-related ecologies. *In Preparation*

222. van Opijnen T, Bodi K, Camilli A. 2009. Tn-seq: High-throughput parallel sequencing for fitness and genetic interaction studies in microorganisms. *Nat Meth* 6:767-72.

223. van Opijnen T, Camilli A. 2013. Transposon insertion sequencing: a new tool for systems-level analysis of microorganisms. *Nat Rev Microbiol* 11:435-42.

224. Vastenhouw N, Plasterk R. 2004. RNAi protects the *Caenorhabditis elegans* germline against transposition. *Trends Genet* 20:314-9.

225. Vergara-Irigaray M, Maira-Litrán T, Merino N, Pier GB, Penadés JR, Lasa I. 2008. Wall teichoic acids are dispensable for anchoring the PNAG exopolysaccharide to the *Staphylococcus aureus* cell surface. *Microbiology (Reading, Engl)* 154:865-77

226. Vinogradov E, Sadovskaya I, Li J, Jabbouri S. 2006. Structural elucidation of the extracellular and cell-wall teichoic acids of *Staphylococcus aureus* MN8m, a biofilm forming strain. *Carbohydr Res* 341:738-43

227. Volkman BF, Zhang Q, Debabov DV, Rivera E, Kresheck GC, Neuhaus FC. 2001. Biosynthesis of D-alanyl-lipoteichoic acid: the tertiary structure of apo-D-alanyl carrier protein. *Biochemistry* 40:7964-72

228. Vollmer W, Blanot D, de Pedro MA. 2008. Peptidoglycan structure and architecture. *FEMS Microbiol Rev* 32:149-67

229. Waldron D, Lindsay J. 2006. Sau1: a novel lineage-specific type I restriction-modifications system that blocks horizontal gene transfer into *Staphylococcus aureus* and between *S. aureus* isolates of different lineages. *J Bacteriol* 188:5578-85.

230. Walsh C. 2000. Molecular mechanisms that confer antibacterial drug resistance. *Nature* 406:775-81

231. Walter J, Loach DM, Alqumber M, Rockel C, Hermann C, et al. 2007. D-alanyl ester depletion of teichoic acids in *Lactobacillus reuteri* 100-23 results in impaired colonization of the mouse gastrointestinal tract. *Environmental Microbiology* 9:1750-60

232. Wang H, Claveau D, Vaillancourt J, Roemer T, Meredith T. 2011. HIgh-frequency transposition for determining antibacterial mode of action. *Nat Chem Biol* 7:720-9.

233. Wang H, Gill CJ, Lee SH, Mann P, Zuck P, et al. 2013. Discovery of Wall Teichoic Acid Inhibitors as Potential Anti-MRSA β-Lactam Combination Agents. *Chemistry & biology* 20:272-84

234. Ward J, Wyke A, Curtis C. 1980. The effect of tunicamycin on wall-polymer synthesis in Bacilli. *Biochem. Soc. Trans.* 8:164-6.

235. Ward JB. 1981. Teichoic and teichuronic acids: biosynthesis, assembly, and location. *Microbiological Reviews* 45:211-43

236. Wecke J, Madela K, Fischer W. 1997. The absence of D-alanine from lipoteichoic acid and wall teichoic acid alters surface charge, enhances autolysis and increases susceptibility to methicillin in *Bacillus subtilis*. *Microbiology* 143:2953

237. Weidenmaier C, Kokai-Kun JF, Kristian SA, Chanturiya T, Kalbacher H, et al. 2004. Role of teichoic acids in *Staphylococcus aureus* nasal colonization, a major risk factor in nosocomial infections. *Nat Med* 10:243-5

238. Weidenmaier C, Kokai-Kun JF, Kulauzovic E, Kohler T, Thumm G, et al. 2008. Differential roles of sortase-anchored surface proteins and wall teichoic acid in *Staphylococcus aureus* nasal colonization. *Int J Med Microbiol* 298:505-13

239. Weidenmaier C, Kristian SA, Peschel A. 2003. Bacterial resistance to antimicrobial host defenses--an emerging target for novel antiinfective strategies? *Curr Drug Targets* 4:643-9

240. Weidenmaier C, Peschel A. 2008. Teichoic acids and related cell-wall glycopolymers in Gram-positive physiology and host interactions. *Nat Rev Microbiol* 6:276-87

241. Weidenmaier C, Peschel A, Xiong Y-Q, Kristian SA, Dietz K, et al. 2005. Lack of wall teichoic acids in *Staphylococcus aureus* leads to reduced interactions with endothelial cells and to attenuated virulence in a rabbit model of endocarditis. *J Infect Dis* 191:1771-7

242. Wickham JR, Halye JL, Kashtanov S, Khandogin J, Rice CV. 2009. Revisiting magnesium chelation by teichoic acid with phosphorus solid-state NMR and theoretical calculations. *J Phys Chem B* 113:2177-83

243. Will O, Jacobs M. 2006. Estimating the number of essential genes in random transposon mutagenesis libraries.

244. Wyke AW, Ward JB. 1977. Biosynthesis of wall polymers in Bacillus subtilis. *J Bacteriol* 130:1055-63

245. Xayarath B, Yother J. 2007. Mutations blocking side chain assembly, polymerization, or transport of a Wzy-dependent *Streptococcus pneumoniae* capsule are lethal in the absence of suppressor mutations and can affect polymer transfer to the cell wall. *J Bacteriol* 189:3369-81

246. Xia G, Corrigan RM, Winstel V, Goerke C, Grundling A, Peschel A. 2011. Wall teichoic Acid-dependent adsorption of staphylococcal siphovirus and myovirus. *J Bacteriol* 193:4006-9

247. Xia G, Kohler T, Peschel A. 2010. The wall teichoic acid and lipoteichoic acid polymers of *Staphylococcus aureus*. *Int J Med Microbiol* 300:148-54

248. Xia G, Maier L, Sanchez-Carballo P, Li M, Otto M, et al. 2010. Glycosylation of wall teichoic acid in *Staphylococcus aureus* by TarM. *Journal of Biological Chemistry* 285:13405-15

249. Yamamoto H, Miyake Y, Hisaoka M, Kurosawa S-I, Sekiguchi J. 2008. The major and minor wall teichoic acids prevent the sidewall localization of vegetative DL-endopeptidase LytF in *Bacillus subtilis*. *Molecular Microbiology* 70:297-310

250. Yang S-J, Bayer AS, Mishra NN, Meehl M, Ledala N, et al. 2012. The *Staphylococcus aureus* two-component regulatory system, GraRS, senses and confers resistance to selected cationic antimicrobial peptides. *Infec Immun* 80:74-81.

251. Yokoyama K, Miyashita T, Araki Y, Ito E. 1986. Structure and functions of linkage unit intermediates in the biosynthesis of ribitol teichoic acids in *Staphylococcus aureus* H and *Bacillus subtilis* W23. *Eur J Biochem* 161:479-89

252. Yotis W, Barman S. 1970. Action of diethylstilbestrol on staphylococci: further observations on the effect of resting cells. *Appl Microbiol* 19:474-8

253. Young M, Mauël C, Margot P, Karamata D. 1989. Pseudo-allelic relationship between non-homologous genes concerned with biosynthesis of polyglycerol phosphate and polyribitol phosphate teichoic acids in *Bacillus subtilis* strains 168 and W23. *Mol Microbiol* 3:1805-12

254. Zapun A, Contreras-Martel C, Vernet T. 2008. Penicillin-binding proteins and beta-lactam resistance. *FEMS Microbiol Rev* 32:361-85

255. Zhang Y-H, Ginsberg C, Yuan Y, Walker S. 2006. Acceptor substrate selectiveity and kinetic mechanism of *Bacillus subtilis* TagA. *Biochemsitry (Moscow)* 45:10895-904

256. Zoll S, al. e. 2010. Structural basis of cell wall cleavage by a staphylococcal autolysin. *PLoS Pathog* 6:e1000807

257. Zolli M, Kobric D, Brown E. 2001. Reduction precedes cytidylyl transfer without substrate channeling in distinct acive sites of the bifunctional CDP-ribitol synthase from *Haemophilus influenzae*. *Biochemistry* 40:5041-8

258. Zomer A, Burghout P, Bootsma H, Hermans P, van Hijum S. 2012. ESSENTIALS: software for rapid analysis of high throughput transposon insertion sequencing data. *PLos ONE* 7:e43012